Università degli Studi di Cagliari

PHD DEGREE

Chemical Sciences and Technologies

Cycle XXX

TITLE OF THE PHD THESIS

Versatility and Clinical Applications of Metabolomics: Tissues and Biofluids Investigation for Pathological Clustering

Scientific Disciplinary Sector(s)

CHIM06 - ERC LS2_4

PhD Student: Francesco Palmas

Coordinator of the PhD Programme Prof. Stefano Enzo

Supervisor Dr Claudia Fattuoni, Prof. Mariano Casu

Final exam. Academic Year 2016 – 2017
Thesis defence: February-March 2018 Session

Abstract

Metabolomics is the discipline that comprehensively and simultaneously profile the metabolome within a sample or organism. Investigating the downstream processes from gene expression and protein synthesis to the metabolic network, metabolomics may be of pivotal importance for the design of new screening methodology, for the identification of novel biomarkers and for the study of diseases at molecular and biochemical level. To this end, the versatility of metabolomic strategy was exploited for the investigation of diverse clinical conditions and different phenotypes regarding pregnancy, neonatology, oncology, odontology, treatment response, and autoimmune diseases. In particular, GC-MS, ^{1}H-NMR or HRMAS-MRS were applied on AF, intact kidney tissue, extracts from placenta, plasma, saliva, and urine specimens. In most studies, metabolomic strategy was able to highlight significant alteration related to various mechanisms (e.g. dietary intake and oxidative stress) that affected the relative concentrations of the metabolome. In conclusions, while larger, multicentre samples size and parallel microbiological analyses should be used to confirm data, these metabolomics-based findings are an interesting promise for the future discovery of novel biomarkers, phenotypical investigations, and translation into medical setting to improve clinical practice.

Keywords

Metabolomics, GC-MS, ^{1}H-NMR, HRMAS-MRS, Amniotic Fluid, Intact Kidney Tissue, Placenta, Plasma, Saliva, Urine, foetus' sex recognition, obesity, PROM, pPROM, meconium, HCMV, primary infection, NEC, RCC, CRC, hypothermia response, SSc

Summary

List of Abbreviations

10-fold CV	10-fold Cross Validation
1D	One Dimensional
β-HCG	β-Subunit Of Human Chorionic Gonadotropin
ACI	Asymptomatic Congenital Infection
Ad	Adjacent benign
AF	Amniotic Fluid
AFP	α-Fetoprotein
AMDIS	Automated Mass Spectral Deconvolution and Identification System
AML	Angiomyolipoma
ANOVA	Analysis Of Variance
APC	Antigen Presenting Cells
AOU	Azienda Ospedaliera Universitaria
ATP	Adenosine Triphosphate
a.u.	Arbitrary Units
AUC	Area Under the Curve
BMI	Body Mass Index
BW	Birth Weight
CA19-9	Carbohydrate Antigen 19-9
CC	Clear Cell
Chr	Chromophobe
CI	Confidence Interval
CPMG	Carr-Purcell-Meiboom-Gill
CRC	Colorectal Cancer
DHA	Docosahexaenoic Acid
ED	Entner–Doudoroff
EDTA	Ethylenediaminetetraacetic acid
FIGO	International Federation of Gynaecology and Obstetrics
FDR	False Discovery Rate
FOBT	Faecal Occult Blood Test
FX	Guanosine Diphosphate Keto-6-Deoxymannose-3,5-Epimerase-4-Reductase
GC-MS	Gas Chromatography Mass Spectrometry
GDP	Guanosine Diphosphate
GDM	Gestational Diabetes Mellitus
GHS	Glutathione
GMD	Golm Metabolome Database
GMDS	Guanosine Diphosphate Mannose-4,6-Dehydratase
GPC	Glycerophosphocholine
GR	Glyoxylate Reductase
HC	Histological Chorioamnionitis
HCA	Hierarchical Cluster Analysis
HCMV	Human Cytomegalovirus
HIE	Ischemic Encephalopathy
HIF-1α	Hypoxia-Inducible Factor Alpha Subunit
HRMAS	High Resolution Magic Angle Spinning
IGF-BP1	Insulin Growth Factor Binding Protein-1
IL-1	Interleukin-1
IOM	Institute of Medicine
IUI	Intrauterine Infection/Inflammation
LC-PUFA	Long Chain-Polyunsaturated Fatty Acids
LC-MS	Liquid Chromatography-Mass Spectrometry
LGR5	Leucine-Rich Repeat-Containing G Protein-Coupled Receptor 5
LOOCV	Leave One Out Cross Validation
MMP-12	Matrix Metalloproteinase 12
MRS	Magnetic Resonance Spectroscopy
MRSI	Magnetic Resonance Spectroscopy Imaging
MSEA	Metabolite Sets Enrichment Analysis
MSTFA	*N*-Methyl-*N*-trimethylsilyltrifuoroacetamide
mTOR	Mammalian Target Of Rapamycin
NEC	Necrotising Enterocolitis

NIST	National Institute of Standards and Technology
NMR	Nuclear Magnetic Resonance
NOESY	Nuclear Overhauser Spectroscopy
OGTT	Oral Glucose Tolerance Test
Onc	Oncocytoma
OPLS-DA	Orthogonal Partial Least Square-Discriminant Analysis
OR	Odds Ratio
Pap	Papillary
PBS	Phosphate-Buffered Saline
PC5	D1-pyrroline-5-carboxylate
PCA	Principal Component Analysis
PCho	Phosphocholine
PLS-DA	Partial Least Square Discriminant Analysis
PMN	Polymorphonuclear
PRODX	Proline Dehydrogenase
PPROM	Preterm Premature Rupture Of Membranes
PROM	Premature Rupture Of Membranes
POX	Proline Oxidase
PTFE	Polytetrafluoroethylene
RCC	Renal Cell Carcinoma
Rh	Rhesus
ROC	Receiver Operating Characteristic
ROI	Region Of Interest
ROS	Reactive Oxygen Species
SCI	Symptomatic Congenital Infections
SSc	Systemic Sclerosis
SSRI	Selective Serotonin Reuptake Inhibitor
TBD	To Be Determined
TCA	Tricarboxylic Acid
TNF-α	Tumour Necrosis Factor A
TNM	Tumour/Regional Nodal Involvement/Distal Metastasis
TRAIL	Tumor Necrosis Factor-Related Apoptosis inducing Ligand
TSP	Trimethylsilyl Propionate
VIP	Variable Importance for the Projection

1. Introduction

1.1 Metabolomics

Originally, several "omics" approaches shared the goal to analyse the plethora of metabolites, i.e. the relatively small molecules involved in metabolic pathways, characterising a biofluid or tissue. Indeed, the label of "metabolomics" was reserved to studies on plants and *in vivo* microbiological systems through mass spectrometry. However, over the years, many of these strategies merged into a single term to avoid redundancy. Currently, the term "metabolomics" refers to the disciplines that comprehensively and simultaneously profile the entire set of metabolites, known as metabolome, within a sample or organism [1]. Nowadays, it is well established that relative concentrations among metabolites within cells, tissues, biofluids, and organisms vary according to several factors such as the physiology, development and/or pathological state of the system under study. For study purposes, Biology considers each metabolic pathway as an isolated system; however, this is not an accurate perspective. Conversely, holistic disciplines attempt to fill this gap, considering and highlighting the complicated network among the different pathways of primary and secondary metabolites. For instance, the perturbation on a particular metabolic cycle may affect several others, causing different ratios among a number of metabolites. Unlike other "omics" approaches, metabolomics may investigate both the endogenous mechanisms and the effects of external factors. Whilst genomics is of great importance for the study of potential inheritance states (pathological and non-pathological) and proteomics may deliver useful information regarding how the provided genes are effective in the organism, metabolomics may add the influence of diet, social behaviour, and environment. In fact, these variables may affect the genome or the proteome at some level, but metabolites should be more susceptible to such influences. Furthermore, another advantage of metabolomics is that metabolites can be readily detected and measured, allowing for an easier application into clinical or pharmaceutical settings. Moreover, although the number or metabolites is substantially lower than that of genes or other variable, metabolomics may deliver the same information. An important aspect of metabolomics is that, following qualitative and quantitative/semi-quantitative detection of the biomolecules, multivariate statistical analysis is conducted. Such powerful tool enables the interpretation of the obtained data. Among the multiple applications of this discipline, clinical metabolomics showed the fastest development [2–5]. Indeed, investigating the downstream processes from gene expression and protein synthesis to the metabolic network [6], metabolomics may be of pivotal importance for the design of new screening methodology (having low invasivity level), for the identification of novel biomarkers and for the study of diseases at molecular and biochemical level. Therefore, it may accurately describe

pathological and phenotypical status and, in a further stage, allow for the design of patient-tailored medicine.

1.2 Analytical Techniques and Platforms

Metabolites' relative concentration is commonly detected by high throughput techniques such as Nuclear Magnetic Resonance (NMR) spectroscopy, gas chromatography-mass spectrometry (GC-MS), or liquid chromatography-mass spectrometry (LC-MS). During the PhD Programme, GC-MS and NMR-based platforms were exploited. As commonly known, each analytical technique presents advantages and disadvantages, meaning there is no such thing as a perfect platform. Nevertheless, the choice of the technique to apply may be of importance for the study results. In particular, GC-MS shows high sensibility, allowing for the analysis of biofluids and tissue extracts in extremely low amounts, and the recognition of unknown compounds is possible by means of dedicated libraries, i.e. digital databases containing retention times and mass spectra of a plethora of compounds. Moreover, if unknown analytes are not present in a library, the study of mass fragments may help in the identification and the classification into certain chemical groups such as carbohydrates, oxidised sugars, etc. Other advantages consist in the moderate cost of the instrument and its maintenance, helping the spreading of such technique in different settings, and the fact that a high degree of specialisation is not required for routine analyses. However, biological specimens require sample pre-treatment for the detection of most metabolites and such procedures are time consuming. Indeed, as described in the successive chapter, for the preparation of a set of samples are necessary about two days. Moreover, molecules under a certain molecular weight (e.g. propanoic acid) and large molecules (e.g. folic acid) are not detectable. Regarding NMR-based platforms, two main techniques were applied: ^{1}H-NMR and high-resolution magic angle spinning magnetic resonance spectroscopy (HRMAS-MRS). The former strategy allows for the analysis of liquid specimens such as biofluid or tissues extracts and requires almost no sample pre-treatment. Therefore, it appears as a fast route to obtain data. HRMAS-MRS is mainly designed to maximise the resolution for the observation of mobile metabolites within solid-state specimens such as intact tissues [2]. This platform is characterised by an important advantage compared to the previous analytical tool: it maintains the accurate structure of the sample [7–14]. Indeed, the absence of an actual pre-treatment (see successive chapter) is optimal because it prevents any relative concentrations alteration that may occur during extraction, and it preserves the specimens for further investigations. For instance, following a HRMAS-MRS experiment is possible to prepare slides for histopathological reading of the exact same specimen, hence providing gold standard diagnosis to strengthen the obtained data. In addition, results from this tool may be exploited for the

improvement of *in vivo* MRS analyses [2]. Nevertheless, both NMR-based techniques display low sensibility, instrument and maintenance costs are elevated, and operators require highly specialised training, limiting the wide application in diverse settings. Furthermore, although the development of certain databases and the possibility to virtually detect the entire metabolome without any molecular weight restriction, identification is less immediate that in the case of mass spectrometry. As a result, a lower number of biomolecules is usually suitable for data processing. Therefore, while GC-MS shows great potential in the detection and identification of small amounts of multiple metabolites, it is a slow technique with a confined range of observable molecular weights. ^{1}H-NMR and HRMAS-MRS are fast means of analysis and preserve the structure of the samples, but are expensive and characterised by limitations for operators and analytes recognition. For these reasons, a study aimed at the complete and accurate description of physiopathological mechanisms would attempt to apply more techniques for the comprehensive characterisation of the metabolome. While this so-called "data fusion" approach would be redundant for certain metabolites, it would expand the range of observable variables. Nevertheless, important insights may derive from single instrument studies and the design of multi-instrumental projects is of difficult feasibility for practical and economic reasons. Notably, if the objective of a study is the development/implementation of a diagnostic methodology or the discovery of novel biomarkers, the model resulting from a single platform may suffice according to suitable accuracy. In this context, GC-MS may be of easier translation into clinical practice with the exception of cases in which fast analysis are strictly necessary or for *in vivo* investigations. For these particular events, NMR would probably be the most useful choice. Within the PhD Programme, the majority of studies were conducted through GC-MS, while one study was performed by HRMAS-MRS (intact kidney tissue in relation to renal cell carcinoma) and another by ^{1}H-NMR (urine sample for necrotising enterocolitis).

1.3 Pathologies ad Phenotypical Conditions

Multiple clinical and phenotypical states were explored through metabolomic analysis. As shown in Table. 1.3.1, the majority of phenotypes under study regarded pregnancy-related and perinatal events, followed by oncological area, treatment response, autoimmune diseases, and odontology. Furthermore, different biofluids or tissues were analyses depending on the project: amniotic fluid, intact kidney tissue, placenta, plasma, saliva, and urine (Table 1.3.1).

Distribution According to Clinical Area of Investigation		
Area	**Studies**	**Number**
Pregnancy-related	foetus' sex recognition obesity during gestation gestational diabetes mellitus premature rupture of membranes at term preterm premature rupture of membranes	5
Perinatal	meconium stained amniotic fluid primary human cytomegalovirus infection chorioamnionitis necrotising enterocolitis	4
Oncology	renal cell carcinoma colorectal cancer	2
Treatment Response	hypothermia for hypoxia occurrences	1
Autoimmune Diseases	systemic sclerosis	1
Odontology	apical periodontitis	1
Distribution According to Specimen of Investigation		
Specimen	**Studies**	**Number**
Amniotic Fluid	gestational diabetes mellitus foetus' sex recognition meconium stained amniotic fluid primary human cytomegalovirus infection	4
Intact Kidney Tissue	renal cell carcinoma	1
Placenta (extracts)	obesity during gestation	1
Plasma	colorectal cancer	1
Saliva	apical periodontitis	1
Urine	chorioamnionitis hypothermia for hypoxia occurrences necrotising enterocolitis premature rupture of membranes at term preterm premature rupture of membranes systemic sclerosis	6

Table 1.3.1: *Distribution of the studies according to clinical area of investigation or to the type of specimen analysed*

In this work, chapters were divided by biofluids or tissues rather than by the clinical area of interest for two main reasons:

1) Division by biofluid/tissue would better highlight the versatility of the metabolomic approach even when the same mean of investigation was considered.

2) Although some studies could be grouped under the same clinical area, the condition described were highly different. The biochemical mechanisms characterising such events were specific for the conditions and not related to each other. For instance, pregnancy cases comprised foetus' sex recognition, obesity during gestation, gestational diabetes mellitus, premature rupture of membranes at term, and preterm premature rupture of membranes. Even for the last two investigations, each study required different explanation; therefore, chapter's division by biofluid/tissue was preferred.

1.4 Aim of the project

The aim of this PhD project was to exploit the versatility of metabolomics, i.e. its capacity to adapt to different functions/research objectives, for the investigation of diverse clinical conditions and different phenotypes. The clusterisation of groups regarding pregnancy, neonatology, oncology, odondology, autoimmune diseases, and treatment response may deliver useful information on their physiopathological dynamics through the alteration of specific metabolic behaviours and hence for future discovery of novel biomarkers. This would indeed represent a powerful tool towards the improvement of clinical practice.

2. Materials and Methods

2.1 Population

During my PhD programme, given the variety of pathologies investigated, different populations were considered for different studies. The populations of each project were selected to analyse samples from matched subjects. Indeed, grouping of individuals with similar characteristics (i.e. age, sex, health status, etc.), prevent the introduction of confounding factors and allows for the underlining of the differences that are solely related to the conditions under study. For this reason, data regarding populations will be separately discussed in each section.

2.2 Sample Preparation, Analysis, and Data Processing

2.2.1 Gas Chromatography-Mass Spectroscopy

General Considerations

Five different biofluids were analysed, for different projects, by means of GC-MS platform: amniotic fluid, placenta tissue extracts, plasma, saliva, and urine. The applied pre-analytical sample treatments are a modification of a protocol previously reported [15,16]. In details, the amount of sample considered for the analysis increased according to the trend urine < amniotic fluid < plasma < saliva because of the increasing natural dilution of the biofluid under study (Table 2.2.1). For the same reason, smaller final dilution was applied to amniotic fluid specimens.

Biofluid	Sample Volume (µL)	Methoxylamine (µL)	MSTFA (µL)	Hexane (µL)
Amniotic fluid	200	60	80	100
Plasma	400	50	50	200
Saliva	1000	30	30	600
Urine	150	30	30	600

Table 2.2.1: *Different volumes of sample, methoxylamine, MSTFA, and hexane for each biofluid under study*

The addition of acetone in amniotic fluid and saliva samples was introduced for protein denaturation and precipitation, hence to subtract such molecules that cannot be analysed through this platform. In urine specimens, a solution of urease was used. In fact, such enzyme is responsible for the transformation of urea in NH_3 and CO_2 (Scheme 2.2.1. Given the prominent amount of urea in urine, the consumption of this molecule has two main advantages. The first is the possibility to detect the compounds that may elute at similar retention times to urea's peak, while the second consists in the larger availability, hence the necessity of smaller amounts, of the derivatising agents.

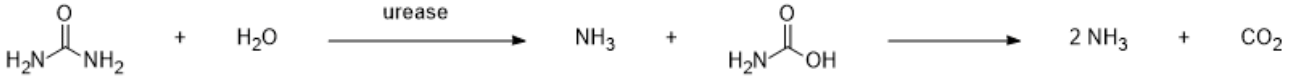

Scheme 2.2.1: *Urease catalyses the transformation of urea in NH_3 and CO_2*

Derivatisation processes, methoxymation and silylation, were applied to all the samples analysed by means of GC-MS. Different volumes of derivatization agents were used according to natural dilution of the specimen. Methoximation procedure is necessary to reduce the number of detectable carbohydrates forms that are normally present in solution. Indeed, carbohydrates are in equilibrium, through intramolecular hemiacetalization and mutarotation, with different forms. For instance, D-glucose is found as open structure, α- and β–pyranose and α– and β–furanose (Scheme 2.2.2). The addition of a solution of methoxylamine in pyridine to the dried sample yields the methoximes derivatives as the geometrical isomers E and Z (Scheme 2.2.3). This means the carbonyl group is substituted by a C-N double bond, which can no longer react to produce hemiacetals. Therefore, instead of detecting more than 4 peaks for the same analytes, only the 2 peaks are observed. Such procedure was not applied for the preparation of placental lipophilic phase due to the absence of carbohydrates in this fraction.

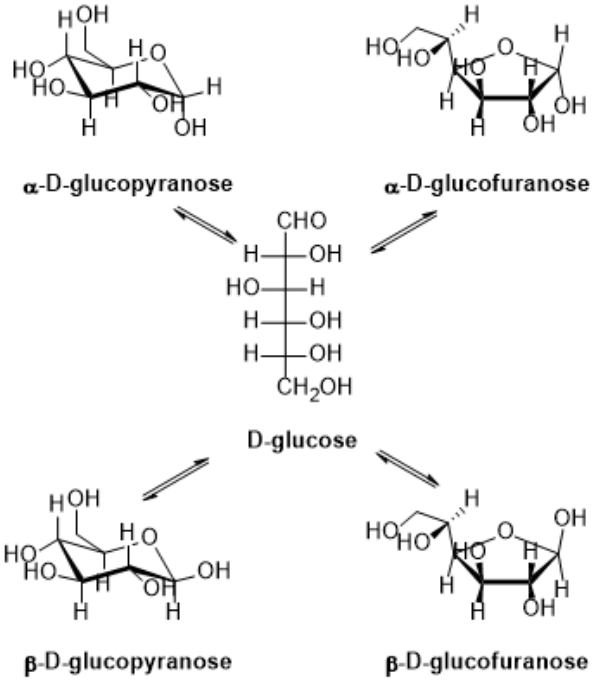

Scheme 2.2.2: *Different forms of D-glucose in solution*

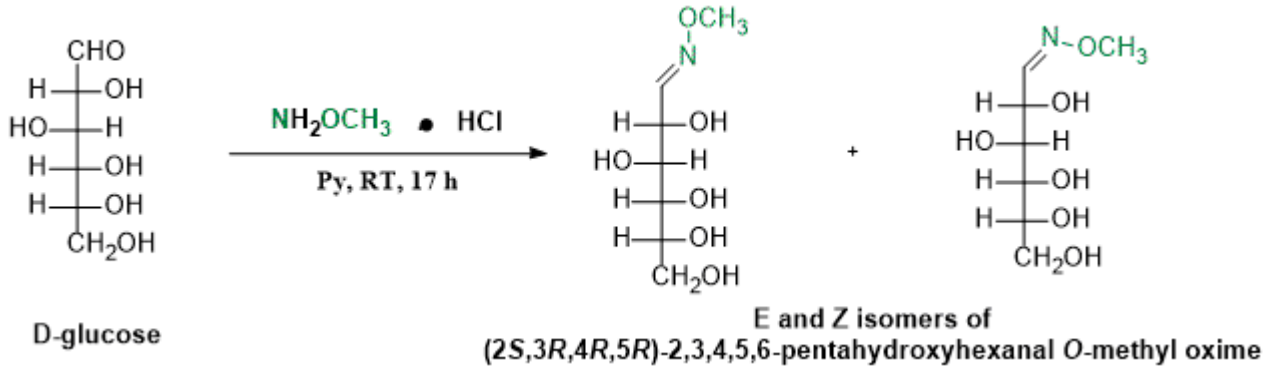

Scheme 2.2.3: *Methoximation of glucose*

Conversely, to methoxymation, silylation has a wider target. Indeed, several metabolites are polar compounds characterised by the possibility of hydrogen bonds formation. Since hydrogen bonds increase the boiling point, this may prevent their eligibility for GC analysis. For this reason, silylation reaction aims at the substitution of the so-called "acidic hydrogens", i.e. those hydrogens bound to more electronegative heteroatoms that may induce hydrogen bonds (Scheme 2.2.4). The impairment of such phenomena leads to more volatile compounds. Interestingly, amniotic fluid analysis required the largest volume of reactant due to the significant presence of glucose.

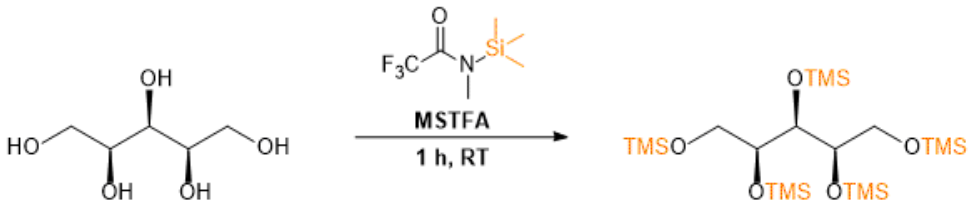

Scheme 2.2.4: *Silylation of a compound bearing acidic hydrogens, e.g. xylitol*

In the case of the lipophilic phase of placenta extraction, methylation reaction was performed instead of silylation (Scheme 2.2.5). Although different procedures, the reasons behind such strategies are the same.

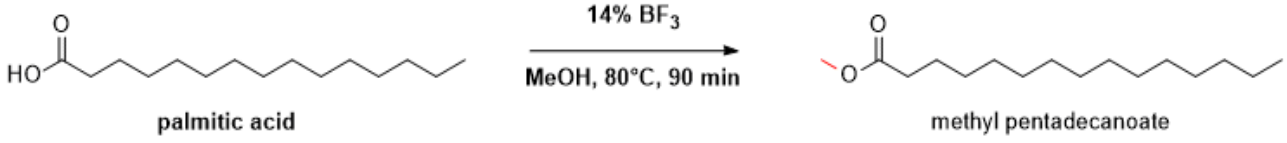

Scheme 2.2.5: *Methylation of a fatty acid*

Amniotic Fluid

Samples were thawed at room temperature and mixed by vortex in order to homogenize the matrix. 200 µL were then transferred in tubes (1.5 mL in capacity) and treated with 400 µL of acetone for protein precipitation. The mixture was mixed by vortex for 30 s and then centrifuged (1400 rpm for 10 min at 4 °C). 400 µL of supernatant were transferred into glass vials and evaporated to dryness overnight in a vacuum centrifuge. 60 µL of a 0.24 M (20 mg/mL) solution of methoxylamine hydrochloride in pyridine was added to each vial; samples were mixed by vortex and left to react for 17 h at room temperature. Subsequently, 80 µL of *N*-Methyl-*N*-trimethyl-silyl-trifuoroacetamide (MSTFA) were added and incubated for 1 h at room temperature. The derivatized samples were diluted with hexane (100 µL) just before GC-MS analysis [17–21].

Samples were analysed using a Agilent 5975C interfaced to the GC 7820 equipped with a DB-5ms column (J & W), injector temperature at 230 °C, detector temperature at 280 °C, helium carrier gas flow rate of 1 mL/min. The GC oven temperature program was 90°C initial temperature with 1 min hold time and ramping at 10 °C/min to a final temperature of 270 °C with 7 min hold time. 1 µL of the derivatized sample was then injected in split (1:20) mode. After a solvent delay of 3 min mass spectra were acquired in full scan mode using 2.28 scans/s with a mass range of 50–700 Amu [17–21].

Placental Extracts

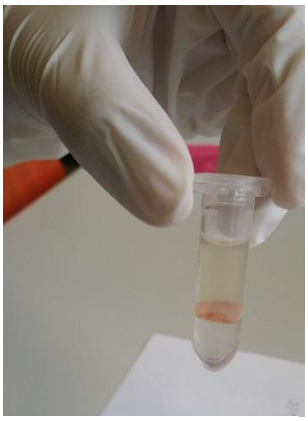

Fig. 2.2.1: *placenta extraction mixture*

The extraction method was optimized from literature methods [22–26]. A piece of placental tissue of about 100 mg was rapidly weighted, put in a glass mortar on ice with chloroform/methanol/water (1.4/1.4/1 - 700/700/500 µL) and homogenized with a Potter-Elvehjem homogenizer with a polytetrafluoroethylene (PTFE) pestle. The solvent mixture was then transferred in a 2 mL Eppendorf tube. The volume of extraction solution was normalised to 100 mg of tissue, considering 1000 µL for the upper (hydrophilic) phase and 600 µL for the lower (lipophilic) one. For example, for a placenta sample of 96 mg, 1042 µL (100 mg/96 mg*1000 µL) for the upper phase and 625 µL (100 mg/96 mg*600 µL) for the lower phase were used [23]. Samples were kept at 4 °C for 15 min and then centrifuged at 14000 rpm for 10 min at 4°C.

The upper phase and the lower phase were separated. While the hydrophilic phase was dried in a vacuum concentrator (Eppendorf), the lipophilic one was transferred into a glass vacuum desiccator under fume-hood. The dried fractions were stored at -80°C until analysis.

The dried hydrophilic phase was then treated with 30 µL of a 0.24 M (20 mg/mL) solution of methoxylamine hydrochloride in pyridine. Samples were vortex mixed and left to react for 17 h at room temperature. Subsequently, 30 µL of MSTFA were added and left to react for 1 h at room temperature. Finally, derivatized samples were diluted with 600 µL of tetracosane in hexane (0.01 mg/mL) just before GC–MS analysis. Samples were analysed using a Agilent 5975C interfaced to the GC 7820 equipped with a DB-5ms column (J & W), injector temperature at 230 °C, detector temperature at 280 °C, helium carrier gas flow rate of 1 mL/min. The GC oven temperature program was 90°C initial temperature with 1 min hold time and ramping at 10 °C/min to a final temperature of 270 °C with 7 min hold time. 1 µL of the derivatized sample was then injected in

split (1:20) mode. After a solvent delay of 3 min, mass spectra were acquired in full scan mode using 2.28 scans/s with a mass range of 50–700 Amu.

150 µL of chloroform:methanol (1:1) and 100 µL of 14% BF_3 in methanol was added to each vial of the dried lipophilic phase. Samples were vortex mixed and left to react for 90 min at 80 ºC into a heating block. Once samples had cooled, 600 µL hexane and 300 µL H_2O were added, samples were vortex mixed and transferred in 1.5 mL Eppendorf tubes. After centrifugation for 2 min at 1400 rpm the upper organic layer was transferred into glass vials and dried in the Eppendorf vacuum dryer. Samples were reconstituted with 400 µL hexane and injected. Samples were analysed using a Agilent 5977B interfaced to the GC 7890B equipped with a DB-5ms column (J & W), injector temperature at 230 °C, detector temperature at 280 °C, helium carrier gas flow rate of 1 ml/min. The initial GC oven temperature was 60 ºC for 2 min. This was then increased by 15ºC/min to 150 ºC, and then increased by 4 °C/min to a final temperature of 230 ºC, then kept for 20 min. 1 µL of the derivatised sample was injected in split (1:10) mode. After a solvent delay of 4 min, mass spectra were acquired in full scan mode using 2.28 scans /s with a mass range of 50–700 Amu.

Plasma

Plasma samples were collected in EDTA-containing tubes and stored at -80°C. 400 µL of thawed plasma were transferred in Eppendorf tubes, treated with 1200 µL of cold methanol, vortex mixed, and centrifuged for 15 min at 14000 rpm (16.9 G) and 4 °C. 370 µL of supernatant were transferred into glass vials and evaporated to dryness overnight in an Eppendorf vacuum centrifuge. 50 µL of a 0.24 M (20 mg/mL) solution of methoxylamine hydrochloride in pyridine were added to each vial, samples were vortex mixed and left to react for 17 h at room temperature. Then 50 µL of MSTFA were added and left to react for 1 h at room temperature. The derivatised samples were diluted with 200 µL of tetracosane in hexane just before GC-MS analysis.

Fig. 2.2.2: *GC-MS platform*

Samples were analysed using an Agilent 5975C interfaced to the GC 7820 equipped with a DB-5ms column (J & W), injector temperature at 230 °C, detector temperature at 280 °C, helium carrier gas flow rate of 1 mL/min. The GC oven temperature programme was 90°C initial temperature with 1 min hold time and ramping at 10°C/min to a final temperature of 270°C with 7 min hold time. 1 µL of the derivatized sample is injected in split (1:5) mode. After a solvent delay of 3 min, mass spectra were acquired in full scan mode using 2.28 scans/s with a

mass range of 50–700 Amu.

Saliva

Saliva samples were thawed at room temperature. 1000 µL were then transferred in an Eppendorf tube with 1000 µL of cold acetone at -20 °C [27], vortexed for 30 s and centrifuged for 10 min at 14000 rpm (16.9 G) and 4 °C. 1000 µL of supernatant were transferred in glass vials and evaporated to dryness overnight in an Eppendorf vacuum centrifuge. 30 µL of a 0.24 M (20 mg/mL) solution of methoxylamine hydrochloride in pyridine were added to each vial, samples were vortex mixed, and then left to react for 17 h at room temperature. 30 µL of MSTFA were added and left to react for 1 h at room temperature. The derivatized samples were diluted with 600 µL of tetracosane in hexane with (0.01 mg / mL) just before GC-MS analysis.

Samples were analysed using a Agilent 5975C interfaced to the GC 7820 or with a Agilent 5977B interfaced to the GC 7890B equipped with a DB-5ms column (J & W), injector temperature at 230 °C, detector temperature at 280 °C, helium carrier gas flow rate of 1 mL / min. The GC oven temperature program was 90°C initial temperature with 1 min hold time and ramping at 10 °C/min to a final temperature of 270 °C with 7 min hold time. 1 µL of the derivatized sample was then injected in split (1:20) mode. After a solvent delay of 3 min, mass spectra were acquired in full scan mode using 2.28 scans/s with a mass range of 50–700 Amu.

Urine

Samples were thawed at 0 °C and mixed by vortex in order to homogenize the matrix. 150 µL were then transferred in tubes (2 mL in capacity) and treated with 800 µL of urease solution in water (0.050 g/50 mL). The mixture was mixed by vortex for 30 s, subjected to ultrasound for 30 min and then centrifuged for 10 min at 14000 rpm (16.9 G) and 4 °C. 1200 µL of supernatant were transferred into glass vials and evaporated to dryness overnight in a vacuum centrifuge. 30 µL of a 0.24 M (20 mg/mL) solution of methoxylamine hydrochloride in pyridine was added to each vial; samples were mixed by vortex and left to react for 17 h at room temperature. Subsequently, 30 µL of MSTFA were added and incubated for 1 h at room temperature. The derivatized samples were diluted with 600 µL of tetracose in hexane (0.01 mg / mL) just before GC–MS analysis. [28–32]

Samples were analysed using a Agilent 5975C interfaced to the GC 7820 or with a Agilent 5977B interfaced to the GC 7890B equipped with a DB-5ms column (J & W), injector temperature at 230 °C, detector temperature at 280 °C, helium carrier gas flow rate of 1 mL/min. The GC oven

temperature programme was 90°C initial temperature with 1 min hold time and ramping at 10 °C/min to a final temperature of 270 °C with 7 min hold time. 1 µL of the derivatized sample was then injected in split (1:20) mode. After a solvent delay of 3 min, mass spectra were acquired in full scan mode using 2.28 scans/s with a mass range of 50–700 Amu.

GC-MS Data Processing

Each acquired chromatogram was analysed by means of the free software Automated Mass Spectral Deconvolution and Identification System (AMDIS; http://chemdata.nist.gov/mass-spc/amdis) that identified each peak by comparison of the relative mass spectra and the retention times with those stored in an in-house made library comprising 255 metabolites. Other metabolites were identified using NIST08 (National Institute of Standards and Technology's mass spectral database) and the Golm Metabolome Database (GMD, http://gmd.mpimp-golm.mpg.de/). AMDIS analysis produced an Excel data matrix that was successively subjected to chemometric analysis.

2.2.2 Nuclear Magnetic Resonance

Intact Kidney Tissue

Fresh tissue samples were kept on ice from the operating room and analysed within 1 h after excision. Frozen specimens were stored at -80°C for at least 24 h prior to tissue MRS. Successively, fresh or frozen tissues were cut on a frozen metal support, obtaining samples of ~10 mg. Specimens were then inserted into a 4 mm zirconia rotor with Kel-F inserts to generate a 10 µL sample space (Fig. 2). Two to 10 µL of D_2O were then added for field locking.

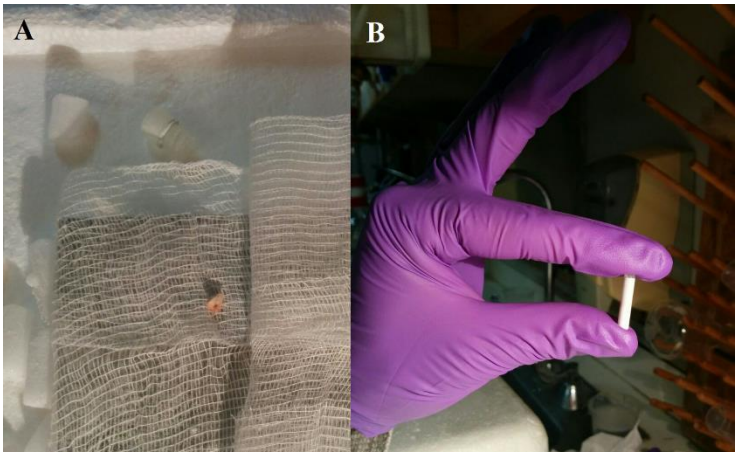

Fig. 2.2.3: *A) Kidney sample on frozen metal support B) Zirconia rotor*

HRMAS-MRS was conducted on a Bruker AVANCE spectrometer operating at 600 MHz. Spectra were recorded at 4 ºC with resonance frequency centred on the water resonance, a rotor-

synchronized Carr-Purcell-Meiboom-Gill (CPMG) filter sequence, and at a spinning rate of 3600 Hz (±1.0 Hz) [33]. Three different spectra were then recorded: one without water suppression, one with water suppression and long *T* relaxation time, and one with water suppression and short *T* [34].

Spectra were phased and baseline correction was performed using an in-house developed MatLab-based curve fitting programme, which exported intensity data on excel files. Values were recorded every 0.001 ppm, centred according to lactate resonance, and normalised by the sum of the metabolic region from 0.5 to 4.5 ppm. In details, relative intensities were calculated using the metabolic region of the water-unsuppressed spectrum of the same sample. In fact, assuming that hydration is constant in tissues (80% of tissues are constituted by water), water amount reflects the weight of the sample. Since water peak can be used but its shape is usually not reproducible, the equation for calculating relative intensity for each ppm value is:

$$[M]=I_{Mx}/I_{Tot} = I_{Mx}/I_{Mrwu} \times((I_{Mrws} \times 55556 \times 0.8))/I_{Tot}$$

Where;

[M] is the normalised concentration values

I_{Mx} is the integral/intensity that has to be normalised

I_{Tot} is the intensity of the total spectrum without water suppression

I_{Mrwu} is the intensity of the metabolic region in the spectrum without water suppression (water unsuppressed)

I_{Mrws} is the intensity of the metabolic region in the spectrum with water suppression

55556 is a factor to convert the water intensity into µmol/g unit

0.8 is the assumed percentage of water in the tissue

This approach allowed for the identification of 58 spectral regions with measurable intensities in >80% of tissues for both long and short *T*. These regions were then defined as regions of interest (ROIs). Since each ROI may include the contributions of diverse metabolites and *vice versa*, metabolites' identity was considered only when majorly contributing and relevant.

Following HRMAS analyses, kidney tissues were stored in 10% formalin solution prior to paraffin embedding. This process was necessary for the preparation of slides for successive histopathological reading. Tissues were cut, and slides were incubated overnight at 65°C prior to treatment with standard haematoxylin and eosin staining: xylenes, 100% ethanol, 95% ethanol, H_2O, haematoxylin, H_2O, bluing reagent, H_2O, 95% ethanol, eosin, 95% ethanol, 100% ethanol, and xylenes. Permount was then applied to secure the coverslips and left to dry for 24 h.

Urine

Aliquots of 800 µL of thawed samples were transferred into 1.5 mL centrifuge microtube with 8 µL of sodium azide (10% w/w) to avoid potential bacterial growth. Samples were then centrifuged at 12000 rpm for 10 min at 4 °C. In order to stabilise the pH, 630 µL of supernatant were mixed with 70 µL of 1.5 M phosphate buffer solution (pH 7.4) containing trimethylsilyl propionate (TSP) for a final concentration of 1 mM. The mixture was vortex mixed and 650 µL were transferred into 5 mm wide NMR tubes.

^{1}H NMR experiments were performed at 300 K using a Varian UNITY INOVA 500 spectrometer (Agilent Technologies, CA, USA) operating at 499.839 MHz. One-dimensional (1D) ^{1}H NMR spectra were obtained using a standard pulse sequence (1D NOESY) with presaturation during relaxation and mixing time for water suppression. For each urine spectrum, a total of 128 scans were collected in 64k data points over a spectral width of 6000 Hz using a relaxation delay of 2 s, an acquisition time of 1.5 s, and a mixing of 0.1 s.

Following Fourier transformation with 0.3 Hz line broadening, spectra were phased, baseline were corrected, and the chemical shift scale was set by assigning a value of $\delta = 0.00$ ppm to the signal for the internal TSP standard. ^{1}H NMR spectra were processed by means of MestReNova (Version 8.1, Mestrelab Research SL, Santiago de Compostela, Spain) and misalignments were corrected manly for pH-dependent chemical shift changes. NMR spectra were considered from 0.5 to 9.5 ppm and subdivided into regions (bins) of 0.0025 ppm each. The spectral regions containing TSP (0.5 - −0.5 ppm) and water (4.6-5.2 ppm) resonances were excluded. Bins were then normalised to the sum of total spectrum to compensate for the overall concentration differences. The obtained data matrix was automatically reduced to ASCII files and converted into an excel file.

2.3 Statistical Analysis

2.3.1 Univariate Statistical Analysis

Univariate statistical analyses consisted in Student's t-test, Pearson correlation coefficient, Wilcoxon paired signed rank tests, and analysis of variance (ANOVA). Depending on the specific study, two-tailed, homoscedastic unpaired or paired Student's t-test was used. In the cases of non-normal distribution, such as for NMR ROIs, Wilcoxon paired signed rank test was applied instead. Mann-Whitney-Wilcoxon test was also applied for the chorioamnionitis study. Calculations were performed through Excel from OFFICE Windows, MetaboAnalyst 3.0 [35,36], or JMP 13, depending on the project. Results were considered significant only for $p<0.05$. Regarding the investigation on

intact kidney tissues, the notations *, **, ad *** were used for $p<0.05$, $p<0.005$, and $p<0.0008$, respectively.

2.3.2 Multivariate Statistical Analysis

Prior to statistical analysis, data matrices were subjected to normalisation by sum, log data transformation, and scaling by unit variance (UV)/auto-scaling method. Pareto scaling method was applied for the urine NMR data. HRMAS data were processed as described in the previous section. Multivariate analyses comprised unsupervised principal component analysis (PCA) and supervised partial least squares discriminant analysis (PLS-DA), orthogonal partial least square-discriminant analysis (OPLS-DA), and hierarchical cluster analysis (HCA). These calculations were performed by means of MetaboAnalyst 3.0 [35,36], JMP 13, or the soft independent modelling of class analogy (SIMCA) software (version 14.0, Umetrics, Umeå, Sweden) depending on the project.

PCA

PCA, an unsupervised pattern recognition method, was performed to examine the intrinsic variation in the data set [19]. Briefly, PCA reduce the number of variables, i.e. the metabolites in the samples, to a lower number of uncorrelated variables, the PCs, which are the result of combinations among of the initial measurements. Therefore, PCA allows for the underlining of the variance within the data set and the removal of redundancies. Notably, most of the descriptive information is contained in the first few PCs. Subsequently, each sample is assigned with a score for each PC and it can be plotted as a single point in a two-dimensional PCA scores plot. This help to visualise the clustering of samples based on metabolomic/phenotypical similarity. The metabolites responsible for such separation may then be reported into loading plots.

Partial Least Squares Regressions

Unlike PCA, which attempts to reveal the maximum variance between variables, partial least square regressions are supervised statistical means used to identify a direction that may explain such variance. During these projects, PLS-DA was the most exploited variant for such task. Furthermore, OPLS-DA approach was sometimes used in order to reduce the model complexity by removing the systematic variations in the X matrix that were not related to Y response, i.e. the structured noise, hence maximising the separation among samples [25]. To determine the optimal number of components necessary for the PLS-DA model, 10-fold cross validation (10-fold CV) or leave one out cross validation (LOOCV) methods were applied. Performance measures were the sum of squares errors divided by total sum of squares captured by the model (R^2), the cross-validated R^2

(Q^2), and the prediction accuracy (Accuracy). Permutation test was then applied to the models to investigate its predictive ability using the prediction accuracy test to set a permutation number (n=100 and $p< 0.01$). The discriminant metabolites were visualised as variable importance for the projection (VIP) plots [19,37].

2.3.3 Power Analysis, Metabolic Pathway Analysis, and MSEA

Power analysis tool from MetaboAnalyst was exploited to identify the necessary sample size to detect the observed metabolic perturbation with a certain probability (power) and false discovery rate (FDR) [19,36]. Metabolic Pathway Analysis or metabolite set enrichment analysis (MSEA) were used to highlight the metabolic pathways which resulted most affected by the phenotypical difference. In particular, Metabolic Pathway Analysis measures the pathway impact through the number of detected metabolites involved in a certain pathway, while -log(p) is an indication of the statistical correlation between a pathway and the case under study [36].

3. Amniotic Fluid

3.1 General Aspects of Amniotic Fluid

Amniotic fluid (AF) is a biological fluid in which foetal lung secretion, foetal urine, and the fluid from foetal swallowing and/or resorption through foetal membranes dynamically interact to change its volume and composition [38,39]. This dynamic system ismainly regulated by the placenta, which is not only a metabolic barrier, but it also constitutes a connection between mother and foetus circulations [40], hence influencing absorption and secretion capacity. Moreover, metabolites may be transported from foetal plasma through the permeable skin of the foetus [41]. Notably, also hormones play a significant role in metabolites' exchange. In human species, the volume of AF varies from 25 mL, at the 10th week of gestation, to 800 – 1000 mL at the end of gestation. During the initial part of the pregnancy, AF composition is similar to the interstitial fluid of the mother; however, at the 14th week foetal urine starts to be formed, having a predominant effect on the biofluid composition from the 20th week on. As previously mentioned, tracheobronchial and salivary glands secretions and buccal mucosa are other components of this system. Currently, several qualitative and quantitative aspects regarding AF composition are well known. The main component of AF (90%) is glucose, which is related to the mother's glycaemia [42]. In case of normal pregnancies, glucose concentration ranges from 30 to 35 mg/dL. Nevertheless, glucose level lowers to 20-25 mg/dL after the 26th week, due to Rhesus(Rh)-isoimmunisation. In the presence of diabetes, the beginning of the pregnancy is characterised by higher levels (circa 70 mg/dL), while values similar to normal pregnancies are observed after the 36th week. Electrolytes constitutes the second most influent portion of AF [42]. Indeed, several and diverse ionic species contribute to maintain an optimal osmolarity value of 275 mOsm/L, which prevent the occurrence of certain pathological conditions such as preeclampsia and gestational diabetes mellitus (GDM), which may lead to asphyxia. Usually, the overall protein content decreases throughout gestation [42]. Although the origin of the protein species present in AF is not always clearly understood, some compounds dynamics are satisfactorily described. Among them, α-fetoprotein (AFP) is used to predict foetal maturation because it is known to be produced by the foetus and delivered through urine since the 9th week of gestation. Successively, its level lowers from the 14th week to the end of the pregnancy. Furthermore, high concentrations of AFP are observed for neural tube damages and are therefore related to foetal suffering or malformations (especially anencephaly, meningocele, and spina bifida). AF lipid fraction has probably been the most studied for clinical practice. In the late stages of pregnancy, the presence of lipids increases, probably due to the development of the respiratory system [42]. Among the entire range of compounds belonging to this class, lecithins (phosphatidylcholine) are the most considered because of their anti-atelectasis activity in the lungs.

There are two different types of lecithins, dipalmitic (palmitic fatty acid in two positions), and palmitomyristic (palmitic and myristic fatty acids), which show different biosynthesis starting time and amounts during gestation. Therefore, their levels are an important index for foetus lung maturity and health. Other biologically active components present in AF are hormones, both as protein and steroid species, small amounts of bilirubin, creatinine, and orange cells [42]. In clinical practice, AF is routinely subjected to *in vivo* ultrasound to detect malformations. Moreover, it can be collected through amniocentesis, usually at second trimester, to assess pregnancy risks such as advanced maternal age and to reveal the presence of several chromosome defects, open-tube occurrences, cystic fibrosis, or to evaluate foetal lung maturity in case of preterm birth [41]. Since AF reflects mother's and foetus's health status at the same time [43], it has the potential to serve as an important diagnostic tool for a wider spectrum of clinical conditions. Indeed, although the collection of the biofluid through amniocentesis may be invasive and hazardous [44], aliquots of it may be taken from routine analysis. Previous metabolomic research on AF focuses on diverse pathologies such as preterm birth/labour, gestational age, GDM, foetal malformations, etc [4].

3.2 Diagnosis of Gestational Diabetes Mellitus

3.2.1 Gestational Diabetes Mellitus

GDM is a form of hyperglycaemia occurring during pregnancy that has not a fully described mechanism. Such pathology is increasing in pregnant women from most ethnic groups, although different rates depending on the different ethnicity are observed. In particular, while Caucasians seem to be less affected by this condition, Asians are characterised by the highest incidence rate [45]. Notably, also other variables such as obesity may influence the predisposition toward this pathology. The reason why GDM is of clinical relevance is its association with higher risks of adverse perinatal, pregnancy, and delivery outcomes. Indeed, for women which experienced GDM, type II diabetes incidence increases more than seven-fold within 5-10 years after pregnancy.

3.2.2 Aim of the Project

The aim of this particular project was to highlight alteration in AF composition in relation to the occurrence of GDM. Indeed, significant changes may deliver useful information for physiopathological purposes.

3.2.3 Population

A preliminary retrospective cohort study was conducted on 37 pregnant women (healthy subjects n = 29 and GDM patients n = 8). Gestational age of the enrolled patients was from 36th to 41st weeks

and median gestational age of 39 weeks. AF specimens were collected by means of amniocentesis at the 15th or 16th week of gestation at Department of Surgical Sciences, Dentistry, Gynecology and Pediatrics, Pediatric Division, University of Verona (Italy).

3.2.4 Results

Preliminary data were published in 2015 [21] and further investigated by implementing the data set. Although a few discriminant metabolites changed, the models were similar. Following PCA for a more homogenous set of samples, t-test highlighted significant alterations in nonanoic acid, asparagine, and pyroglutamic acid levels ($p < 0.002$). Moreover, PLS-DA showed accuracy = 0.72973, $R^2 = 0.47977$, $Q^2 = 0.2105$, calculated by LOOVC. Therefore, although the accuracy of the prediction seems satisfactory, fitting is not statistically significant probably due to small sample size. According to this model, the majority of the compounds seems to increase in GDM cases; nonanoic acid, asparagine, pyroglutamic acid, monostearin, stearic acid, 1,2-propandiol, monopalmitin, arabinofuranose, 2-aminoheptadioic acid, and 5 unknown/non-identified endogenous compounds seem to follow this trend, while ethanolamine decreased in pathological cases. Further metabolic pathway analysis and enrichment analysis highlighted the contribution of phenylalanine metabolism and fatty acid biosynthesis pathways for the clusterisation of the two phenotypes. Power analysis calculated a FDR of 0.1 and a predicted power of 0.65 for a 200 samples model, 0.82 for 400 samples, and 0.91 for 600 samples.

3.2.5 Discussion

Notably, only univariate analysis produced statistically significant values. Nevertheless, these findings are of difficult interpretation. For this reason, together with the low multivariate model's fitting performance, there is a clear necessity to expand the sample size for the confirmation of such data.

3.3 Foetus' Sex Recognition

3.3.1 Importance of Foetus' Sex in Pregnancy

Knowledge of the sex of the future child is not commonly an issue unless relevant for treatment planning related to sex-linked genetic diseases [46]. Sexual morphogenesis starts around the 6th week of gestation and it seems to be triggered by hormone secretion. Interestingly, sex dependent differences were observed regarding placental size [47], trophoblast epithelium, and villous vessel endothelium [48]. Although such phenomena are not fully understood yet, different biological behaviours in such an early life stage are interesting and may be informative of different biological

needs. For this reason, the detection of divergent sex-depending metabolic profiles may add interesting insight in the understanding of human development. Currently, foetus' sex is mainly assessed through ultrasonography techniques [46] that are reliable from 13th week of gestation [49–52]. These methods are based on the observation of penis and scrotum/*labia majora* and *minora* or the evaluation of the anogenital distance. In particular, the latter is greater in male foetuses and it depends on testosterone production [53,54]. Moreover, experimental evidence suggests acceptable reliability prior to the 13th week. Nevertheless, although rarely, these approaches may lead to incorrect determinations. The most accurate method for sex assessment is through genetic test following amniocentesis, chorionic villus sampling, and cell-free foetal DNA in maternal blood. Nevertheless, given the risks associated with the former practice and the expenses relative to the latter, [55] these are not routinely performed if not on particular conditions.

3.3.2 Aim of the Project

The objective of this work was to characterise the different AF metabolic profile arising from the difference in the foetuses' sex. Although a sex recognition test would not majorly improve clinical practice, the information related to the changes in biology may be interesting for physiology studies.

3.3.3 Population

A total of 85 samples (41 mothers bearing male foetuses and 44 with female foetuses) were analysed. Gestational age of the preliminary retrospective cohort study subjects enrolled in this project ranged from 36th to 41st weeks (median = 39 weeks). AF was collected through amniocentesis (15th or 16th week of gestation) at Department of Surgical Sciences, Dentistry, Gynecology and Pediatrics, Pediatric Division, University of Verona (Italy).

3.3.4 Results and Discussion

PCA was applied to the entire set of samples to obtain the final matrix without outliers. Although the decent sample size for these analyses, t-test highlighted no significant difference in the two groups. Moreover, PLS-DA produced an unsatisfactory model (accuracy = 0.43529, R^2 = 0.18916, Q^2 = -0.2713 calculated by LOOVC) and power analysis with FDR of 0.1 could not deliver a predicted power even for a 1000 samples. Therefore, experimental evidence showed no statistically significant alteration in the metabolic profile of healthy female and healthy male foetuses. This suggest that, although other physiological differences may be present, excretion and metabolisation are independent on the sex of the yet unborn child. Therefore, differentiation in this context may begin in successive developmental stages and it may be interesting to identify such moment through further studies.

3.4 Meconium Stained AF and Delivery Dynamics

3.4.1 Meconium Stained AF

The term meconium refers to the earlies faeces of an infant, which are exclusively produced due to the various substances ingested by the foetus during the pregnancy, i.e. mainly AF and uterus epithelium cells. Meconium is usually released by the newborns after birth; however, this phenomenon may also occur during labour or delivery, staining the AF. At delivery, AF may be hence classified as clear or, in the presence of meconium, into grades depending on colour, shade, and visual consistency of the biofluid. Nevertheless, these grades are not indicative of a certain outcome. From a clinical perspective, meconium stained AF may be a sign of foetal distress, hence not optimal health status of the baby. The most common adverse events are the presence of meconium in foetal lungs, causing meconium aspiration syndrome and asphyxia, or the thickening of meconium, which may congest foetal intestines (meconium ileus). In the clinical experience of our medical collaborators, meconium stained AF is observed in faster deliveries. Although an adverse environment for foetus' health may be hypothesised, the causes triggering this event are not fully understood.

3.4.2 Aim of the Project

The aim of this work was to describe the changes in AF composition in the presence of meconium, and among the different grades of staining. In addition to a physiological description, these data may be linked to the dynamics causing faster deliveries and, consequently, putting the basis for future clinical applications.

3.4.3 Population

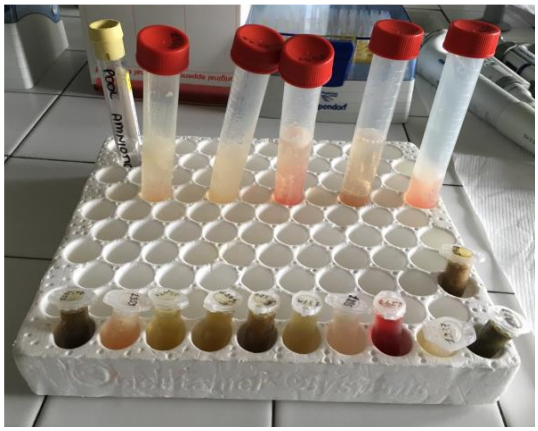

Fig. 3.4.1: *Samples of stained AF displaying a number of different colours and shades*

Within this project, 53 AF specimens were collected at the Unit of Obstetrics and Gynaecology of the University-Hospital of Cagliari. In details, 32 samples were clear AF, while the remaining were characterised by the presence of meconium (stained 1 n = 5, stained 2 n = 8, and stained 3 n = 8) (Table 3.4.1). Gestational age of the subjects varied from 37 to 41 weeks and maternal age between 20 and 30 years old. Sampling was performed during delivery by means of a cannula positioned behind the neck of the newborn.

Total Enrolled Subjects (n = 53)			
Clear AF (n = 32)	Stained AF (n = 21)		
	Stained 1 (n = 5)	Stained 2 (n = 8)	Stained 3 (n = 8)

Table 3.4.1*: Summary of the groups and phenotypes in which the total 68 enrolled subject were divided into.*

3.4.4 Results

Four Classes Analysis

ANOVA calculations conducted on the four phenotypes (clear and the three stained) under study highlighted 13 compounds that could differentiate among the different pairs of classes (Table 3.4.2). Notably no discriminant metabolite was found for "stained 2 vs. stained 3" groups and most of the metabolites were statistically different between clear and stained 2 or stained 3 samples.

Metabolite	**Clear *vs.* Stained 1**	**Clear *vs.* Stained 2**	**Clear *vs.* Stained 3**	**Stained 1 *vs.* Stained 2**	**Stained 1 *vs.* Stained 3**
N-acetylglucosamine		*	*	*	*
galacturonic acid		*	*	*	*
N-acetylneuraminic acid		*	*		*
allantoin	*	*	*		
fucose		*	*	*	*
tryptophan		*	*		
maltose		*	*		
threonic acid		*	*		
glucaric acid		*	*		*
quinic acid	*	*	*		

Table 3.4.2: *Identified compound which were found statistically different by means of ANOVA*

Although statistical parameters were not optimal (accuracy = 0.59615, R^2 = 0.65964, Q^2 = 0.46625, by LOOCV), 2 components PLS-DA model confirmed the significance of *N*-acetylglucosamine, galacturonic acid, *N*-acetylneuraminic acid, allantoin, fucose, tryptophan, maltose, threonic, glucaric, and quinic acid, and three other unknown compounds (Fig. 3.4.2). However, power analysis for such model delivered a FDR of 0.6 for 600 samples per group.

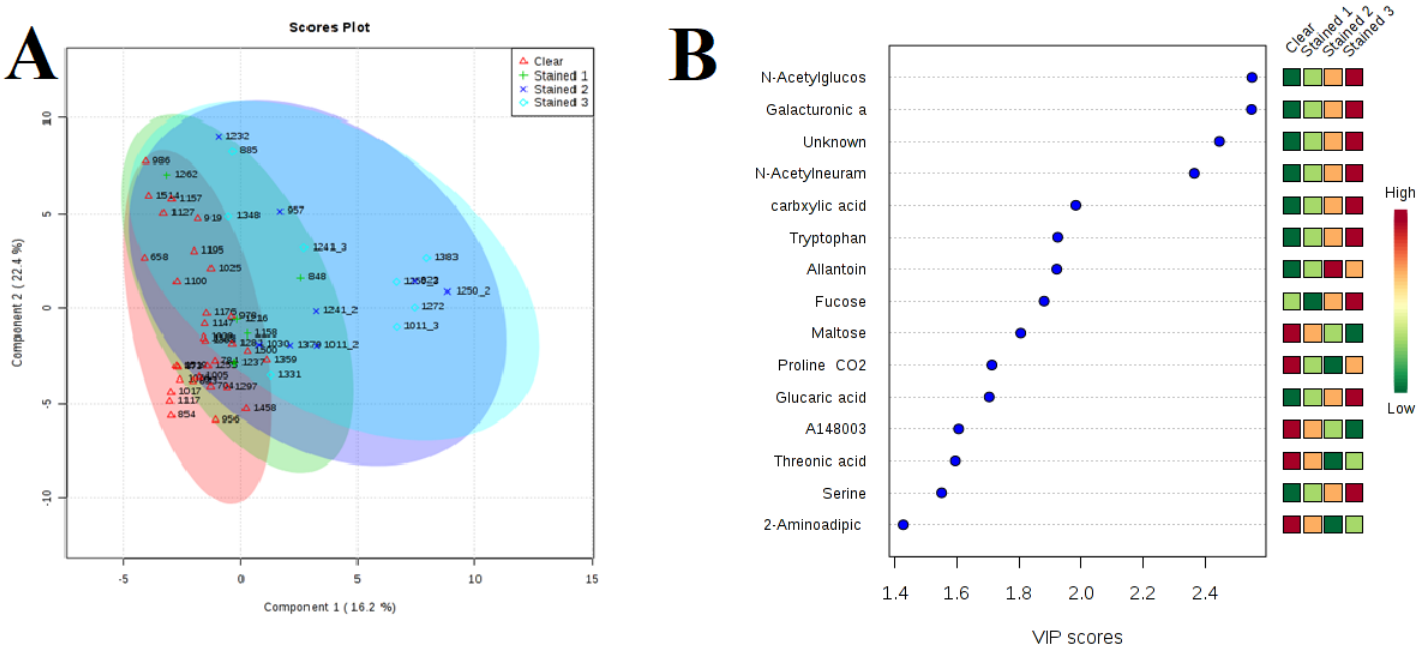

Fig. 3.4.2: *PLS-DA results showing A) 2D score plot and B) VIP features and trend for the four classes under study*

Clear vs. Stained

Grouping the stained samples together, PCA excluded two entries. Similarly to the previous analysis, Student's t-test and PLS-DA (accuracy = 0.76667, R^2 = 0.64086, Q^2 = 0.35245 by LOOCV) revealed alteration in *N*-acetylglucosamine, galacturonic acid, allantoin, *N*-acetylneuraminic acid, tryptophan, threonic acid, quinic acid, maltose, fucose, glucaric acid and four unknown compounds. In addition, 2-aminoadipic acid was highlighted as a significant feature (Fig. 3.4.3). Power analysis showed a FDR of 0.6 for 200 samples per group. Therefore, the trend exposed by the calculations on the four phenotypes seem to be confirmed.

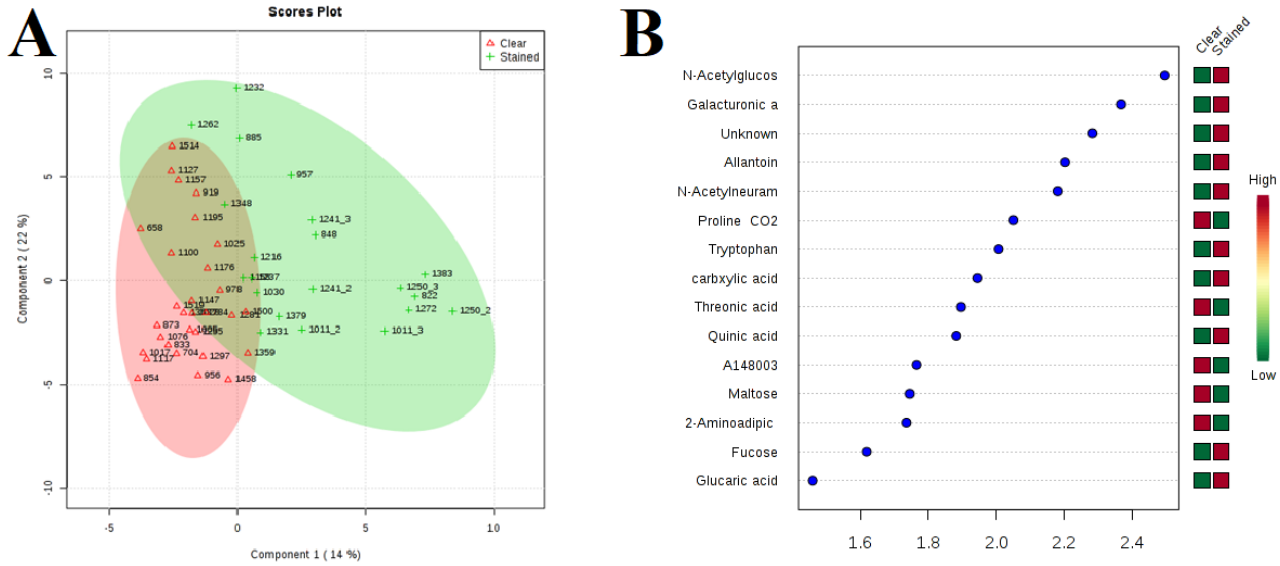

Fig. 3.4.3: *PLS-DA results showing A) 2D score plot and B) VIP features and trend for the clusterisation between clear and stained AF samples*

Stained Analysis

Considering solely the difference among the three grades of stained AF, neither ANOVA, nor PLS-DA could highlight relevant differences.

3.4.5 Discussion

Results indicate that separation among the four different phenotypes is mainly due to the changes characterising all the stained specimens considered in one single group. Indeed, not only alterations among the three grades of stained AF were not significant, but also similar changes between the four-classes and the clear *vs.* meconium stained AF analyses were observed. In particular, *N*-acetylglucosamine, *N*-acetylneuraminic acid, and fucose were expected in higher levels within the meconium stained samples because of their role in the composition of amniotic mucins [56,57]. Such complex structures are constituted by several carbohydrate and carbohydrate-derivative moieties and are also related to meconium glycoproteins. Furthermore, *N*-acetylglucosamine and glucuronic acid form hyaluronic acid, a glycosaminoglycan that exerts modulating action on inflammatory processes [58]. Hyaluronic acid may either promote or inhibit inflammation through diverse mechanisms. Among the inhibiting mechanisms, oxidation by reacting with reactive oxygen species (ROS) lead to production of glucaric acid [59]. Therefore, increase in these metabolites may be a sign of oxidative stress. Interestingly, also the higher levels of allantoin (Fig. 3.4.4) in stained specimens, may be caused by oxidation of uric acid by means of ROS [60,61]. Although both hyaluronic acid and allantoin prevents additional tissue damage and prompt would healing through different dynamics [58,60], these phenomena may not be of interest in this particular case. Further relation to oxidative stress is the decrease in threonic acid, a product of ascorbic acid breakdown [62]. Indeed, such behaviour was observed in diabetic animal model. The only metabolites against this hypothesis is 2-aminoadipic acid which should increase in the presence of ROS [63]. Consequently, the apparently faster delivery may be attributed to a harmful environment for the foetus. Regarding the increase in quinic acid and tryptophan, a 2009 study [64] reported accumulation of the former compound in the gastrointestinal tract of adult subjects after several weeks administration. Part of quinic acid was then transformed in tryptophan by the intestinal flora and gradually released in the successive months. For this reason, meconium presence in the amniotic fluid may contribute to metabolic alteration due to the previous accumulation of the two species inside the foetus. Nevertheless, although meconium seems not to be sterile [65], it is not known if foetal microbiota is capable of such transformations.

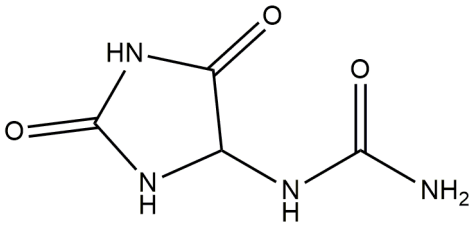

Fig. 3.4.4: *Allantoin*

3.5 Primary HCMV Infection In Pregnancy

3.5.1 Human Cytomegalovirus

Human cytomegalovirus (HCMV) is the most common viral infection in developing foetuses. Vertical transmission, i.e. from the mother to her child, may follow either primary or non-primary HCMV maternal infection. Interestingly, although transmission rate from a woman with serological evidence of immunity to her child is estimated to be around 1–2%, primary maternal infection shows higher risks of 30–35% throughout the gestation [66–71]. The presence of symptoms at birth seems to be mainly influenced by gestational age at the time of maternal primary infection. In details, 33.3% of symptomatic congenital infections are periconceptional, 25.5% occur during the 1st trimester, 14.3% during the 2nd, and only 8% during the last one [72]. Moreover, primary infections before or in early pregnancy differently affect foetal risks incidence and clinical outcome at birth [73]. For instance, long-term neurological sequelae such as abnormal hearing and neurodevelopmental impairment are observed in 35–45% of symptomatic births [74], while significantly lower rates have been reported for asymptomatic ones [75,76]. Although blood and urinary viral loads in congenitally infected newborns could be associated with symptomatic births and long-term sequelae [77,78], the accurate detection of HCMV transmission and subsequent effects on the foetus is still a challenging task. Currently, HCMV foetal infection is diagnosed by amniocentesis. However, only an AF DNA level of N105 copies/mL may be considered as predictive for symptomatic congenital infection [79]. Nevertheless, similar high viral loads have been reported in either symptomatic or asymptomatic cases [80–83] and only very low levels (b103 copies/mL) consistently accounts for asymptomatic congenital infection at birth [84]. In fact, although polymerase chain reaction (PCR) sensitivity ranges between 70–90%, and it can reach 100% with right timing [85–87], it is 100% accurate only when positive. When negative, there is 8% of chance that foetal infection actually occurred. Such a discrepancy can be explained by a delayed transmission of HCMV to the foetus [88,89]. Furthermore, other variables such as time of HCMV intrauterine transmission and time of prenatal diagnosis may negatively affect this test [72]. Therefore, in order to deliver proper counselling on foetal risk and prognosis at birth, it is necessary to confirm or dismiss and to determine the onset of a primary HCMV infection. Indeed, for this reason, parental counselling aims at predict, if possible, which infected foetuses may develop symptoms at birth or later in life. To our knowledge, only one previous paper investigated the effects of HCMV in congenitally infected newborns. This NMR-based study analysed urine samples collected within the first two weeks of life and could identify discriminant metabolites to recognise infected from uninfected newborns [90–92].

3.5.2 Aim of the Project

The aim of this investigation was to elucidate the changes in metabolic pathways due to congenital HCMV infection in mothers and foetuses and to identify new potential diagnostic and/or prognostic biomarkers. This project seems to be the first metabolomic investigation on AF in HCMV infected foetuses/mothers in relation to foetal health. [4]

3.5.3 Population

A retrospective cohort study was conducted on 63 pregnant subjects; 20 contracted primary HCMV infection during pregnancy and, subsequently, transmitted the virus to the foetus (transmitters); 20 contracted the infection without transmitting the virus to the foetus (non-transmitters) (Table 3.5.1). Twenty-three healthy subjects, who underwent amniocentesis for cytogenetic-based diagnosis, were enrolled as controls. Median age of mothers was 34 and 37 years for infected (transmitters and non-transmitters) and for controls, respectively. Among the 20 infected foetuses, 9 were symptomatic congenital infections (SCI). In details, 2 showed pathological findings through ultrasound investigation and, for this reason, pregnancies were interrupted by caesarean section; 4 babies showed hearing impairment and motor deficit (n = 1), hearing impairment alone (n= 2) or IUGR (n= 1); 3 foetuses were found with DNAemia, high levels of virus-specific IgM antibodies and β2-microglobulin, and low platelets count. Since these latter features are prognostic markers of symptomatic congenital infection, [84] pregnancies were interrupted. The remaining 11 infected foetuses resulted asymptomatic (ACI): 10 were diagnosed at birth and 1 after voluntary interruption of pregnancy and autoptic examination.

<table>
<tr><th colspan="3">Total Enrolled Subjects (n = 63)</th></tr>
<tr><td colspan="2">Primary HCMV Positive (n = 40)</td><td rowspan="3">Controls (n = 23)</td></tr>
<tr><td colspan="2">Transmitters (n = 20)</td><td rowspan="2">Non-transmitters
(n = 20)</td></tr>
<tr><td>SCI
(n = 9)</td><td>ACI
(n = 11)</td></tr>
</table>

Table 3.5.1: *Summary of the groups and phenotypes in which the total 63 enrolled subject were divided into.*

Median viral load in AF (HCMV DNA) was lower in asymptomatic foetuses (9.8 × 105 copies/mL) when compared with symptomatic ones (2.3 × 106 copies/mL) (p=0.10). All the AF samples were obtained by amniocentesis performed at the Departments of Obstetrics and Gynecology, Fondazione Istituto di Ricovero e Cura a Carattere Scientifico (IRCCS) Policlinico San Matteo, Pavia, Italy. The 40 HCMV infected subjects underwent amniocentesis at a median gestational age of 21 weeks (range 19–25), while the 23 controls, at 16 weeks of gestation. Estimated median

gestational age of maternal infection was 6 weeks (range 2–14). Results of prenatal diagnosis were confirmed in newborns at birth by testing their urine or by collecting autoptic samples obtained after delivery. After routine serological tests for the most common viruses, the remaining volume of AF samples was aliquoted and stored at −80 °C until metabolomics analysis.

3.5.4 HCMV Diagnosis

Diagnosis of maternal primary HCMV infection was based on the presence of at least two of the following criteria: [90–92]

a) HCMV-specific IgG seroconversion (with an interval of 1–2 months between the last seronegative and the first seropositive result)
b) virus-specific IgM antibodies and low IgG avidity index (AI)
c) HCMV DNA in maternal blood

In the majority of the enrolled subjects, timing of maternal infection was determined by **a)** (13/40, 32.5%), **b)** (27/40, 67.5%), the *de novo* appearance of neutralizing antibodies in human embryonic fibroblasts (21/40, 52.5%), and the observation of clinical signs and symptoms. In the case of non-reported symptoms, IgG, IgM, and AI kinetics were analysed over time for identification of maternal infection onset. HCMV transmission to the foetus was diagnosed by viral DNA detection and quantitation in AF.

3.5.5 Results

Controls vs. Transmitters

Although not ideal, PLS-DA showed a statistically significant separation between controls and transmitters, as reported in Fig. 3.5.1A (accuracy= 0.88, R^2 = 0.75, Q^2 = 0.58 with 10-fold CV, performance measure $p<0.01$). Among the 58 detected metabolites, those responsible for discriminating HCMV infected subjects were higher glutamine, glycine, serine, pyruvic acid, threonine, threonic acid, and cysteine levels, and lower unknown U1715 and U1804, glutamic acid, U1437, fructose, sugar-like A203003 and A203005, and tyrosine. Moreover, metabolic pathways analysis allowed for the recognition of the metabolisms that were most altered by the transmission of HCMV (Fig. 3.5.1B). Glutamine and glutamate, pyrimidine, purine, alanine-aspartate-glutamate, arginine and proline, cystine and methionine, and glycine-serine-threonine metabolisms resulted the most influenced pathways.

Controls vs. Non-Transmitters

Applying PLS-DA statistical approach, a significant separation was observed between controls and non-transmitters mothers (Fig. 3.5.2A; accuracy = 0.88, R^2 = 0.78, Q^2 = 0.54 with 10-fold CV, performance measure $p<0.01$). In non-transmitters, glutamine; serine; glycine; threonic acid; threonine; 1-monostearin; urea; and cystine were found increased, while sorbitol; unknown U1804; sugarlike A203003; U1751; xylitol; leucine; and fructose decreased. Interestingly, similar trends were observed for glutamine, glycine, serine, threonic acid, cystine, threonine, fructose, sugar-like compound A203003, and unknowns U1751 and U1804 in both controls *vs.* transmitters and controls *vs.* non-transmitters models. Such finding suggests the presence of a perturbation caused by the maternal viral load rather than by the viral transmission to the foetus. Furthermore, metabolic pathways analysis highlighted glutamine and glutamate, pyrimidine, purine, alanine aspartate-glutamate, arginine and proline, primary bile acids biosynthesis, cysteine and methionine, and glycine-serine-threonine metabolisms as the most affected (Fig. 3.5.2B).

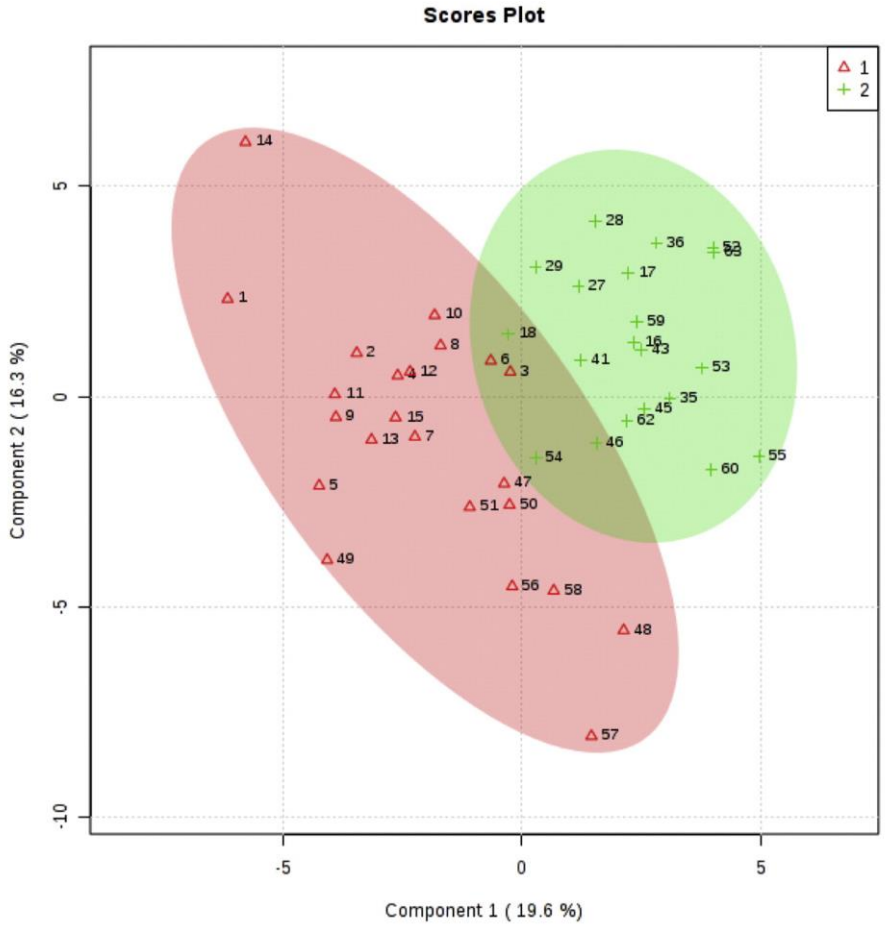

A

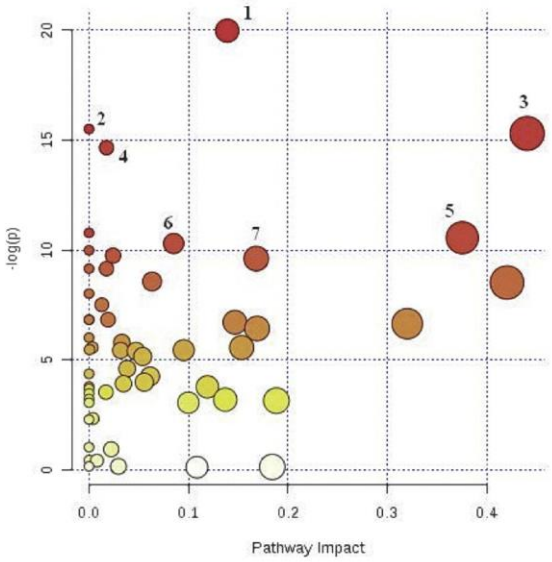

B

No.	Metabolic Pathway/Metabolism
1.	Glutamine and glutamate
2.	Pyrimidine
3.	Alanine, aspartate and glutamate
4.	Purine
5.	Arginine and proline
6.	Butanoate
7.	Cysteine and methionine

C

Fig. 3.5.1: *Comparison between controls and transmitters. A=2D scores plot showing PLS-DA discrimination for controls (1) vs. transmitters (2) groups. B=metabolic hubs mainly affected by HCMV presence and transmission: controls vs. transmitters. C = corresponding list of metabolic hubs mainly affected by HCMV presence and transmission*

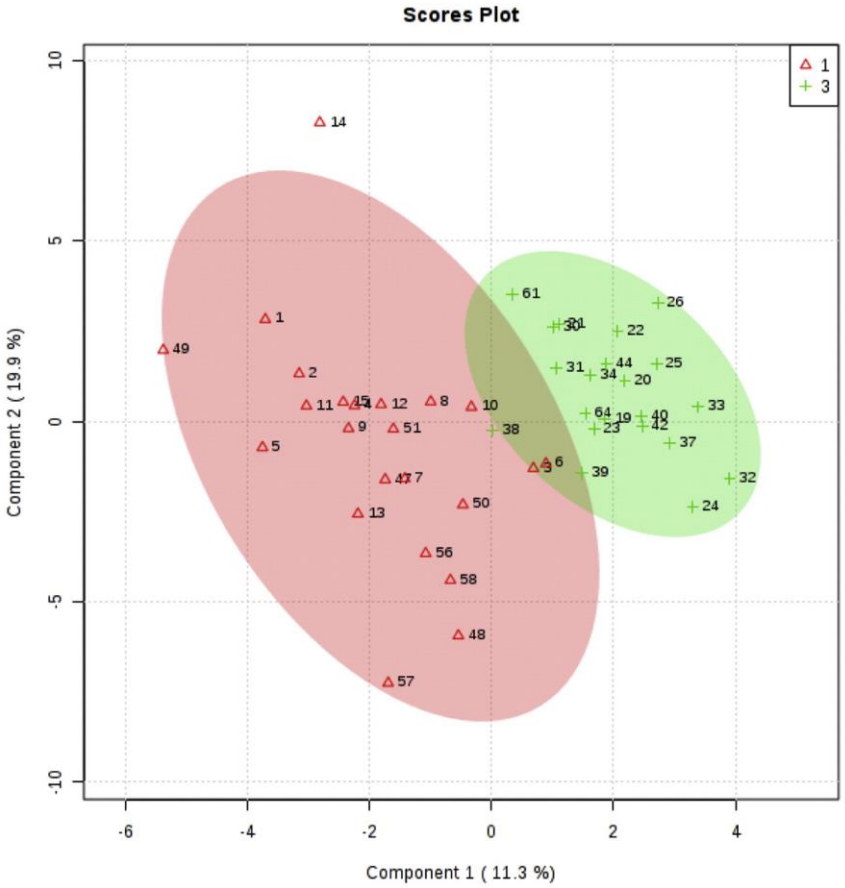

A

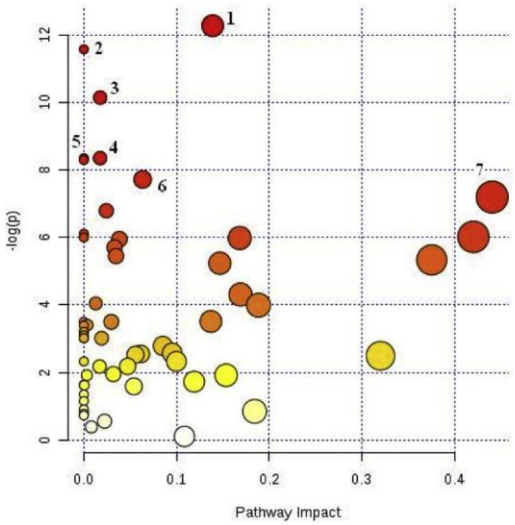

B

No.	Metabolic Pathway/Metabolism
1.	Glutamine and glutamate
2.	Pyrimidine
3.	Alanine, aspartate and glutamate
4.	Purine
5.	Arginine and proline
6.	Butanoate
7.	Cysteine and methionine

C

Fig. 3.5.2: *Comparison between controls and non-transmitters. A=2D scores plot showing PLS-DA discrimination for controls (1) vs. non-transmitters (3) groups. B=metabolic hubs mainly affected by HCMV presence: controls vs. non-transmitters. C = corresponding list of metabolic hubs mainly affected by HCMV presence*

Transmitters vs. Non-Transmitters

No statistically significant separation between the two phenotypes was achieved through PLS-DA (accuracy = 0.44, R2 = 0.46, Q2= −0.14 with 10-fold CV, performance measure p = 0.37). The reasons behind this result may be the samples noise masking the metabolic differences between the groups or the limited samples size. Indeed, applying power analysis on transmitters *vs.* non-transmitters matrix, a robust separation with a predictive power of 0.83 should be obtained by increasing the sample size to 200 for each group.

Transmitters Outcome: Asymptomatic vs. Symptomatic

PLS-DA calculations were then performed on transmitters AF specimens to observe potential metabolome alteration between infected foetuses showing ACI or SCI. Unfortunately, the separation was not statistically significant.

3.5.6 Discussion

HCMV Infected vs. Controls

Interestingly, results emerging from the comparison between 'controls *vs.* transmitters', and 'controls *vs.* non-transmitters' showed some similarities. Indeed, increase in glutamine, glycine, serine, threonine, threonic acid, and cystine levels were revealed in transmitters and non-transmitters. Conversely, fructose, sugar-like compound A203003, and unknowns U1751 and U1804 decreased in HCMV infected subjects. Furthermore, both comparisons highlighted the glutamine-glutamate metabolism as the most involved pathway in the separation. The role of glutamine in HCMV metabolism and development was described in infected fibroblasts by Munger and Chambers [93–96]. Regarding the higher levels of serine found in infected specimens, it may be a consequence of phosphatidylserines breakdown. This compound is indeed observed as threefold lower content in virion membranes [97]. The enhancement of pyrimidine biosynthesis may be explained by HCMV infection promotion of nucleotides production for viral RNA and DNA synthesis (Scheme 3.5.1) [93].

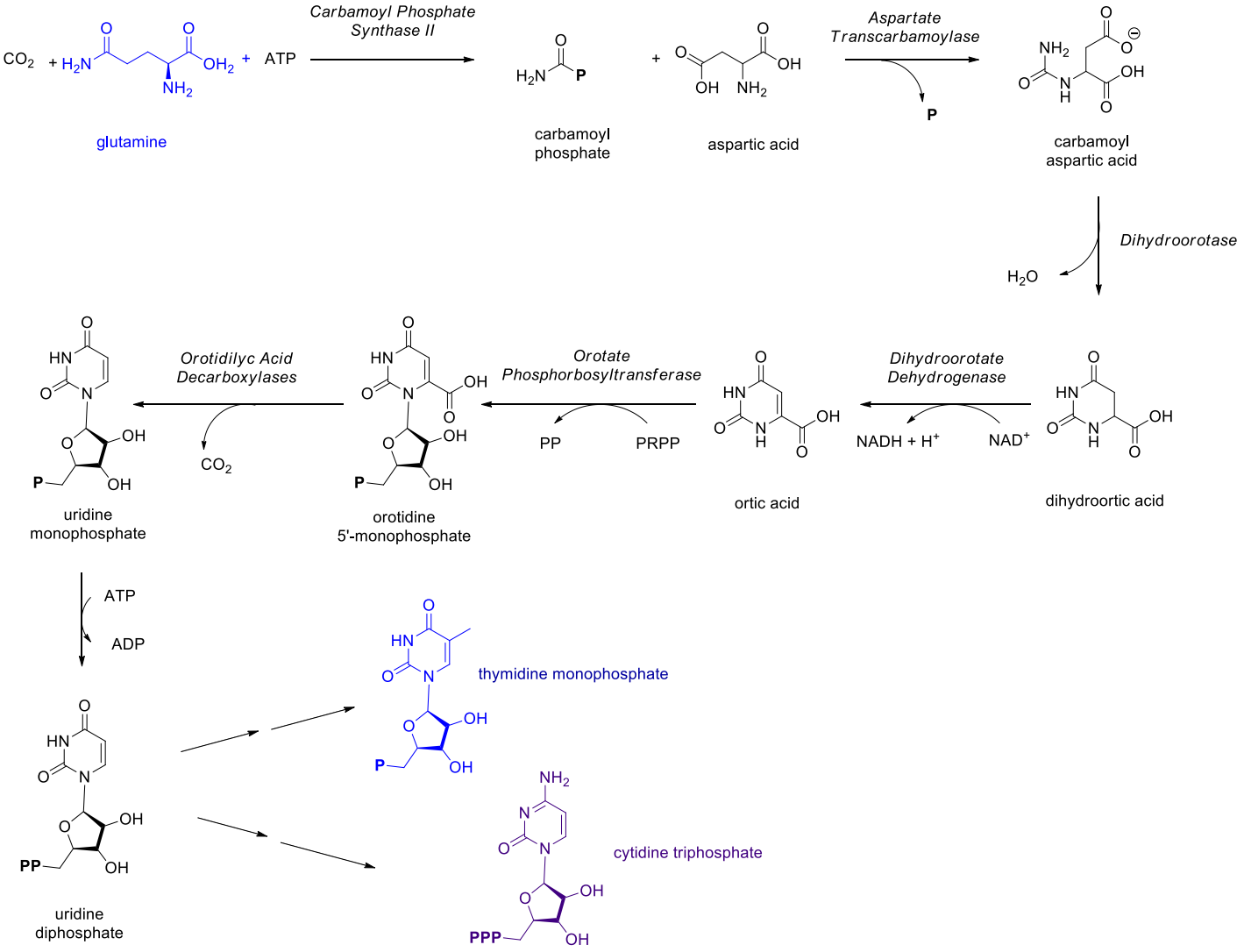

Scheme 3.5.1: *Pyrimidine Biosynthesis Pathway.* ***P*** *= phosphate*

Therefore, high similarity in the comparisons between controls and each of the two groups of infected subjects (transmitters and non-transmitters) was observed. These findings suggested a stronger influence of the maternal primary infection than that of the transmission to the foetus. Accordingly, the influence of the foetal infection on AF could be hidden by the mother's metabolic changes induced by the virus. Supporting this argument, HCMV DNA-positive placentas were observed in both infected and uninfected newborns [98]. Consequently, placenta may play a role in the defence against HCMV transmission.

Transmitters vs. Non-Transmitters

Overall, the predominant metabolic effects of maternal HCMV transmission should be highlighted through the comparison between transmitters and non-transmitters. However, PLS-DA model did not reach statistical significance, probably due to small sample size. Nevertheless, data showed

alteration of fatty acids pathways, i.e. decrease in palmitic and stearic acids with their monoglyceride derivatives (1-monopalmitin, 1-monostearin, and 2-monopalmitin) within transmitters group (Appendix Fig. A1). In case of confirmation by further studies, it may be accounted for higher demand of lipids for the membrane of this envelop virus [94–96].

Transmitters Outcome: Asymptomatic vs. Symptomatic

Similarly to the previous comparison, although PLS-DA delivered no significant results, data showed perturbation in biotin, lysine, and in β-alanine pathway (Appendix Fig. A2), hence alteration of fatty acid biosynthesis. Indeed, biotin is the coenzyme of carboxylase enzymes and it may also derive from proteolytic degradation of biocytin (biotinyl-L-lysine) or biotinyl-peptides. Regarding β-alanine, it converts to 3-oxopropanoate, and it turn to malonyl-CoA or acetyl-CoA (Fig. 3.5.3), which are key intermediates of fatty acids biosynthesis. If confirmed, these findings may be reasonable for the above mentioned arguments.

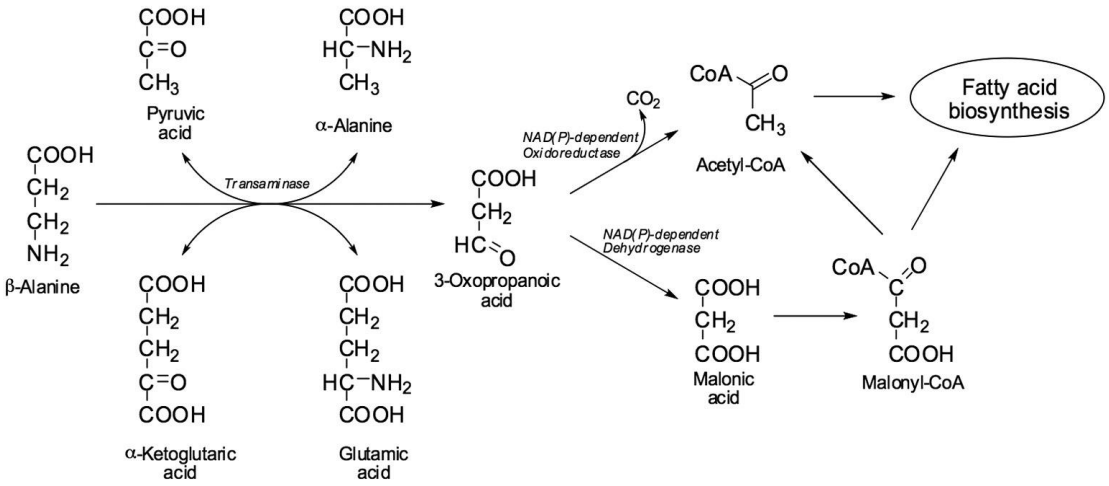

Fig. 3.5.3: *Scheme summarising the β-alanine transformations to key fatty acid biosynthesis intermediates.*

Overall Comments

AF is considered a foetal biofluid, hence the presence of HCMV in it is commonly considered diagnostic for foetal infection, while its absence accounts for the exclusion of HCMV intrauterine transmission. Nevertheless, metabolomic strategy could highlight significant changes only when comparing HCMV-infected *vs.* controls subjects, but not to reliably investigate transmission or symptomatic birth phenomena. Therefore, it is most interesting that the maternal - and maybe placental – health played a pivotal role in the metabolic characteristic of AF, i.e. the conception of this biofluid as solely dependent on the foetus might be questioned.

3.6 Conclusions on Amniotic Fluid

In the majority of these pilot studies, GC-MS analyses of AF proved to be an efficient strategy to deliver useful information regarding pregnancy- and delivery-related pathologies. The absence of relevant results in the characterisation of GDM may be attributed to the exiguous sample size, needing future recruiting and investigations [21]. Conversely, the non-observation of significant changes for sex recognition, may be a sign of differentiation in physiological excretion and metabolisation between sexes after the considered gestational age. Moreover, important alterations between meconium stained and clear AF samples were observed. Indeed, metabolites characterising mucins, response to oxidative stress, and maybe foetal gastrointestinal tract, were highlighted through metabolomic approach. Nevertheless, the most interesting data were relative to the primary HCMV infection during pregnancy [17,18,20]. This preliminary study questioned the role of the foetus as the solely responsible of AF metabolic profile, implying the additional and significant influence of the mother and maybe the placenta. Furthermore, the importance of glutamine and serine as potential biomarkers was underlined. Therefore, while larger samples size should be used to confirm data, these metabolomics-based findings are an interesting promise for the future discovery of AF biomarkers and phenotypical investigations.

Kidney

4.1 Preliminary Study for RCC Tumour Diagnosis

4.1.1 Renal Cell Carcinoma

Renal cell carcinoma (RCC), also known as hypernephroma, renal adenocarcinoma or Grawitz tumour, is a clinical occurrence that develops from the lining of the proximal convoluted tubule. It contributes to 70-80% of all solid kidney tumours and to 80-90% of kidney cancers. Its incidence is higher in Europe and North America, accounting for 89,000 and 62,000 new cases in 2016, and it is the 8th most common type of cancer in the western world [99–101] and the 3rd among US genitourinary malignancies (over 61,000 new cancer diagnoses and 14,000 deaths per year) [102]. From a histopathological point of view, the main subtypes of RCC are clear cell (75%–85% of RCC cases), papillary (10%–15%), and chromophobe (4%–5%). Interestingly, histopathological examination is usually able to distinguish the different types of tumour; nevertheless, some cases may be of difficult visual interpretation. Therefore, novel assessment, based on metabolic fingerprint, may be of help. These malignancies are usually diagnosed around the 65 years of age [100] and, although their aetiology seems to not be clearly described, obesity, smoking, and hypertension contribute to their incidence. To a lesser extent familiality and comorbidity with von Hippel-Lindau and Birt-Hogg-Dubé syndromes may play a role in the development of some types of RCC [99,100,103]. Currently, primary tumour/regional nodal involvement/distal metastasis (TNM) stage at the time of diagnosis is a reliable prognostic tool [99,103,104], while the Fuhrman nuclear grading system, which additionally considers nuclear and nucleolar morphology, is less informative [101]. Surgery is the common treatment for early stage RCC; however, alternative, less-invasive approaches have been investigated, such as image-guided radiofrequency, microwave, and cryo-ablation percutaneous ablation [2,101].

4.1.2 Aim of the Project

The project focused on the description of RCC metabolic patterns in order to discover novel biomarkers for early diagnosis or physiopathological characterisation. This may facilitate translation to *in vivo* platforms, such as magnetic resonance spectroscopy imaging (MRSI), which means improving clinical practice through less invasive and more accurate procedures. Furthermore, differences in spectroscopic intensities between the analysis of frozen and fresh samples were investigated to further understand the implications of and to validate the use of tissue biobanks. This study was performed at the Athinoula A. Martinos Center for Biomedical Imaging (Charlestown, MA), during an exchange period abroad within the collaboration with the

Departments of Pathology, Radiology, and Urology of Massachusetts General Hospital, Harvard Medical School, Boston, MA, (USA)

4.1.3 Population

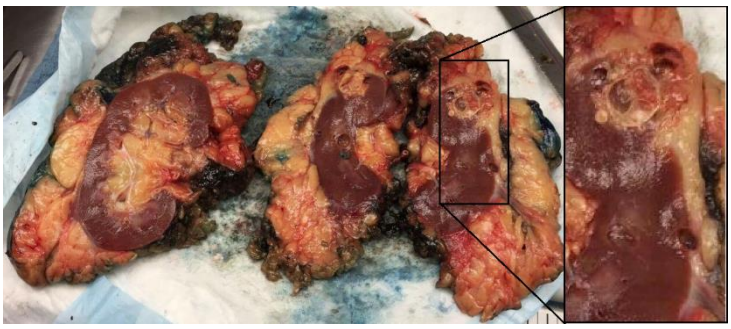

Fig. 4.1.1: *Kidney removed by nephrectomy; inset shows RCC portion*

Human RCC

Frozen biopsy samples were collected from 76 subjects (median age=56, from 37 to 83 years old). Among these patients, 33 were female and 56 were male, while ethnicity composition was homogeneous beside 2 persons. Samples were first divided into two groups, tumorous (n=57) and adjacent benign tissues (Ad, n=19), Tumorous cases were further divided according to histological nature. In particular, 5 types of tumours were included in this study: benign tumour angiomyolipoma (AML, n=7), chromophobe (Chr, n=12), clear cell (CC, n=17), benign oncocytoma (Onc, n=10), and Papillary (Pap, n=11).

Fresh-Frozen

Thirteen fresh-frozen sample pairs from 7 subjects were selected for the validation of the employment of biobanks. Fresh specimens were kept on ice from the operation room and then analysed within 1 h following excision. Paired frozen samples were stored at -80 °C for at least 24 h prior to analysis.

4.1.4 Results

Alteration between Ad and Tumour Tissues

In comparing spectra from cancer tissues and from Ad ones, 29 spectral regions were significantly different. Such regions are shown in Table 4.1.1. Notably, beside the region from 3.13 to 3.15 ppm, which characterises spermine presence, all spectral intensities were decreased in the adjacent benign cases. Other metabolites associated with these spectral regions were *myo*-inositol (3.42-3.23 ppm), taurine (3.45-3.43 and 3.24-3.23 ppm), alanine (3.80-3.78 ppm), glutathione (GSH, 3.80-3.78 ppm), glycerophocholine (GPC) and phosphocholine (PCho) and threonine (3.22-3.21 ppm), glucose (3.45-3.43 ppm), valine (1.06-1.03 ppm), and a “to be determined” (TBD) compound (4.02-4.00 ppm)

Regions (ppm)	p value	Trend Respect to Adjacent	Regions (ppm)	p value	Trend Respect to Adjacent
3.24-3.23	***	lower	2.84-2.82	***	lower
3.93-3.91	***	lower	3.90-3.89	**	lower
2.45-2.42	***	lower	3.86-3.85	*	lower
2.15-2.11	**	lower	3.05-2.98	*	lower
3.15-3.13	*	higher	2.36-2.31	*	lower
3.88-3.87	**	lower	1.00-0.94	*	lower
4.02-4.00	*	lower	2.10-2.07	*	lower
3.95-3.94	***	lower	3.72-3.70	***	lower
4.15-4.10	**	lower	1.35-1.33	***	lower
3.80-3.78	**	lower	2.81-2.79	**	lower
3.69-3.67	**	lower	0.91-0.89	*	lower
4.35-4.24	*	lower	2.06-2.03	***	lower
3.63-3.62	*	lower	2.02-2.00	*	lower
3.45-3.43	*	lower	2.77-2.75	*	lower
2.38-2.37	**	lower			

Table 4.1.1: *Statistically different ROIs, associated metabolites, and trend for the comparison between tumours and Ad.*

Malignant vs. Non Malignant

When comparing the group of malignant specimens (Chr, CC, and Pap) with that of non-malignant ones (Ad, AML, and Onc), 33 significantly different ROIs were observed to differentiate the groups based on increased levels in malignant tissues. Relevant metabolites for this separation were TBD, taurine, glucose, alanine (3.80-3.78 ppm and 1.49-1.46 ppm), GSH, *myo*-inostol, valine, and GPC and PCho.

Comparison Among All Types of Histopathologically Different Tissues

Interestingly, ANOVA and Wilcoxon tests highlighted 44 of the 58 ROIs as able to differentiate between at least two tumour types or adjacent benign samples. Among them, the 12 regions shown in Table 4.1.2 were particularly significant for subtypes' characterisation.

Spectral Regions	Major Contributing Metabolites	Ad					AML				Onc			CC		Chr
		AML	Onc	CC	Chr	Pap	Onc	CC	Chr	Pap	CC	Chr	Pap	Chr	Pap	Pap
1.00-0.94	valine	***	*	***					**	***			**	**	***	
1.06-1.03	valine	***	*	***			*		**	***		*	*		***	
1.49-1.46	alanine	***	***	***	***					***			**		***	**
3.15.3.13	spermine	***	***	***	***	***			*	**					*	
3.22-3.21	GPC, PCho	***		***	***	***	***				***	***	***			
3.24-3.23	myo-inositol, taurine		***		***		**		**		***		*	***		*
3.45-3.43	taurine, glucose	*			***	***				***			***	*	***	***
3.80-3.78	alanine, GSH	**	*		*		***	*	***	*	**	***	*			
3.99-3.96	histidine, phenylalanine, PCho, serine	***	**	***	***	***	*	*								
4.02-4.00	TBD				*	***			**	***		**	***	**	***	
4.07-4.05	Cho, myo-inositol	*		***		***	*				***	*	***			*
4.35-4.24	GPC, Pcho, theronine		***	*	*			**		*	***		***	***		**

Table 4.1.2: *Twelve most significant 12 ROIs for separation between at least two tumour types or Ad samples.*

Furthermore, a score plot of the first three components for the separation between Ad *vs.* benign tumours (Fig. 3.1.2A) and Ad *vs.* RCC (Fig 4.1.2B) are shown below.

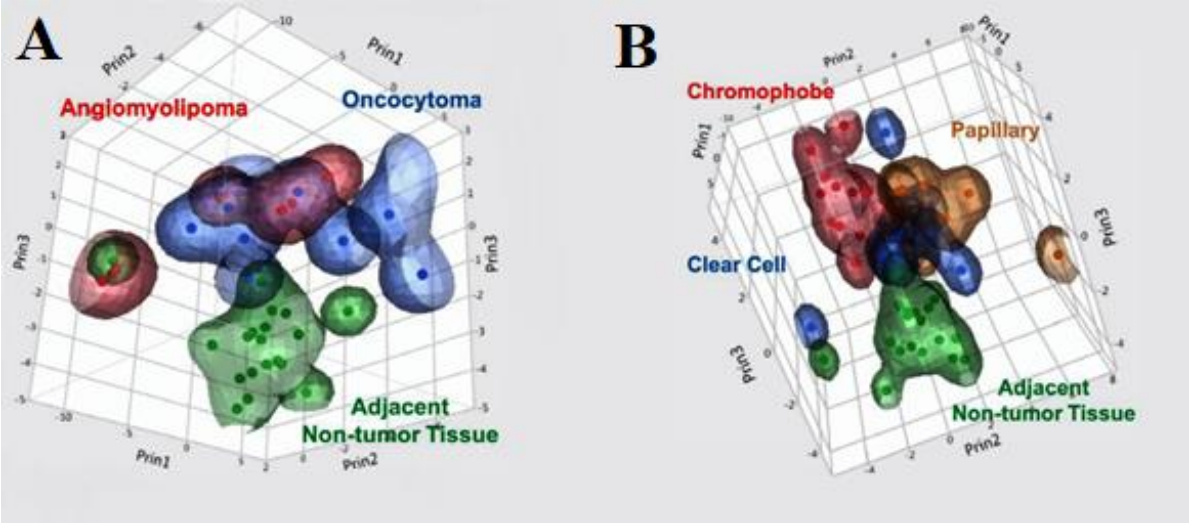

Fig 4.1.2**:** PCA *3D plots of the first three PCs, dividing* A) *Ad from benign tumours (Onc and AML) and B) Ad from RCC (CC, Chr, and Pap)*

Similarity of fresh-frozen paired samples

Paired t- and Wilcoxon tests delivered no statistically significant difference for any ROI between samples scanned fresh or following freezing process. Moreover, regression analysis for the means of the two groups showed linear relation with a slope of 1.008 (Fig. 4.1.3).

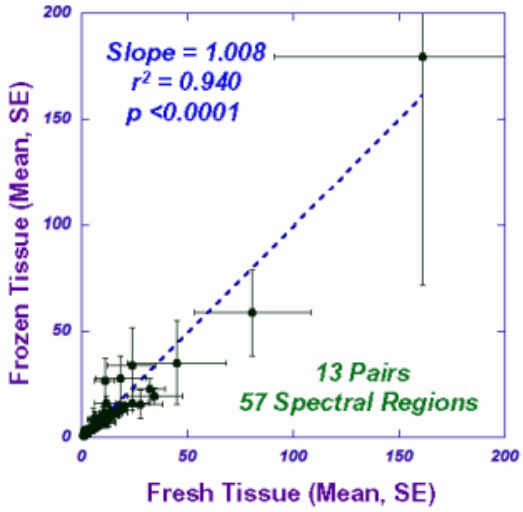

Fig. 4.1.3: *Linear regression analysis for Fresh vs. Frozen groups*

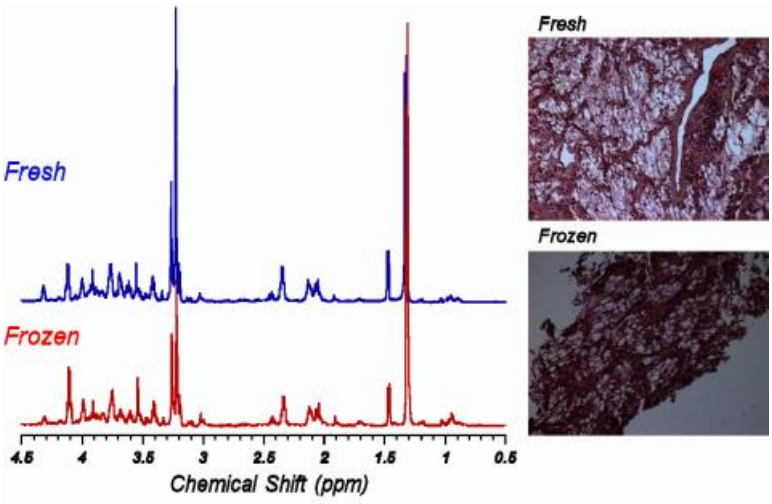

Fig. 4.1.4: *Fresh and Frozen NMR spectra and histopathological reading*

4.1.5 Discussion

Metabolic Changes in Histopathological Types

HRMAS-based metabolomic analysis was able to highlight statistically significant alterations in several spectral regions. Increases in *myo*-inositol, taurine, alanine, and choline-containing compounds (GPC and PCho) levels were common in cancer [2]. Interestingly, not only these molecules are more abundant when comparing Ad with tumorous specimens, but also when malignant *vs.* non-malignant and cases are examined. Moreover, these compounds could separate tumour types. Since GPC and PCho are major cell membrane constituents, their higher values may be signs of stimulation of cell proliferation, cell membrane turnover, choline phosphorylation, and phosphatidylcholine pathway activity [105–107]. Moreover, the increase in taurine and the antioxidant GSH may be related to an endogenous response to tumour proliferation and its oxidative stress [108–110]. Being a glycolysis product, the amino acid alanine may be the result of higher glycolytic flux, cytosolic amino acid transformations, and protein synthesis [111]. Regarding *myo*-inositol, its alteration may derive from cellular signal transduction messengers, such as membrane-associated phosphatidyl inositols and inositol phosphates [112], or by its action as protein kinase C activator. Notably, this enzyme appears in more aggressive brain tumours [2]. Unexpectedly, glucose values were found higher in tumorous specimens and especially in malignant ones. In fact, due to the Warburg effect, an opposite trend should be observed. In details, this phenomenon involves adenosine triphosphate (ATP) production through the less efficient enhanced glycolysis, followed by lactate fermentation [113–115]. This occurs instead of the normal lower glycolysis, followed by pyruvate oxidation through oxidative phosphorylation. Nevertheless, recent works have been published regarding the so-called “reverse Warburg effect” [115–117]. According to these results, the

cells of some types of cancer may induce the Warburg effect also in the surrounding stromal fibroblasts. Therefore, the metabolism of the neighbouring tissues may be altered to supply ATP and lactate to cancerous cells. Other significantly different metabolites highlighted by this study were threonine, valine, spermine, and TBD. While the first two entries, as well as an alternative cause for alanine, may be explained by protein degradation in the case of tumours, spermine is of difficult interpretation. Indeed, literature seems to report information about spermine only in relation to prostate cancer [2].

Similarity of Fresh-Frozen Paired Samples

The absence of significant differences in any spectral ROI in the comparison of fresh-frozen pairs suggested that freezing may be considered as an appropriate preservation strategy due to the stability of kidney tissues. Therefore, results supported the reliability of data obtained from metabolomic analyses of previously banked tissues. Being an accurate representation of *in vivo* behaviour, frozen tissue analysis may help translation to clinical practice.

4.2 Conclusions on Intact Kidney Tissue

HRMAS MRS metabolomics investigation strategy could successfully highlight the metabolic differences, between tumours and benign adjacent tissues, malignant (Chr, CC, and Pap) and non-malignant (Ad, Onc, and AML) specimens, and among the 6 diverse phenotypes. Although this is a preliminary study that requires a larger sample size to validate these findings, it may be of interest to better understand RCC dynamics. Indeed, these findings indicate potential metabolomic biomarkers to be further tested. Ultimately, translation of such information into *in vivo* platform may improve clinical practice through earlier and more accurate diagnosis and prevent overtreatment. Moreover, data from this work supports and encourages the organisation of biobanks. Future developments of this project will aim at correlating quantitative histopathology evaluations, Furhman, and TNM scores data with metabolites' alterations. Another goal could be the assessment of the spatial extent of the so-called "metabolic field", i.e. metabolic perturbation of the cells adjacent to those affected by a pathological status. This would deliver useful information about cancer metabolism, to potentially aid treatment design. Furthermore, as previously mentioned, a larger sample size should be considered to produce a more robust model.

5. Placenta

5.1 General Aspects of Placenta

Placenta is the highly specialised organ connecting the embryo's umbilical cord and the uterine wall of the pregnant woman, hence developing from the junction of the vascular systems of the two of them [118]. The organ may be divided into two compartments: the foetal *chorion frondosus* and the maternal *decidua basalis*. Throughout gestation, the former portion grows to become the major part [119]. Normal placenta at term has a diameter of circa 22 cm, a thickness of 2-2.5 cm, and it weight about 470 g [120]. Such structure, which has been described as a "transitory liver", mainly acts by means of diffusion through villi, capillary walls, and other membranes at the places of contact between the uterus and the foetus [118]. It is responsible for the uptake and storage of nutrients necessary to the foetus, gas exchange with the mother, pregnancy hormones production, elimination of foetal metabolic end products, regulation of the temperature, and water retention [118,119]. Moreover, placenta serves as a barrier against certain internal infections. Due to placenta's nutrition functions, its main components are carbohydrate, protein, lipids, enzymes, vitamins, hormones, and minerals [119]. Nevertheless, the ratios among these compounds vary during the gestation to supply different needs. In details, glycogen levels seem to increase for the stages of *decidua basalis*, foetal lungs, and foetal liver formation. Carbohydrates and lipids decrease during the last quarter of pregnancy, probably due to modulation of permeability and secretory activity. Notably, foetal lipid content is different from that of the mother by higher values of palmitic acid and lower values of oleic and stearic acids. Vitamin C content rises throughout pregnancy to decrease at its termination. Furthermore, vitamin D and A, ascorbic acid, thiamine, riboflavin, and carotene can be detected in placental tissues. Interestingly, large proteins are broken down to amino acids prior to transfer to the foetus. From a clinical perspective, visual examination of size, shape, consistency, and completeness of placenta may be performed after delivery in order to observe signs of abnormal foetal development and perinatal morbidity [120]. Regarding metabolomic strategy applied to investigate placenta's dynamics, only a few studies were reported focusing on hypoxia [121–125], preeclampsia [23,121,126,127], neural tube defects [22], and rat foetal growth [128] using mass spectrometry or HRMAS MRS platforms.

5.2 Maternal Obesity

Maternal obesity is caused by calories imbalance and incorrect dietary intake and represent a risk factor for adverse pregnancy outcomes and children's complications afterbirth [129,130]. Such condition has been associated with a lipotoxic placental environment, higher levels of intracellular fatty acids, inflammation, and oxidative stress, which may impair placental function and

metabolism [131]. Indeed, increased maternal Body Mass Index (BMI) was found related to decreased placental efficiency and histopathologic signs of hypoxia and inflammation [131–134].

5.2.1 Aim of the Project

The aim of this preliminary study was to examine, solely by GC-MS platform, the key metabolites from both hydrophilic and lipophilic fractions of placenta associated with maternal obesity. Furthermore, it was attempted to observe separation in obese patients due to GDM.

5.2.2 Population

A total of 38 pregnant women were enrolled for this study. Pregnant women were divided into two different groups based on their pre-gestational BMI according to the Institute of Medicine (IOM) guidelines [135]: Normal weight (NW, 18.5 ≤BMI< 25 Kg/m^2, n = 20) and obese (OB, BMI≥ 30 Kg/m^2, n = 18). Among obese subjects, 8 women showed GDM (OB/GDM+) diagnosed, according to International Federation of Gynaecology and Obstetrics (FIGO) guidelines [136], through oral glucose tolerance test (OGTT, 75 g). Only singleton spontaneous pregnancies, with maternal age between 18 and 40 years old and of Caucasian ethnicity were included in the study (Table 5.2.1). Exclusion criteria consisted in maternal pre-existing diseases, foetal and maternal infections, alcohol or drugs abuse, foetal malformations or chromosomal disorders, and BMI< 18.5 or between 25 and 30. Obese patients were followed with specific nutritional recommendations on weight gain during pregnancy. Glycemia levels of OB/GDM+ group were routinely examined and these patients received lifestyle and dietary indications for glycaemic control. None of the enrolled women needed insulin therapy. The protocol of the study was approved by the ethical committee of the Sacco Hospital (Milan) and all women signed a written informed consent.

Maternal/Delivery Data	Parameter	NW n=20	OB n=18
Maternal Data	Maternal Age [yrs]	33.7 ± 5.7	33.9 ± 5.2
	Maternal Pre-Pregnancy BMI [kg/m^2]	21.5 ± 1.6	36.4 ± 4.8 ***
	Maternal Gestational weight gain [kg]	11.2 ± 3.6	8.8 ± 4.0
	Maternal Basal Glycemia [mg/dL]	78.6 ± 6.9	89.3 ± 11.0 *
Delivery Data	Gestational Age [wks]	39.1 ± 0.2	39.1 ± 0.3
	Fetal Weight [g]	3420.0 ± 401.1	3390.3 ± 461.6
	Placental Weight [g]	479.0 ± 80.8	508.6 ± 80.7
	Placental Efficiency	7.34 ± 1.28	6.76 ± 1.01
	Placental Area [cm^2]	287.0 ± 77.5	247.51 ± 59.1
	Placental Thickness [cm]	1.78 ± 0.56	2.19 ± 0.60

Table 5.2.1: *Maternal and delivery data (foetal and placental parameters). Data are presented as average ± SD. OB group comprised both OB/GDM- and OB/GDM+ subjects. Placental Efficiency is expressed as foetal/placental weight ratio.*

5.2.3 Sample Collection

Placentas from elective caesarean section were measured recording placental weight, area and thickness [133]. Following discard of the maternal decidua layer, placental tissues were collected from a not-impaired part of the placental disc, washed in phosphate-buffered saline (PBS) solution, cut, and immediately snap frozen. Specimens were then transferred into a -80 °C freezer and sent to University of Cagliari for metabolomic analysis.

5.2.4 Results

OB vs. NW

Student's t-test applied on the hydrophilic phase highlighted significantly higher levels of uracil in obese group, which was then confirmed by PLS-DA calculations (accuracy= 0.77, R^2 = 0.79, Q^2 = 0.48 with 10-fold CV method) (Fig. 5.2.1A and Fig.5.2.1B). Together with uracil, this model showed an increase in nucleobases (hypoxanthine and a purine derivative), glucose-6-phosphate, 3-phoshoglycerate, glycerol, nicotinamide, tyrosine, isoleucine, phenylalanine, leucine, and serine, while lower values were observed for lysine, taurine, glutamine, the nucleosides inosine and guanosine, an inositol isomer, and gluconic and aspartic acids. Regarding lipophilic phase, t-test

revealed no significant differences between the groups, while PLS-DA delivered satisfactory results (accuracy = 0.86 R^2 = 0.62 Q^2 = 0.33, performance measure p< 0.01). The most interesting features were higher levels of palmitic acid in obese subjects, and lower values of arachidonic, stearic, and docosahexaenoic acids (DHA) within the same group (Fig. 5.2.1C and Fig. 5.2.1D).

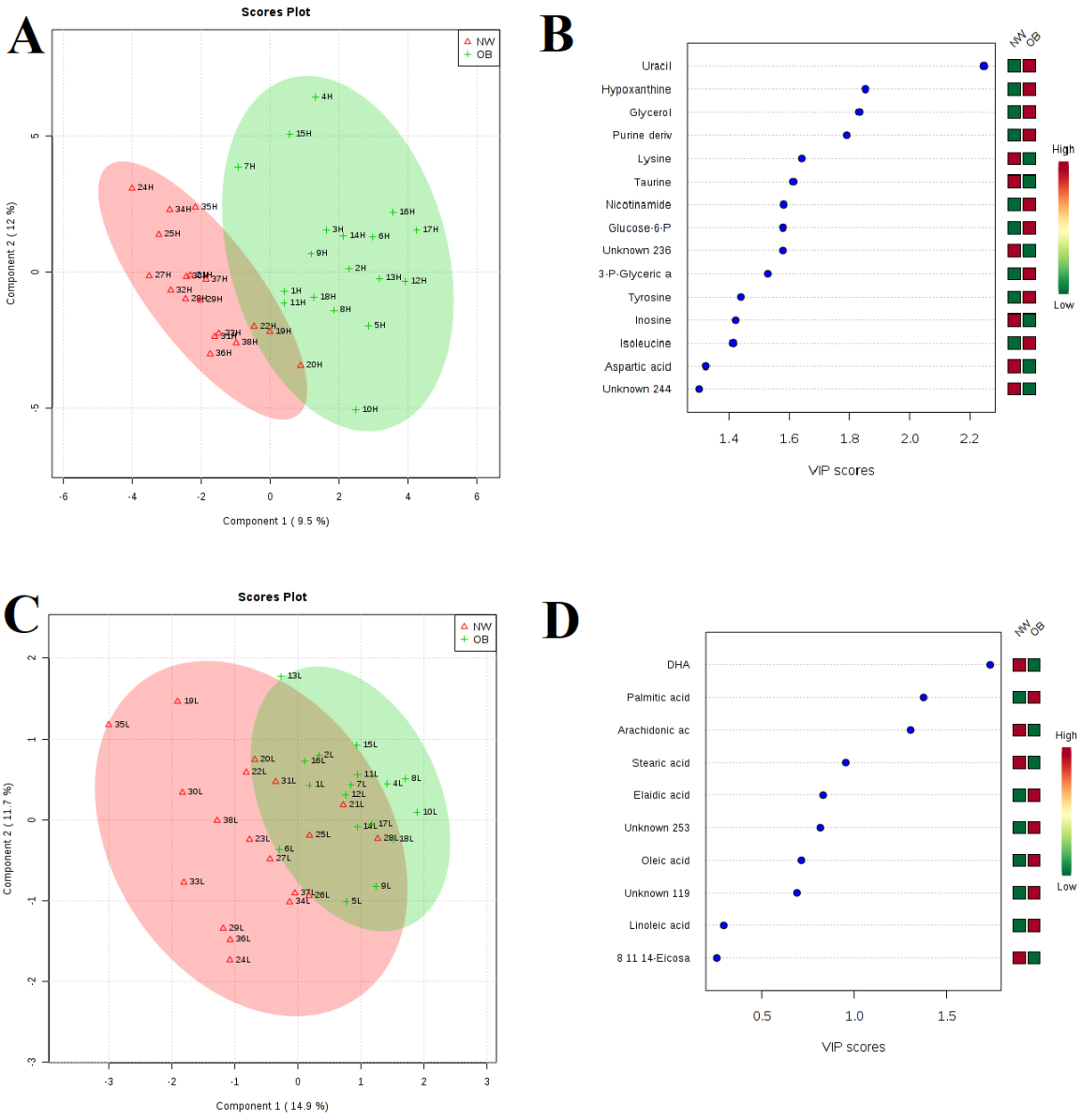

Fig. 5.2.1: *PLS-DA results showing A) 2D score plots for placental hydrophilic fractions B) VIP features and trends for placental hydrophilic fractions C) 2D score plots for placental lipophilic fractions D) VIP features and trends for placental lipophilic fractions*

Furthermore, joining the hydro- and lipophilic matrices into a single one, PLS-DA delivered a predictive 4 components model displaying accuracy = 0.80435, R^2 = 0.89354, and Q^2 = 0.18716

(Fig. 5.2.2). Although showing lower performance, these calculations remarked the results from the separate matrices, highlighting the global characteristic metabolites for each phenotype.

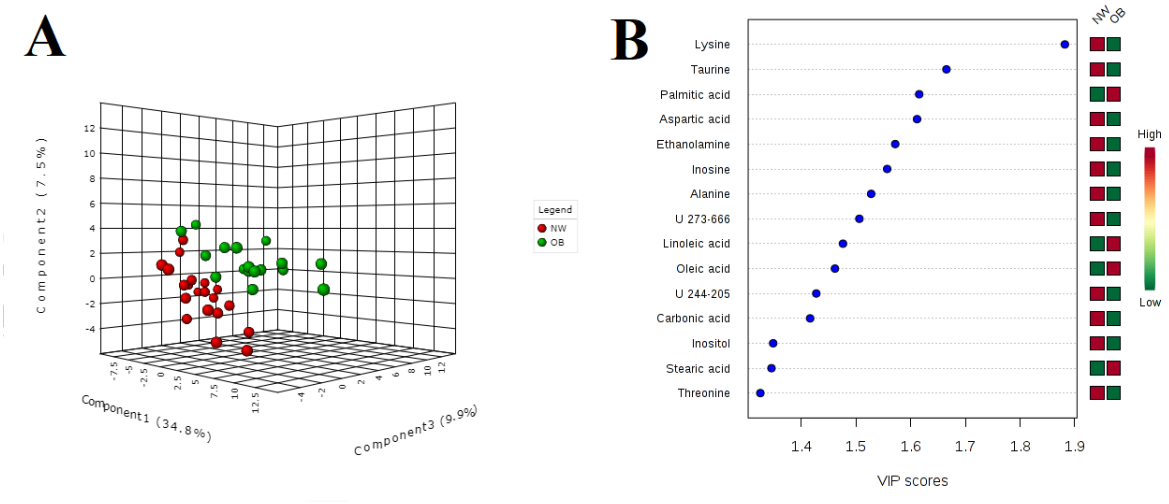

Fig. 5.2.2: *PLS-DA results showing A) 3D score plot for the placental hydro- and lipophilic matrices jointed together B) VIP features and trends for jointed placental hydro-and lipophilic matrices*

OB/GDM- vs. OB/GDM+

Performing ANOVA with Tukey's HSD post-hoc test on both hydro- and lipophilic fractions for the separation among OB/GDM+, obese patients with no GDM (OB/GDM-), and NW, no significant result was observed. Interestingly, while PLS-DA model of the hydrophilic fraction of three classes delivered satisfactory values (accuracy= 0.61 R^2= 0.83 Q^2= 0.55, performance measure $p<0.01$) (Fig. 5.2.3A and 5.2.3B), the same calculations on the lipophilic fraction were not statistically significant.

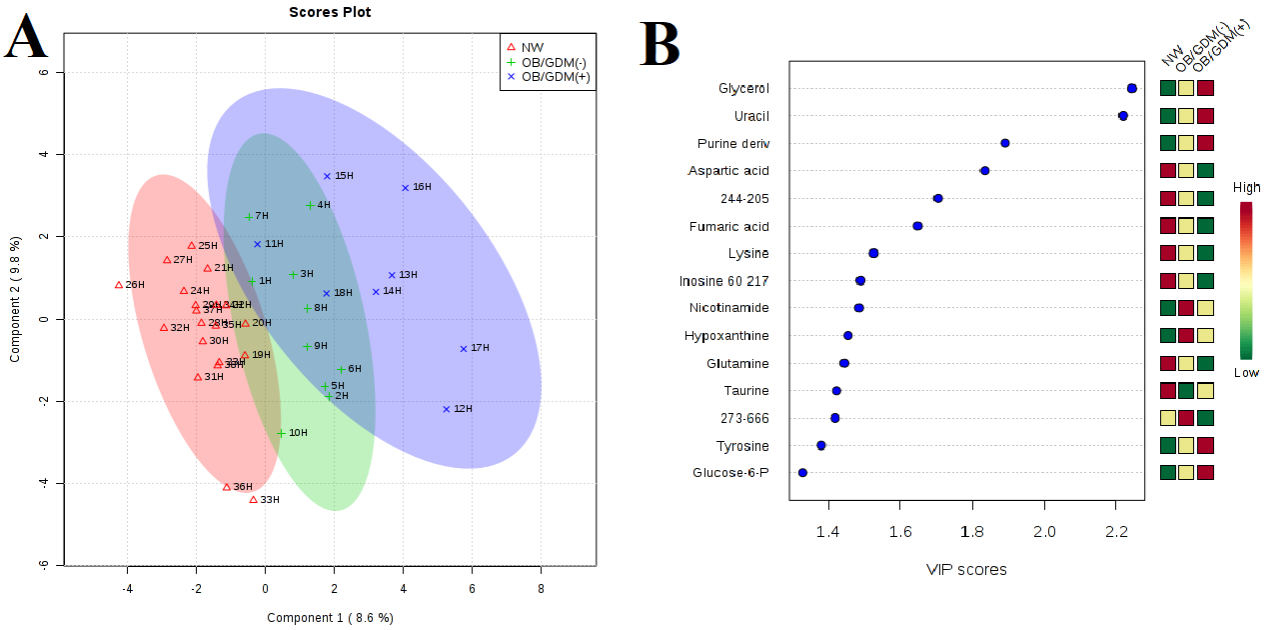

Fig. 5.2.3: *PLS-DA results showing A) 2D score plot for placental hydrophilic fractions for the separation of the three phenotypes B) VIP features and trends for placental hydrophilic fractions of the three different phenotypes*

5.2.5 Discussion

OB vs. NW

GC-MS analysis of the hydrophilic phase revealed altered amounts of several metabolites in obese placentas. Although amino acids are normally accumulated within the placenta by active transport systems located on the microvillus membrane [137,138], different trends for different amino acids were highlighted in this study. In fact, maternal obesity has been associated with enhanced placental transporters, mammalian target of rapamycin (mTOR), and IGF-1 signalling pathways activity [139]. Nevertheless, as mentioned above, obese subjects showed higher values of taurine, tyrosine, isoleucine, phenylalanine, leucine and serine and decreased levels of lysine, aspartic acid, and glutamine. In particular, decrease in the aminosulfonic metabolite taurine was supported by previous findings in obese or diabetic subjects [140] and in placental villous explants of obese pregnancies showing reduced activity of taurine transporters [141]. Glutamine trend may be caused due to foetal liver overgrowth [138,139]. Interestingly, collected data seem to indicate the disruption of placenta's mitochondrial metabolism. Indeed, several discriminant amino acids, together with glycerol, uracil, hypoxanthine, a purine derivative, nicotinamide, glucose-6-phosphate, 3-phosphoglycerate, guanosine, and inosine are involved in metabolic pathways supporting nucleotides production, antioxidant defences, and lipid synthesis. In details, among the variety of its

metabolic functions, serine contributes to mitochondrial NAPDH production through folate cycle [142]. Nicotinamide, an important component of NAD^+-NADH co-enzymatic factor, is involved in mitochondrial energy production and in several redox transformations [143]. Glycerol is present in lipid and energy metabolism as backbone of triglycerides' structure. Therefore, its higher levels may be related to enhanced placental fatty acid availability and uptake from the maternal circulation of obese women [144]. Regarding the trend of inositol and gluconic acid, lower amounts may suggest a reduced carbohydrate metabolism, hence induced insulin sensitivity [145]. Supporting these hypotheses on mitochondrial impairment, a recent work [146] highlighted increased mitochondrial DNA content in placentas of obese women, which may potentially lead to less foetal oxygen availability and in turn altered metabolism [147,148]. Furthermore, mutated genes affecting mitochondrial function and energy production were already observed in obese placentas and maternal blood [149,150]. Analysing the lipophilic fraction, other significant features were highlighted. Lower levels of long chain-polyunsaturated fatty acids (LC-PUFA) derivatives, arachidonic acid, and DHA were revealed in OB group, while saturated palmitic acid was increased. Changes in the maternal lipid profile have been reported in obesity, with increased triglycerides and decreased levels of high density lipoproteins [144]. Moreover, placental expression of fatty acid binding proteins is stimulated in obesity [151] together with higher lipid accumulation. Therefore, independently of GDM, OB patients seemed characterised by disruption of physiologic LC-PUFA biomagnification, leading to reduced availability of arachidonic acid and DHA for the foetus. This may induce adverse foetal outcomes and the development of a number of chronic diseases such as metabolic and cardiovascular diseases throughout postnatal life [152,153].

OB/GDM- vs. OB/GDM+

Although less information could be drawn from GDM exploration, the observed alterations in amino acid levels were previously reported for hyperglycemic mothers [154] and in umbilical blood from GDM subjects [155].

5.3 Conclusions on Placenta

Broad-range placental metabolomic analysis was able to reveal differences in obese pregnancies [26,156]. Results suggested changes in nucleotide production, antioxidant defences, lipid synthesis, and NADPH-based signalling, i.e. a generalised shift towards higher placental mitochondrial metabolism. Moreover, common features usually associated with obesity such as higher glycerol and saturated fatty acids levels were observed. Therefore, highlighting potential modifications in the intrauterine metabolic environment, this study supports the necessity of a precise planning of

maternal BMI before conception. Although limitations to this work were represented by the small sample size and by the specific recruiting, which may not reflect general obese population with diverse outcomes, such data may be considered as a basis for the exploration of potential markers for afterbirth diseases.

6. Plasma

6.1 Plasma Composition

Blood plasma is the extracellular matrix in which blood cells are suspended. It is a clear, light yellow solution constituted by circa 90-95% of water and 5-10% of dissolved solutes of organic and inorganic nature [157,158]. In particular, the major portion of the solutes is proteins: albumins responsible for osmotic concentration, globulins for lipid and lipophilic vitamins transport, and fibrinogen [157]. Other compounds dissolved in plasma are clotting factors, glucose, hormones, electrolytes (sodium, chloride, potassium, and calcium in decreasing order), and gasses such as oxygen and CO_2 [158]. The main biological functions of such biofluid comprise intravascular osmosis, achieved through the above-mentioned albumins and electrolytes, and as protein reserve. Currently, whole blood, plasma, and serum tests are widely used for a plethora of routinary and non-routinary clinical analyses.

6.2 Colorectal Cancer

Colorectal cancer (CRC) is one of the most prevalent types of cancer, ranking as the 3rd most common malignancy and the 4th leading cause of cancer death worldwide [159]. Although 5-years survival rate for CRC can reach 90% when cancer is detected at an early and localised stage, survival rate dramatically drops to 12% if the cancer has spread to distant organs [160]. Currently, several screening and detection methods are available for CRC upon clinical, endoscopic, histologic, and radiographic techniques that often cause pain and discomfort to patients for their invasiveness [161]. Other non-invasive stool-based tests, such as faecal DNA [162] and faecal occult blood test (FOBT), and serum analysis for cancer markers such as carcinoembryonic (CEA) and carbohydrate antigen 19.9 (CA19-9) are commonly used. Nevertheless, due to low sensitivity, the clinical application of these strategies is limited [163]. Moreover, microRNA tests for the observation of genetic alterations have been extendedly studied, but not routinely employed because of low reliability and sensitivity [164]. Therefore, it is important to develop simple and non-invasive screening tools to improve detection of the disease in its early stages. Notably, previous Metabolomic studies were able to successfully recognise CRC tissues from adjacent mucosal [165] or control specimens [166] and to associate rate of recurrence and patients' survival with metabolome variations [167].

6.2.1 Aim of the Project

In this study, metabolic profiles of colon and rectal cancer plasma were characterised by means of GC-MS-based metabolomic analysis and compared to normal volunteer controls to find potential plasma biomarkers.

6.2.2 Population

Twenty-four subjects (median age 62, from 30 to 90 years old) were recruited and divided into two groups according to the histopathological analysis of bioptic tissues: CRC patients (n = 15; colon cancer n = 8; rectal cancer n = 7) and healthy controls (n = 9). Plasma sampling from patients was performed before any specific therapy. Healthy controls showed no evidence of actual disease following physical examination. Patients and healthy controls were recruited at the Colorectal Surgery Unit of the University of Cagliari between July 2015 and September 2015. Informed consent was obtained from all subjects in the study, according to institutional guidelines.

6.2.3 Results

Following t-test, PCA, and PLS-DA (accuracy = 0.875, R^2 = 0.99, Q^2 = 0.436 for 5 components model) the comparison between cancers group (rectal and colon) and controls showed a main increase in mannose, fructose, erythritol, 3-methyl-3-hydroxybutyric acid, and aminomalonic acid and a decrease in 3-amino-1,2-propanediol, methionine, iminodiacetic acid, valine, leucine, serotonin, lysine, tyrosine, proline, and glucoheptonic acid (Table 6.2.1). Interestingly, the same trends for mannose, fructose, 3-amino-1,2-propanediol, methionine, valine, and serotonin were observed when separately observing rectal or colon cancers *vs.* controls. Therefore, a similarity in the two diseases seems to be highlighted. Nevertheless, some differences may be noted in the separation of the two different malignancies with the healthy cases. In particular, rectal tumours displayed enrichment in 3-methyl-3-hydroxybutyric acid and 2-piperidinecarboxylic acid and depletion in iminodiacetic acid and proline (accuracy = 0.8125, R^2 = 0.71862, Q^2 = 0.37968 for 1 component model), while colon phenotypes were characterised by higher levels of erythritol and lower levels of lysine, leucine, and histidine (accuracy = 0.88235, R^2 = 0.99932, Q^2 = 0.61032 for 5 components model). Notably, although the univariate analysis displayed a larger number of metabolites, only the main metabolites confirmed by both methods are reported.

Populations	Discriminants
Cancers *vs.* controls	**Increase:** mannose, fructose, erythritol, aminomalonic acid, 3-methyl-3-hydroxybutyric acid **Decrease:** 3-amino-1,2-propanediol, methionine, iminodiacetic acid, valine, leucine, serotonin, lysine, tyrosine, proline, glucoheptonic acid
Rectal cancers *vs.* controls	**Increase:** mannose, 3-methyl-3-hydroxybutyric acid, fructose, and 2-piperidinecarboxylic acid **Decrease:** iminodiacetic acid, 3-amino-1,2-propanediol, serotonin, methionine, valine, proline
Colon cancers *vs.* controls	**Increase:** mannose, erythritol, fructose **Decrease:** 3-amino-1,2-propanediol, lysine, valine, methionine, leucine, histidine, serotonin

Table 6.2.1: *Discriminant metabolic trends for the separation of cancers vs. control, rectal cancers vs. controls, and colon cancers vs. controls phenotypes.*

Regarding the metabolic differences between rectal and colon cancers, application of t-test on the rectal-control separation, showed that the former condition was characterized by higher levels of ornithine, citric acid, *cis*-aconitic acid, and lysine. Further PLS-DA investigation revealed that higher levels of citric acid, lysine, *cis*-aconitic acid, threonic acid, arachidonic acid, ornithine, threonine, 3-hydroxybutyric acid, oleic acid, 4-deoxythreonic acid, and palmitoleic acid were found in rectal cases, while inositol-like compound, a diglyceride, and mannitol levels decreased. However, the obtained model was not statistically significant, probably due to the exiguous sample number and to the strong resemblance between the two conditions. Similarly, a model considering the 3 phenotypes at the same time was not able to reach statistical significance. MSEA, performed to explore the different dynamics in pathological and healthy cases, highlighted several altered metabolisms (Fig. 6.2.1).

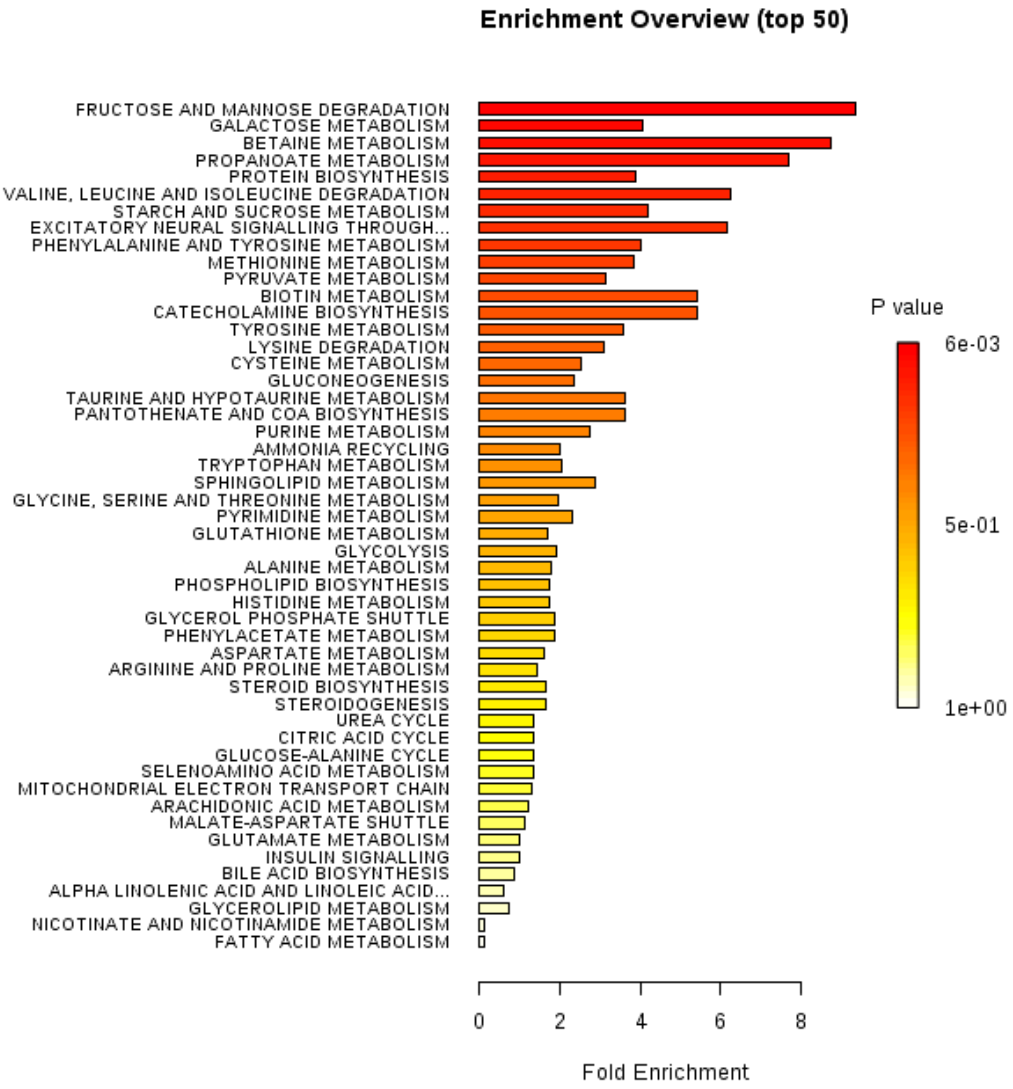

Fig. 6.2.1: *MSEA on cancers (rectal and colon) vs. controls groups shows the pathways that are most affected by the morbidity.*

6.2.4 Discussion

Cancers vs. Controls

Interestingly, the set of metabolites involved in the separations of the two cancer forms with healthy subjects is extremely similar. This may suggest that similar mechanisms underlie the cancer occurrences. As mentioned above, both cancers present the metabolic feature of higher levels of mannose and fructose and lower levels of 3-amino-1,2-propanediol, methionine, valine, and serotonin. Regarding mannose higher concentrations in CRC patients, no direct relationship between the pathology and this metabolite may be defined. However, the guanosine diphosphate mannose-4,6-dehydratase (GMDS) gene is responsible for the enzyme involved in the transformation of guanosine diphosphate mannose (GDP-mannose) into GDP-fucose. In turn, this latter molecule is a key compound in fucosylation processes. Indeed, fucosylation regulates the

tumor necrosis factor-related apoptosis inducing ligand (TRAIL) signalling, which allows for the detection of colon cancer cells by natural killer cells [168–170]. (Scheme 6.2.1) In the presence of GMDS deficiency, the transformation between GDP-mannose and GDP-fucose is impaired and fucosylation is lost, inducing cancer progression and metastasis. Therefore, the higher levels of mannose may derive from a GMDS defect, which prevents the normal formation of the fucose moiety [170,171].

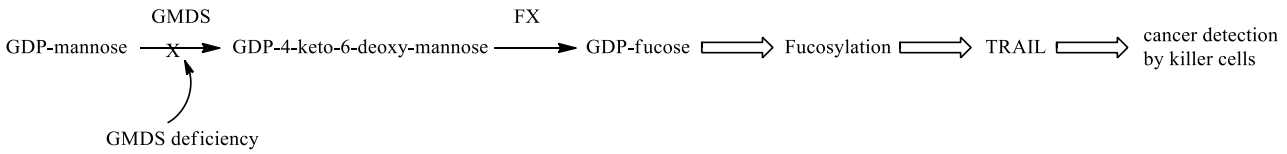

Scheme 6.2.1:. *Scheme describing the relationship among GMDS, TRAIL, and CRC development. The missing conversion of GDP-mannose leads to loss of fucosylation and, in turn, TRAIL signalling. This mechanism impairs cancer detection.*

More information is available for fructose trend. This molecule is a pentose monosaccharide with unrestrained cellular uptake [172]. It may be found as second constituent of the disaccharide sucrose or as a key component in high-fructose corn syrup. Since such compounds are largely used for the production of soft drinks and processed food, the increased consumption of fructose may be reasonable. Furthermore, although mainly derived from diet, fructose can also be converted from glucose *via* pentose phosphate or polyol pathways [173]. In literature, different studies reported the association of high dietary glycemic load, glucose or fructose intake with higher CRC risk for male subjects and especially for those with elevated body mass index [174] or high sucrose intake with increased CRC risks for smokers and non alcohol drinkers male subjects [172]. However, the higher consumption of these carbohydrates seems to have no significant effect on women [172,174]. Interestingly, an increase in vincristine-accumulated mitotic figures per crypt section and in aberrant crypt foci were correlated to higher intake of sucrose and fructose. Such histological features may be linked to epithelial proliferation and sensitivity to carcinogenesis [175]. Moreover, higher fructose blood levels were related with more aggressive colon, rectum, and pancreatic cancers [176,177]. This may be explained by the promotion on nucleic acids synthesis, i.e. proliferation, in cancer cells through transketolase mediated metabolism [178]. In addition, high intake of fructose may promote ROS production, hence increasing cellular stress which in turn may induce neoplastic growth [173]. Regarding serotonin, contrasting evidence reporting both lower and higher plasma concentrations, may be found in literature. The most reasonable explanation for the depletion in serotonin levels was reported by Tan and co-workers, implying such evidence to abnormal gut

bacterial activity [179]. Some studies [180–182] showed that the administration of selective serotonin reuptake inhibitors (SSRIs) in depressed patients could be inversely associated with CRC risks. Preventing the reuptake of the metabolite, this type of drugs leads to increased levels of serotonin in the extracellular environment, hence lower levels may be expected in CRC affected subjects. Notably, another group related this effect to the inhibition by the drug of the growth hormone and/or IGF-I, which could be responsible for the development of colon, breast, and prostate cancers [183]. Nevertheless, increased serotonin levels were found by other groups [182,184]. Allograft mouse models investigations attributed these findings to the ability of serotonin to promote angiogenesis [184] by imparing angiostatin production through matrix metalloproteinase 12 (MMP-12) limitation in tumor-infiltrating macrophages [185–187]. Causing hypoxia and spontaneous necrosis, lower serotonin values led to slower colon cancer growth [184]. Other clinical evidence are related to overexpression of serotonin receptors in cancer tissues and cell lines [188]. The decrease in amino acids levels reported in literature [189,190] was also observed in this study. In particular, methionine and folate play an important role in the methylation, synthesis, and repair of DNA, preventing CRC occurrences [191–195]. In fact, both molecules are necessary for the synthesis of S-adenosylmethionine, a universal methyl group donor [196], and aberrant DNA methylation may be responsible for initiation and early development of CRC. Previous investigations support the findings of this study by reporting inadequate intakes of methionine associated with higher risks of CRC, especially in the cases of long follow-up, Western countries, and men [160] and higher risks of proximal colon cancer in men and rectal cancer in women [197]. Moreover, increased CRC risks were observed with inadequate intake of both methionine and folate [195] or together with substantial consumption of alcohol [191]. Unfortunately, the application of GC-MS platform does not allow for the detection of folate, limiting the considerations on such link. Interestingly, although methionine protection may derive from diet alone [195], it has to be noticed that this amino acid is present in high-protein foods which may induce CRC event by means of different mechanisms [192,198]. Another amino acid that showed lower levels in CRC occurrences was leucine. Such observation may be related to the leucine-rich repeat-containing G protein-coupled receptor 5 (LGR5), a transmembrane receptor which seems to be overexpressed in certain CRC cell lines [199–201] from the early tumorogenis and especially in lymphatic invasion [199,200], vascular invasion, tumor depth, lymph node metastasis, and tumor stage III. Although LGR5 overexpression correlates with some features such as cancer stage and number of lymph node metastases, the exact function of LGR5-related signalling in still unknown [199]. Nevertheless, leucine depletion may be explained by the use of this amino acid for the enhanced synthesis of LGR5. Similarly, also proline decrease may derive from the overexpression of the proline rich 15 (Prr15) gene, which encodes proline rich proteins, in sporadic CRCs. Unfortunately,

the biological activity of these proteins in still unclear [202,203]. Another explanation may involve proline dehydrogenase/oxidase (PRODH/POX). In fact, this enzyme catalysed transformation of proline into D1-pyrroline-5-carboxylate (P5C), which lead to ATP production for cancers survival in hypoxia and glucose deprivation conditions [204]. Regarding L-tyrosine, such compound is metabolised through the assistance of gut bacteria. The decrease of this metabolite may be a sign of the modification of the gut microbiota in CRC patients [205]. Proline was also found significantly decreased in several other studies [206].

Colon Cancers vs. Controls

Exploring the different metabolic feature of the specimens from colon cancer affected subjects and the controls, lower levels of histidine were observed. This may be caused by a potentially higher activity of histidine decarboxylase to produce histamine [207]. The latter compound has been reported to increase in animal cancerous colon [208] and human CRC cell lines, especially in the case of lymph node and/or hematogenous metastases [209]. Interestingly, histamine may contribute to cancer development by activation of H2 receptors, vascular endothelial growth factor [210], and inhibition of immune response.

Rectal Cancers vs. Colon Cancers

Among the metabolites that may be responsible for the separation between rectal and colon morbidities, threonic acid may be of particular importance. Threonic acid is a breakdown product of ascorbic acid. According to some previous studies [211–213], pharmacologic doses of the latter compound may inhibit cancer cell growth and induce apoptosis and necrosis by, among other mechanisms, ROS-dependent downregulation of a variety of specificity proteins [211]. In particular, ROS may be produced though ascorbate radical intermediate and its effect seems to depend on the cell line and the concentration of ascorbic acids applied *in vitro* [214]. For this reason, a different susceptibility to ascorbic acid between rectal and colon cell lines may be hypothesised, leading to different metabolisation outcome. However, decreasing trends for threonic acid were reported by other authors [213]. Unfortunately, it has to be reminded that this last discrimination has not reached statistical significance, probably due to the small samples size.

Metabolic Pathways

Pathways analysis showed a predominant involvement of fructose and mannose degradation, which may be linked to the processes mentioned above. Furthermore, the analysis performed within this study produced results that are supported by previous works. Indeed, glycolysis, tricarboxylic acid

(TCA) cycle, urea cycle, tryptophan, arginine and proline, pyrimidine, polyamine, amino acid, and fatty acid metabolisms were found significantly affected in CRC occurrences [206,215]. Fatty acid metabolism may be explained by the relationship between high fat/calories diet and cancer proliferation [216–219], while tryptophan and tyrosine and phenylalanine metabolisms may derive from gut microbial cometabolism [219]. Moreover, evidence for altered gluconeogenesis were described and related to uncommon liver activity [220].

6.3 Conclusions on Plasma

In conclusion, metabolomic analysis of plasma specimens from CRC patients compared to those from healthy ones delivered several information. The most evident separation was between CRC and controls, which highlighted metabolites that may be related to dietary intake (fructose, methionine, and fatty acids metabolism), genes activity (proline, leucine, and mannose), and gut bacteria altered production (serotonin, tyrosine, and tryptophan and tyrosine and phenylalanine metabolisms) among other explanations. Although less informative, discrimination of the two different morbidities with control cases was satisfactory. Nevertheless, potential plasma biomarkers were identified for the phenotypical recognition. Unfortunately, the exploration of the two types of cancer did not reach statistical significance and larger sample size is in need to confirm such findings.

7. Saliva

7.1 Saliva General Aspects

Saliva is an exocrine secretion deriving from major (parotid, submandibular, and sublingual) and minor (lower lip, tongue, palate, cheeks, and pharynx) salivary glands, gingival fold, and oral mucosa transudate [221,222]. The average production of saliva accounts for 1-1,5 L per day, and the contribution of the different glands changes depending on absence or presence of stimulation [221,223]. Therefore, given its multiple and variable origin, this clear fluid shows a complex composition. In particular, 99% of it is constituted by water; however, mucous from the nasal cavity and pharynx, non-adherent oral bacteria, food debris, and epithelial and blood cells may be found in normal saliva [221,222]. Furthermore, electrolytes (sodium, potassium, calcium, magnesium, chloride, bicarbonate, and phosphate), proteins (enzymes, albumin, gustin, immunoglobulins, mucosal glycoproteins, etc.), glucose, urea, and ammonia are present. Saliva composition confers hypotonicity to it, allowing mucin glycoprotein to protectively cover mouth inner surface and for not masking taste perception [221]. Interestingly, saliva serves diverse functions [221,222]. Among them, it maintains the pH of the oral cavity around 6-7 by means of bicarbonate, phosphate, and urea. It selects the bacterial flora allowing for the adhesion of only specific microorganisms, modulates demineralisation/remineralisation phenomena for teeth integrity, and it is involved in preliminary phases of digestion. Moreover, the component gustin seems to play a role in growth and maturation of taste buds. Although not routinely employed, analysis of saliva may be used to assess caries risk, to detect genes and biomarkers responsible for certain periodontal or gland diseases/dysfunction, candida or viral infections, sarcoidosis, tuberculosis, liver dysfunction, Sjogren's syndrome, and lymphoma, gastric ulcers, and cancers [1].

7.2 Apical Periodontitis

Apical periodontitis is defined as periradicular inflammatory destruction deriving from infected pulp [224]. Indeed, since immune system cannot act on the pulp, inflammation is a defence mechanism preventing the spreading of infection to adjacent tissues [225]. This pathological condition may be initiated by different stimuli of bacterial nature in the root canal that may further interact with certain yeasts, fungi, and viruses [225–229]. *Streptococcus mutans* and *Lactobacillus acidofilus* are the leading causes of infection. Subsequently, with the progression of the lesions, oral microflora changes toward more specific bacteria. For instance, when lesions are closed, first facultative then strict anaerobic microorganisms such as *Actinobacillus*, *Eikenella corrodens*, *Actinomyces*, *Enterococcus faecalis*, *Pseudomonas*, *Porphyromonas gingivalis*, *Treponema denticola*, and *Tannerella forsythia* find favourable growth condition [226,227]. Apical periodontitis is characterised

by a wide variety of inflammation mediators comprising polymorphonuclear (PMN) leukocytes, lymphocytes B and T (suppressor, natural killer, and helper), and dendritic antigen presenting cells (APC) [230] which are present in different ratio during the different phases of morbidity or healing processes [231–233]. In clinical practice, endodontic interventions aim at inducing periapical tissues healing and at preventing the spreading of infection to other anatomical district, which may result in severe complication [230]. Since 2005, metabolomic exploitation of saliva by means of diverse platforms has focused on several phenotypical alteration such as clinical smoking cessation [234], sport performance [235], Sjögren's syndrome [236], Alzheimer's diseases [237], type 1 diabetes [238], oral, breast, and pancreatic cancers, [40,239–241], etc [242–246]. However, only a few studies are reported on periodontal diseases [239,247], hence additional studies may improve knowledge on this particular subject.

7.2.1 Aim of the Project

This pilot study was designed in order to investigate the salivary metabolome's alterations between patient affected by apical periodontitis and healthy controls. More specifically, the objective of such work was to test the feasibility to identify for the first time a characteristic metabolic profile, descriptive of apical periodontitis.

7.2.2 Population

A total of 21 saliva samples were collected from 21 adult subjects. Twelve of these were affected by chronic apical periodontitis with presence of abscess and fistulas on at least one tooth (median age 48, from 30 to 60 years old), while the remaining 9 were clinically and radiographically healthy subjects (median age 43, from 30 to 60 years old). Both groups showed optimal systemic conditions, satisfactory periodontal health, at least 20 teeth, and underwent no periodontal procedure or drug administration during the 15 days prior to sampling. Collection were performed without forcing salivation and letting saliva accumulate in the mouth. Successively, circa 2 mL of biofluid was let pour into a sampling tube and stored at -80 °C.

7.2.3 Results and Discussion

Neither Student's t-test, nor PCA, nor PLS-DA were able to achieve statistical significance. Table 7.2.1 shows values obtained from PLS-DA. Power analysis applied to such separation indicated a necessary sample size of 700 specimens per group in order to obtain an FDR of 0.55. Therefore, for the observation of any significant alteration between the two phenotypes, the project should proceed

with an extensive samples collection. This result suggest low susceptibility of the biological fluid to this particular status.

Measure	1 comps	2 comps	3 comps	4 comps	5 comps
Accuracy	0.38095	0.33333	0.42857	0.47619	0.57143
R2	0.33667	0.81807	0.93485	0.97106	0.98646
Q2	-0.29788	-1.1134	-0.99081	-0.77103	-0.56838

Table 7.2.1: *Results of PLS-DA for the separation between apical periodontitis-affected and healthy subjects. Notably, no statistically significant value was found.*

7.3 Conclusions on Saliva

Given the low performance of the statistical tools exploited, the characterisation of a pathological metabolic profile was not possible in the case of apical periodontitis. Further investigations on different biofluids may be conducted to assess whether better results may be achieved. However, using such a small sample size, saliva seems not to possess the required metabolic susceptibility to describe such pathological condition. Consequently, it is necessary to drastically increase the number of collected samples prior to proceed with a non-pilot study.

8. Urine

8.1 General Aspects of Urine

Urine is a biofluid that may display several shades of yellow [248]. This property is primarily cause by the concentration and by the presence of molecules such as urochome or uroerythrin that seem to have no clinical interest. However, certain drugs or pathological conditions may affect urine's appearance. Although limpid upon urination, after some time urines show precipitate of low solubility salts. Turbidity is to interpret as a pathological sign. The pH of such fluid is circa 6.0 (from 5.5 to 6.5); however, it fluctuates according to diet and it may assume extreme values due to certain diseases. The average human 24 h production of urine is circa 1.2-1.5 L, varying from 0.6 to 2 L depending from several factors such as hydration, perspiration, physical activity etc. Higher volumes may be symptomatic of certain adverse status such as diabetes or chronic kidney failure, while lower volumes may indicate the presence of dehydration or issues related to kidneys. Notably, urines night production is reduced to half or less of the daily one. Regarding the composition of the biofluid, the main constituent is water, in which the remaining compounds are dissolved. The other major contribution is from urea and creatinine, followed by electrolytes such as chloride, sodium, and potassium, then ammonia, phosphates, uric acid, amino acids, calcium, magnesium, and other minor solid compounds [249]. Moreover, are of pivotal importance the detection and amounts of proteins, glucose and other sugars, blood, ketone bodies, urobilinogen, urobilin, biliary pigments and salts, and other molecules which should be detected under a low thresholds [250]. In addition to the plethora of routinely clinical analyses performed on urines [248–250], this biofluid has been successfully and extensively studied for metabolomics applications over the years [251–254]. Nevertheless, even more information may be obtain from the investigation of the alteration in urinary metabolome.

8.2 Chorioamnionitis Diagnosis through Urinary Metabolome Alteration

8.2.1 Chrorioamnionitis

Chorioamnionitis is an intrauterine infection/inflammation (IUI) occurring between the maternal tissues and the foetal membranes (choriodecidual space) or in the foetal annexes (chorioamniotic membranes, amniotic fluid, umbilical cord) [255]. This condition is a leading cause of preterm birth worldwide, with higher incidence at lower gestational ages [256]. Indeed, up to 50-70% of live births at 24-27 weeks of gestation experience chorioamnionitis. Notably, diverse neonatal adverse outcomes such as death, early- and late-onset sepsis, bronchopulmonary dysplasia, necrotising enterocolitis, and cerebral palsy have been associated with chorioamnionitis [257–261]. Currently, placental histological examination is the gold standard for diagnosis; however, the results are

available only several days after birth [262]. Unfortunately, prenatal diagnosis of chorioamnionitis using clinical criteria provides insufficient specificity and sensitivity with any combination of maternal or foetal clinical signs [263,264]. In order to prevent incorrect clinical diagnoses, different tools based on the combination of clinical and/or laboratory signs into predictive clinical scores, an extended use of amniocentesis, or the introduction of novel biochemical markers have been recently proposed [265–267]. An early and reliable diagnosis of chorioamnionitis around the time of birth would be of pivotal importance for the management of extremely adverse conditions such as early-onset sepsis. In this particular case, given the high incidence in the presence of chorioamnionitis, international guidelines recommend diagnostic evaluation, including blood culture, and preventive postnatal antibiotic treatment. [268,269] Unfortunately, over-treatment is not a rare event due to difficult diagnostic strategies [270]. Furthermore, a more reliable and fast tool for early diagnosis of chorioamnionitis would be useful to counteract the increasing pathogens multidrug-resistance and to prevent short- and long-term adverse outcomes (e.g. toxicity, intestinal dysbiosis, atopy, or wheezing) that may be related to early antibiotics administration [270–273].

8.2.2 Aim of the Project

In the present pilot study, GC-MS-based metabolomic analysis was performed on urine samples collected within the first 24 hours of life from preterm neonates exposed or not exposed to histological chorioamnionitis (HC). The aim of this project was then to investigate the ability of urinary metabolomics to discriminate between neonates born to mothers affected by HC and neonates born to mothers without HC, and to analyse the alteration on newborn's metabolism as a result of HC. Indeed, this could be important to understand the influence of chorioamnionitis. To the best of our knowledge, this is the first time urinary metabolomics has been applied to identify neonates exposed to HC.

8.2.3 Population

This project was designed as a pilot, nested case-control study in the context of a single-center observational prospective cohort study. This work was conducted at the neonatal intensive care unit of Fondazione IRCCS Ca' Granda Ospedale Maggiore Policlinico of Milan, Italy, from November 2011 to September 2015. All inborn neonates admitted to the unit with a gestational age < 35 weeks and/or a birth weight (BW) ≤ 1500 g were consecutively enrolled in the observational study. Exclusion criteria were being outborn, the presence of major congenital anomalies, lack of parental consent or a missing pathological examination of foetal adnexa. Cases (n = 15, group 1) were divided into two groups and matched with controls (n = 30, group 2) for gestational age at birth,

BW, sex, and delivery mode. Sample size was established following the method reported by Julious et al. [274]. HCA was diagnosed and graded using Redline's classification [262]. Gestational age was established on the basis of best obstetric estimates, including last menstrual period and first or second trimester ultrasonography. In details, mean gestational age was 30.2 ± 3.8 weeks for neonates born to mothers with HCA and 30.2 ± 2.9 weeks for controls, while the mean BW was 1415 ± 471.9 g for cases and 1426 ± 569.8 for controls. Three cases out of 15 (20%) developed early-onset sepsis and 2 (13.3%) a late-onset sepsis. Moreover, 5 control subjects (16.6%) showed late-onset sepsis. Nevertheless, no significant difference between cases and controls in demographic characteristics, prenatal management or clinical indicators of adaptation to extra-uterine life was observed (Table 8.2.1). Urine samples were collected within the first 24 h of life using a cotton ball in the disposable diaper that was checked every 60-90 min for the presence of urine. Cotton balls contaminated by stools were discarded and replaced. Urines were squeezed from the cotton ball using a sterile 1 mL syringe and immediately frozen and stored at -80°C until analysis, conducted at the Department of Chemical and Geological Sciences of University of Cagliari, Italy. The study protocol was approved by the Ethics Committee of the Hospital and a written informed consent was obtained from parents before inclusion in the study. All procedures were in accordance with the Helsinki Declaration of 1975, as revised in 2008.

Variable	Group 1 (n=15)	Group 2 (n=30)	p value	OR (95% CI)
maternal age (mean ± SD)	35.2 ± 4.1	33.2 ± 7.3	0.23	-
ethnic group				-
- caucasian	12 (80%)	24 (80%)	1	1
- south-american	0	2 (6.6%)	n.a.	n.a.
- black	1 (6.6%)	1 (3.3%)	0.61	2.07 (0.12 – 34.8)
- asian	2 (13.3%)	3 (10%)	0.74	1.38 (0.1 – 13.6)
clinical choriamnionitis	6 (40%)	6 (20%)	0.16	2.67 (0.54 – 12.8)
positive vaginal swab[1]	5 (33.3%)	11 (36.6%)	0.82	0.86 (0.18 – 3.74)
maternal antibiotics	9 (60%)	13 (43.3%)	0.29	1.96 (0.47 – 8.48)
pre-eclampsia	1 (6.6%)	4 (13.3%)	0.65	0.46 (0.01 – 5.49)
prenatal steroids	13 (86.6%)	26 (86.6%)	1	1
caesarean section	12 (80%)	28 (93.3%)	0.18	0.28 (0.02 – 2.92)
gestational age (weeks[2])	30.2 ± 3.8	30.2 ± 2.9	0.97	-
birth weight (grams)	1415 ± 471.9	1426 ± 569.8	0.95	-
male gender	10 (66.6%)	20 (66.6%)	1	-
twin	5 (33.3%)	18 (60%)	0.09	0.33 (0.07 – 1.44)
small for gestational age	0	4 (13.3%)	n.a.	n.a.
Apgar at 1 min (median, range)	5 (1-9)	6 (1-9)	0.20	-
Apgar at 5 min (median, range)	8 (3-10)	8 (3-10)	0.14	-
umbilical venous blood pH value	7.37 ± 0.03	7.34 ± 0.06	0.19	-
resuscitation in delivery room[3]	12 (80%)	24 (80%)	1	1
oxygen in delivery room	10 (66.6%)	13 (43.3%)	0.14	2.6 (0.61 – 12.1)
endotracheal intubation in delivery room	7 (46.6%)	6 (20%)	0.06	3.5 (0.76 – 16.7)
surfactant therapy in delivery room	2 (13.3%)	4 (13.3%)	1	1
early-onset sepsis	3 (20%)	0	n.a.	n.a.
late-onset sepsis	2 (13.3%)	5 (16.6%)	0.81	0.77 (0.06 – 5.57)
death before discharge	3 (20%)	1 (3.3%)	0.2	7.25 (0.5 – 393)

Table 8.2.1: *Clinical characteristics and neonatal outcomes of the study population. Group 1: cases, neonates born to mothers with histological chorioamnionitis; group 2: controls. Fisher's exact-test for categorical variables; t-test or Mann-Whitney Wilcoxon test for continuous variables (OR: odds ratio; CI: confidence interval). [1]) isolated pathogens (1 or more per swab): Streptococcus agalactiae, Escherichia coli, Pseudomonas aeruginosa, enterococci, fungi, Ureaplasma spp, genital Mycoplasmas [2]) completed weeks of gestation [3]) at least ventilation with mask*

8.2.4 Results

Following univariate analysis, 29 metabolites showed significantly different concentration between cases and controls. Except for gluconic acid, the identified metabolites, were characterised by lower concentration in urine from neonates born to mothers with HC (Table 8.2.2).

Metabolite	**1 *vs.* 2**	**p value**	**Metabolite**	**1 *vs.* 2**	**p value**
Monosaccharide E	*Down*	0.0001	Gluconic acid	***Up***	**0.0109(W)**
Succinic acid	*Down*	0.0002	*N*-Acetylglucosamine	*Down*	0.0109(W)
Mannose	*Down*	0.0012(W)	Ethanolamine	*Down*	0.0118
4-Hydroxyproline	*Down*	0.0015	Glyceric acid	*Down*	0.0130
Arabinose	*Down*	0.0017	3-Hydroxy-3-methylglutaric acid	*Down*	0.0149(W)
Erythritol	*Down*	0.0019	Xylose	*Down*	0.0149(W)
Threonic acid	*Down*	0.0019(W)	Lyxonic acid	*Down*	0.0149(W)
Citric acid	*Down*	0.0019(W)	*N*-Acetylneuraminic acid	*Down*	0.0149(W)
Arabitol	*Down*	0.0021	Glycolic acid	*Down*	0.0160
Glucoheptonic acid 1,4-lactone	*Down*	0.0021(W)	Glycine	*Down*	0.0214
Malic acid	*Down*	0.0023	Lactic acid	*Down*	0.0312
Erythronic acid	*Down*	0.0026	U C	*Down*	0.0341
3,4-Dihydroxybutyric acid	*Down*	0.0032	Glucuronic acid	*Down*	0.0346(W)
Threitol	*Down*	0.0079(W)	2-Hydroxyglutaric acid	*Down*	0.0486(W)
Oxalic acid	*Down*	0.0081			

Table 8.2.2: *Urinary metabolomic profile in neonates born to mothers with histological chorioamnionitis (group 1, cases) vs. controls (group 2). Univariate analysis (t-test) between the groups. P value with (W) is calculated by the Mann-Whitney-Wilcoxon test.*

Successively, PCA highlighted 3 samples from the control group as outliers; therefore, 3 samples from group 1 and the 6 matching controls were removed from the analysis. For this reason, 36 specimens (12 cases and 24 controls) underwent PLS-DA (Fig. 8.2.1 and Fig. 8.2.2).

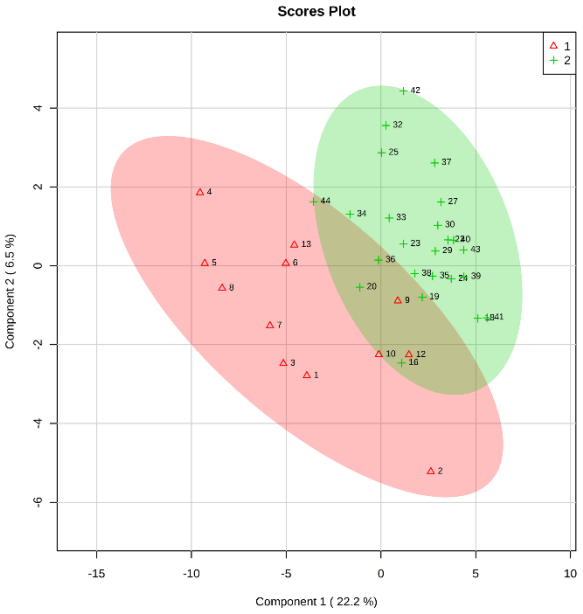

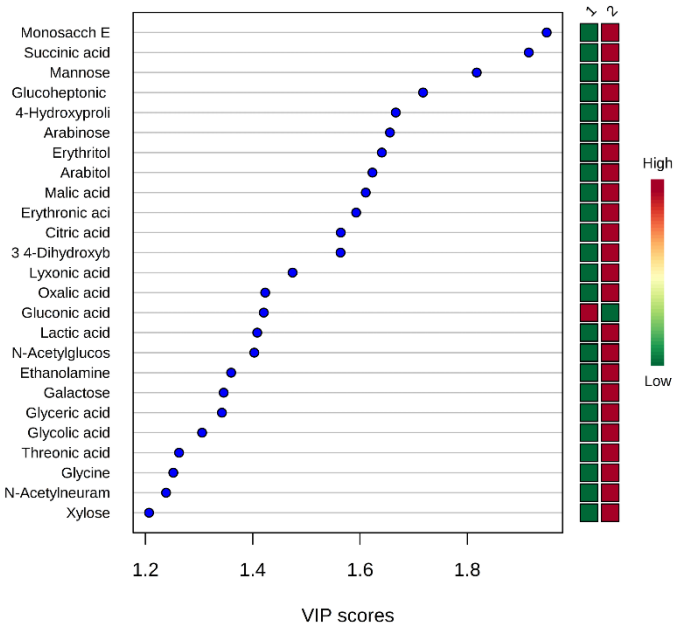

Fig 8.2.1: *2D scores plot showing PLS-DA discrimination between urine samples of neonates born to mothers with HC (group 1, red) and urine samples of controls (group 2, green). Shaded areas indicate the 95% confidence regions.*

Fig 8.2.2: *Summary plot showing the most important metabolites ranked based on VIP score. Group 1) cases; Group 2) controls*

This model was best described by the first four PCs, showing accuracy = 0.79, R^2 = 0.87, and Q^2 = 0.39 by 10-fold CV and corresponding performance measure of p = 0.12. Such values may be attributed to the low number of samples. Among the 131 detected metabolites, those most responsible for the discrimination between the two phenotypes are reported in Fig 8.2.2. These metabolites may be classified into five classes, being: carbohydrates (unknown monosaccharide E, mannose, arabinose, galactose, xylose), amino acids (4-hydroxyproline and glycine), sugar-related polyols (erythritol, arabitol), carboxylic acids (succinic, glucoheptonic, malic, erythronic, citric, 3,4-dihydroxybutyric, lyxonic, oxalic, gluconic, lactic, glyceric, glycolic, threonic, *N*-acetylneuraminic acid), and amine derivatives (*N*-acetylglucosamine, ethanolamine). Similarly to univariate analysis, only gluconic acid revealed higher levels in cases than in controls. Subsequently, MSEA was performed in order to facilitate data interpretation (Fig. 8.2.3). In particular, glutamate metabolism, mitochondrial electron transport chain, citric acid/tricarboxylic acid cycle (TCA), galactose metabolism, and fructose and mannose degradation metabolism were the most significantly altered pathways ($p<0.01$) (Table 8.2.3).

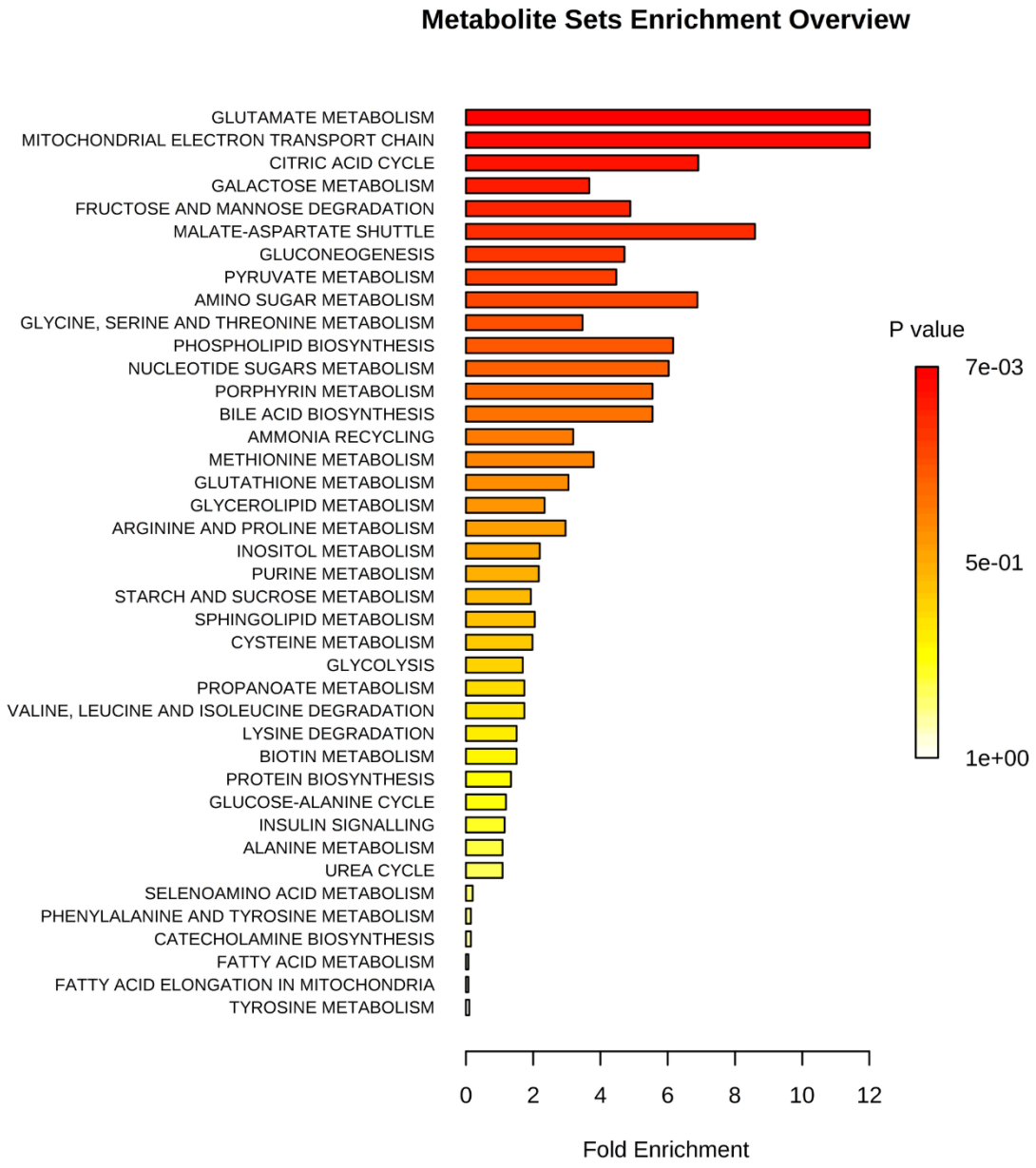

Fig 8.2.3: *Graphical summary of Metabolite Sets Enrichment Analysis (MSEA). Altered metabolic pathways in neonates born to mothers with histological chorioamnionitis compared with controls are shown in order of decreasing P value.*

Metabolite set	Total	Hits	p value	FDR
glutamate metabolism	18	1	0.00017481	0.0034963
mitochondrial electron transport chain	15	1	0.00017481	0.0034963
citric acid cycle	23	5	0.001101	0.012996
galactose metabolism	25	7	0.0014468	0.012996
fructose and mannose degradation	18	3	0.0016245	0.012996
malate-aspartate shuttle	8	1	0.0021231	0.014154
gluconeogenesis	27	4	0.0034039	0.019451
pyruvate metabolism	20	4	0.0046021	0.02301
amino sugar metabolism	15	1	0.0067573	0.030032
glycine, serine and threonine metabolism	26	5	0.009046	0.036184

Table 8.2.3: *Overview of the metabolic pathways most significantly altered ($p<0.01$) in neonates born to mothers with HCA compared with controls. Total indicates the total number of metabolites listed in the pathways; hits indicate the number of significant metabolites identified in the pathways; p value is based on the enrichment analysis.*

8.2.5 Discussion

Metabolomic fingerprinting of urine was able to clusterise the groups of neonates born to mothers with and without HC. All identified metabolites, except for gluconic acid, had a lower concentration in urine from neonates born to mothers with HC compared with controls, even if the statistical significance of the proposed model was affected by the low number of samples. Interestingly, the two most affected metabolic pathways were related to the energy metabolism, including TCA and mitochondrial electron transport chain. Low concentrations of succinic, citric, and malic acid in urine samples from neonates born to mothers with HC may be associated with neonatal mitochondrial dysfunction. This phenomenon may be caused by a systemic inflammatory status triggered by microbial antigens frequently responsible for HC and similar to those observed in septic patients [275]. Therefore, the influence of bacterial metabolism may be considered. Indeed, *N*-acetylglucosamine, *N*-acetylneuraminic acid, 3,4-dihydroxybutyric acid, ethanolamine, and arabinose, which were found decreased in pathological samples. *N*-acetylglucosamine is an amide formed by the condensation of glucosamine and acetic acid and it is a key component of cellular wall of both Gram-positive and Gram-negative bacteria. In particular, *N*-acetylglucosamine is a major component of cell wall peptidoglycan, which contains alternating residues of *N*-acetylglucosamine and *N*-acetylmuramic acid [276]. Reduced amounts of *N*-acetylglucosamine may be related to the higher demand caused by bacterial growth. In addition, the alteration observed for the fatty acid 3,4-dihydroxybutyric acid and the monosaccharide arabinose seems to be a sign of dysbiosis, as was recently reported [277]. Furthermore, the lower concentration of the hexoses

mannose and galactose (along with the not accurately identified monosaccharide E) in urine samples from neonates born to mothers with HC may be a sign of bacterial alterations in the amniotic cavity. Indeed, Romero et al. [6] showed a decreased amount of hexoses, namely mannose and galactose, that might derive from the increased demand of carbohydrates due to bacterial growth. Similar findings were also reported by Dudzik et al. [278] Low hexoses concentration could be explained by the fact that glucose, due to infection may serve as energy source by bacteria and neutrophils. Notably, a previous study described and inverse correlation between glucose and the severity of chorioamnionitis [279]. Another interesting finding was the significant activation of the glycerophospholipid metabolism in neonates born to mothers with HC. This may result in increased production of arachidonic acid, which promotes inflammation and the synthesis of prostanoids that are associated with labour [280]. Regarding the increase in gluconic acid, the action of microbial activity on the pentose phosphate pathway may be hypothesised as potential causes [280]. Indeed, glucose is usually converted to pyruvic acid through glycolysis. However, bacteria can use other metabolic pathways to obtain pyruvic acid and, in particular, the pentose shunt and the Entner–Doudoroff (ED) pathway [281]. Being incapable to phosphorylate glucose to glucose-6-phosphate, some obligate aerobic bacteria initially oxidise glucose to gluconic acid. This compound is then phosphorylated to 6-phosphogluconic and converted into pyruvic acid through the pentose shunt or via ED pathway (Scheme 8.2.1).

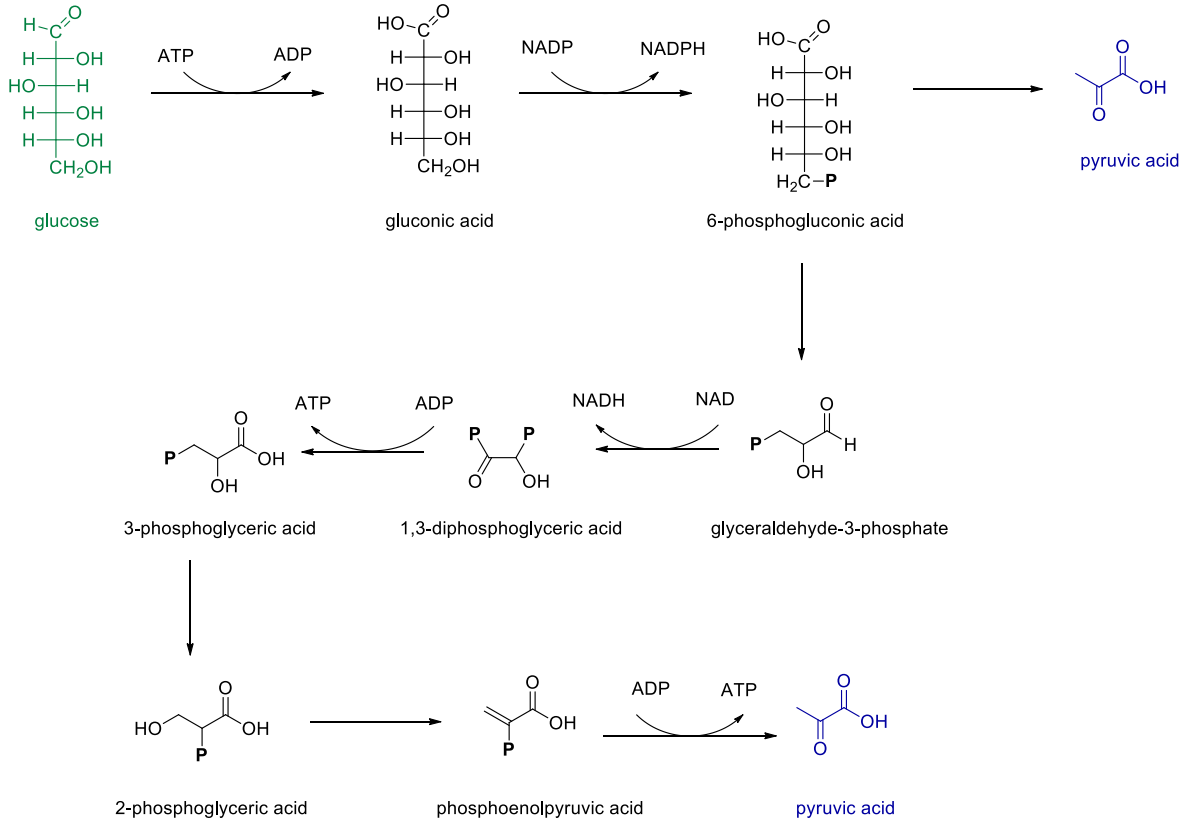

Scheme 8.2.1: *Transformation of glucose to pyruvic acid through ED pathway.* ***P*** *= phosphate*

8.3 Hypothermia Treatment Effects Over the First Month of Life of Asphyxiated Newborns

8.3.1 Perinatal Asphyxia

Perinatal asphyxia is defined as an oxygen deprivation that occurs around the time of birth and it may be caused by perinatal events such as maternal or foetal haemorrhage, intermittent or acute umbilical cord compression, uterine rupture or shoulder dystocia. This medical condition affects circa four million neonates worldwide per year, being lethal for one million subjects [282]. In most cases, infants successfully recover from hypoxia episodes; however, some patients may develop ischemic encephalopathy (HIE), leading to permanent neurological conditions. Moreover, asphyxia and ischemia are responsible for the impairment of different organs and systems (central nervous system 28%, cardiovascular system 25%, kidneys 50%, and lungs 23%) [283]. In particular, HIE seems to affect the terminal electron acceptor in oxidative phosphorylation, and modulation of ATP and ROS. Consequent depolarisation of mitochondrial membranes and increase of intracellular Ca^{2+} may trigger apoptosis. Furthermore, neurological injuries may also derive from glutamate-mediated excytotoxicity and failure of the ATP-dependent ion pumps. Therefore, given its multifactor dependency, the severity and outcome of this disease are of difficult evaluation. For this reason, asphyxia diagnosis is performed assessing several criteria with the two most important being the occurrence of cardiorespiratory or neurological depression and acute hypoxia in the presence of acidemia [284]. Timing and severity of this condition are mainly assessed through Sarnat staging, classifying infant encephalopathy as mild, moderate or severe [285]. Due to the unclear pathological mechanism, a golden standard for treatment has not been defined. For instance, although guidelines are present [286–288], oxygen concentration to be used for neonatal resuscitation is still under debate [289].

8.3.2 Therapeutic Hypothermia

Therapeutic hypothermia is a brain cooling technique applied for 72 h following a hypoxic-ischemic event. This clinical procedure for the treatment of perinatal asphyxia and HIE allowed for the reduction of mortality rate and long-term neurodevelopmental disabilities at 12-24 months of age [290,291]. In details, hypothermia reduces the speed of cerebral metabolism by circa 5% per one-degree fall in temperature, hence delaying the onset of anoxic cell depolarization [292]. Unfortunately, this therapeutic approach is not always efficient and several children continue either to die or to suffer moderate-severe disabilities.

8.3.3 Aim of the Project

The aim of this longitudinal study was to characterise through GC-MS the urinary metabolome of newborns with perinatal asphyxia at the admission to the neonatal intensive care unit (T0) and then to monitor the changes in metabolic levels over time due to hypothermia treatment. In particular, 48 h after starting therapy (T1), the end of therapy (72 h, T2), one week (T3), and one month (T4) from birth were considered for time points. Comparison with adverse outcome was also of interest.

8.3.4 Population

Urine samples were collected from 12 newborns (11 full-terms and one preterm) with perinatal asphyxia were admitted in the neonatal intensive care unit of S. Croce e Carle hospital, Cuneo, Italy. Subjects underwent total body hypothermia treatment for 72 h after birth. Diagnosis was performed by using Sarnat staging [285]. Newborns were treated with hypothermia over 72 hours and urine samples were collected at different time points: at birth, when admitted to the unit (T0); after 48 hours (T1); 72 hours (T2); 1 week (T3); 1 month (T4). A total of 43 specimens were collected for this study. Neurodevelopmental outcome was evaluated at one year of age according to Bayley Scales of Infant and Toddler Development [293]. The project was approved by institutional ethics board of Cagliari (CA-206-18/03/2013) and parents gave written informed consent to the study.

8.3.5 Results

Birth vs. First Month of Life

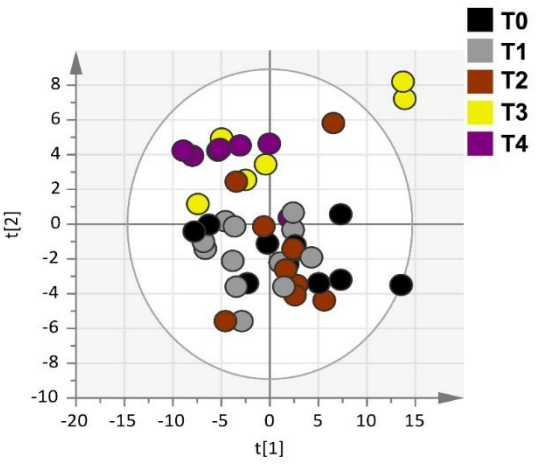

Fig. 8.3.1: *PCA score plot of the samples from asphyxiated newborns collected at five different time points*

To observe the overall changes in subjects metabolome, a first comparison was conducted between specimens collected at birth and those collected at the end of the study. Out of the 12 newborns enrolled in this study, 3 babies died during the 7th day of life. All the deaths were attributable to HIE and comorbid conditions. Although several variables such as clinical conditions (e.g., prematurity), comorbidity, and clinical outcome were present, 2 components-PCA model (R^2 = 0.65 and Q^2 = 0.36), highlighted metabolic changes for each baby, from T0 to T4 (Fig. 8.3.1).

Birth vs. Different Time Points

Urine metabolome at birth, hence before hypothermia treatment, was considered the reference for the monitoring of the metabolic alterations. As reported in Fig. 8.3.2, OPLS-DA model showed clusterisation of T0 samples respect to the other collection times (T1, T2, T3, and T4).

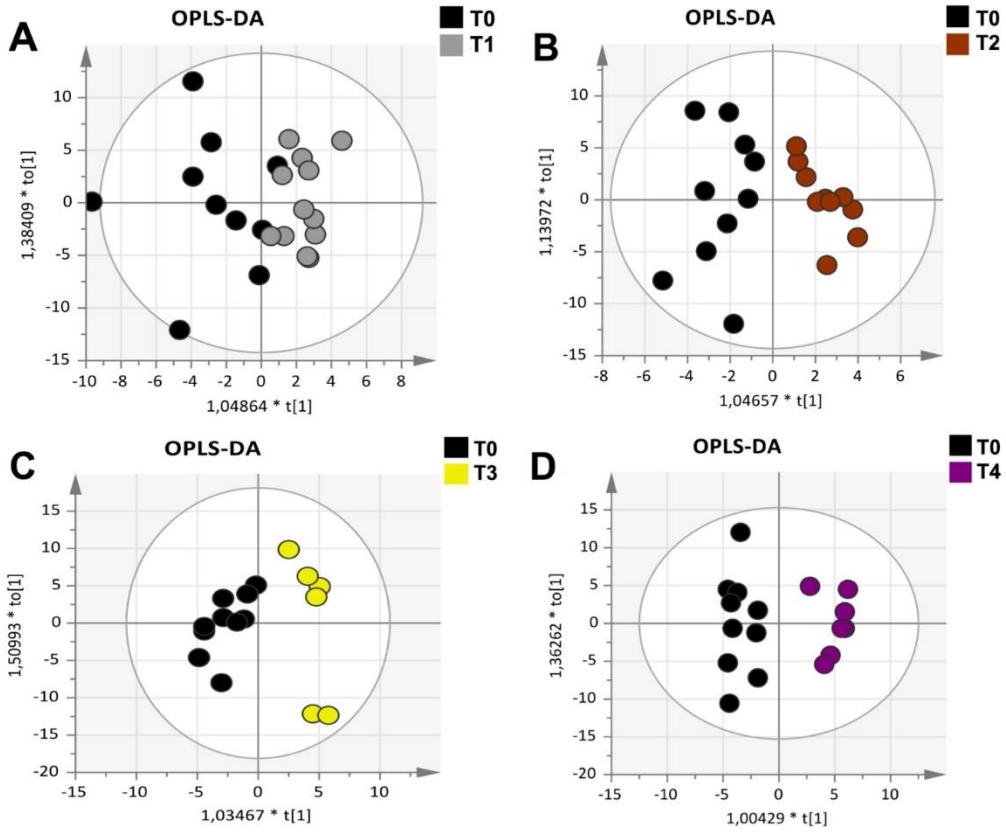

Fig. 8.3.2: *OPLS-DA scores plots for the clusterisation of T0 with A) T1; B) T2; C) T3; D) T4*

After 48 hours of hypothermia (T1), 4 metabolites displayed higher concentrations and 54 lower ones within T1 subjects. At the end of the therapy, i.e. 72 h (T2), 22 features were found increased and 29 decreased. Following 1 week from birth (T3), 24 compounds showed higher levels, while 19 resulted with lower levels. After 1 month from birth, T4 subjects were characterised by an increase in 5 metabolites and a decrease in 33. The most interesting features are reported in Table. 8.3.1.

Trend	T1 *vs.* T0	T2 *vs.* T0	T3 *vs.* T0	T4 *vs.* T0
Increase	Lactose and 1 unknown compound	Lactose, Citric acid, Galactose, Creatinine, 4-Hydroxyproline, and 1 unknown compound	Lactose, Citric acid, Galactose, Creatinine, 4-Hydroxyproline, and Galactitol	Citric acid, Galactose, Galactitol
Decrease	Taurine, Lysine, Mannitol, Oxalic acid, Fructose, N-Acetyl-glucosamine, Kynurenic acid, Sedoheptulose, Ethanolamine, Sucrose, 5-(Acetylamino)-3,5-dideoxy-D-glycero-galacto-2-nonulosonic acid, Scylloinositol, and 3 unknown compounds	Lactic acid, Taurine, Lysine, Mannitol, Fructose, N-Acetyl-glucosamine, Kynurenic acid, Sedoheptulose, Sucrose, 5-(Acetylamino)-3,5-dideoxy-D-glycero-galacto-2-nonulosonic acid, and 2 unknown compounds	Lactic acid, Taurine, Lysine, Mannitol, Oxalic acid, Ethanolamine, Scylloinositol, and 3 unknown compounds	Lactic acid, Taurine, Lysine, Mannitol, Oxalic acid, Fructose N-Acetyl-glucosamine, Kynurenic acid, Sedoheptulose, Ethanolamine, Sucrose, 5-(Acetylamino)-3,5-dideoxy-D-glycero-galacto-2-nonulosonic acid, Scylloinositol, and 4 unknown compounds

Table 8.3.1: *Most relevant changes in metabolites concentration over time in perinatal asphyxia*

Interestingly, lactic acid, taurine, lysine, and mannitol systematically decreased from birth. Conversely, lactose increased as well as citric acid and galactose from T2 to T4. Table 8.3.2 reports the area under the curve (AUC) for each metabolite.

Metabolite	T1	T2	T3	T4
Lactic acid	0.74	0.75	1.0	0.87
Taurine	0.66	0.70	0.98	0.91
Lysine	0.62	0.65	0.67	0.83
Mannitol	0.65	0.65	0.67	0.87
Lactose		0.65	1.0	
Citric acid		0.90	0.98	0.97

Table 8.3.2: *AUC values for lactic acid, taurine, lysine, mannitol, lactose, and citric acid. These metabolites systematically increased or decreased over time*

Metabolic Differences Among Newborns Outcomes

Notably, significant differences were observed between the urinary metabolome of the three babies died after 7 days and that of survivors. This remarkable difference was revealed at birth, before the beginning of hypothermia treatment, and it persisted till the end of therapy (T2) (Fig. 8.3.3).

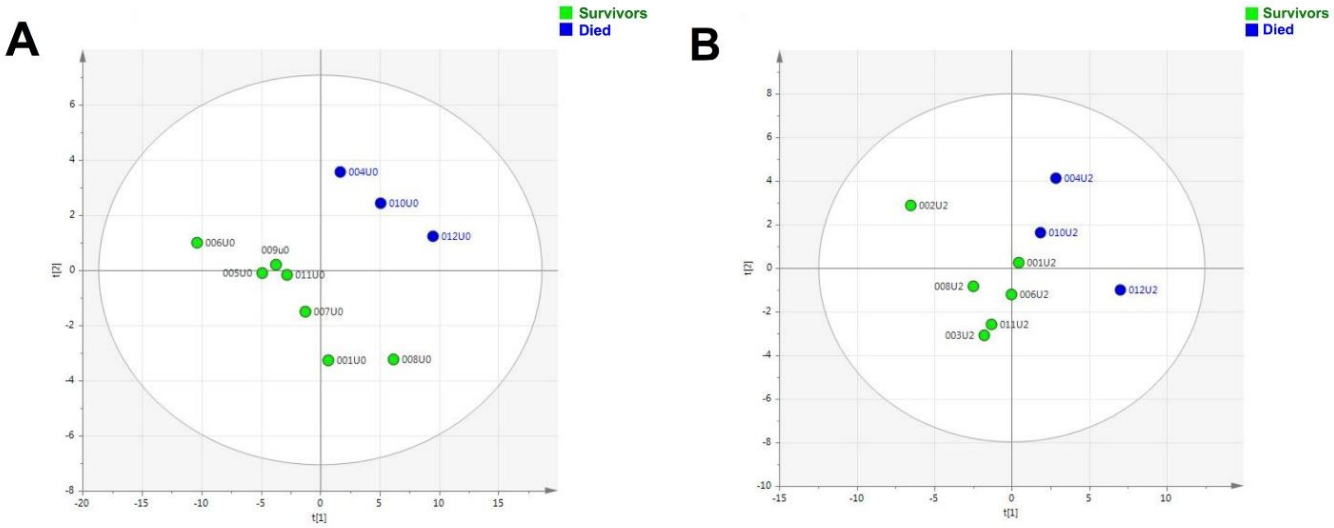

Fig. 8.3.3: *PLS-DA of urine metabolome at T0 and at T2. In this plot, PLS-DA enables class separation between survivors and died newborns.*

Pathway Analysis

Pathway analysis was then applied to underline the most influencing metabolic pathway within a certain phenotype (Fig. 8.3.4 and Fig.8.3.5). During hypoxia (T0, T1, and T2), the most impacting were phenylalanine metabolism, fructose and mannose metabolism, pyrimidine metabolism, glycolysis or gluconeogenesis, starch and sucrose metabolism, pentose phosphate pathway. At T3, molecular phenotypes differed by four pathways: tyrosine metabolism, phenylalanine, tyrosine and tryptophan biosynthesis, ubiquinone and other terpenoid-quinone biosynthesis, nitrogen metabolism. Analysis with T4 delivered similar results.

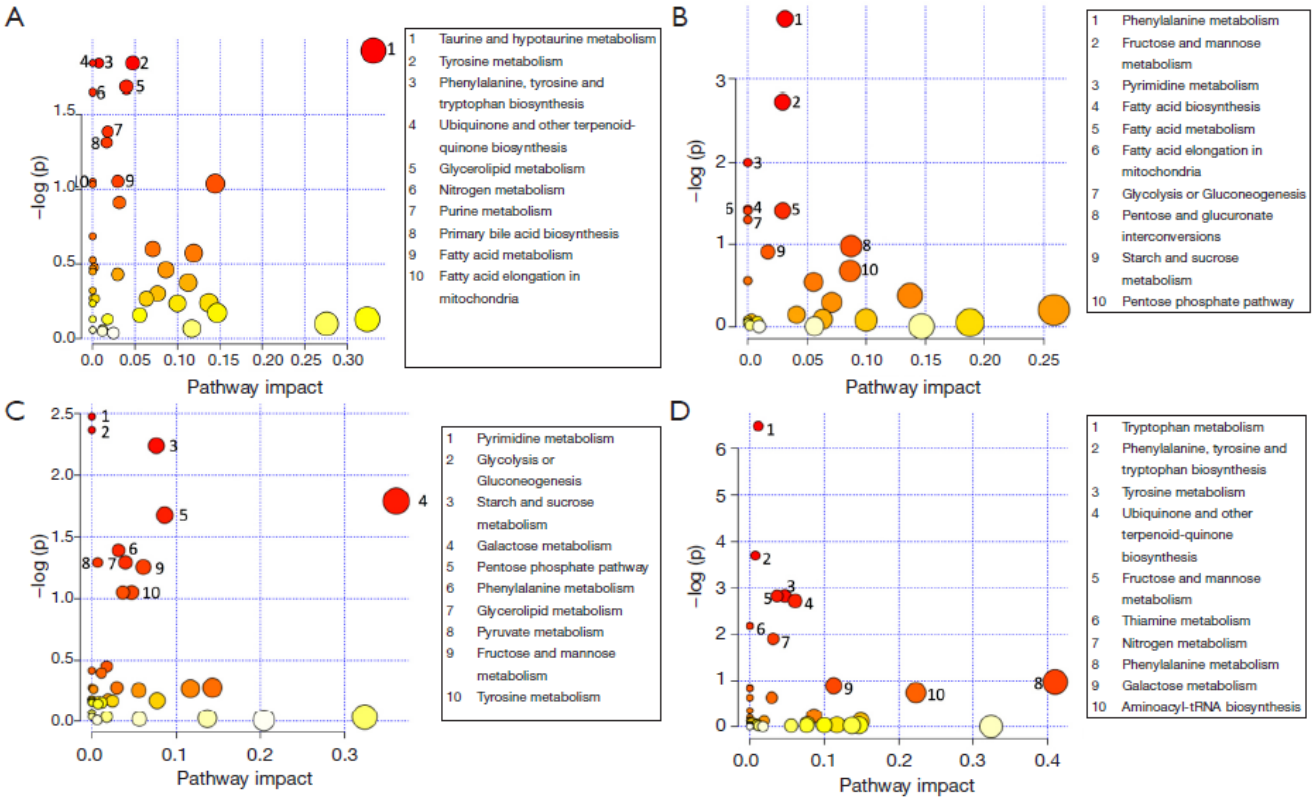

Figure 8.3.4: *Metabolic pathway analysis at A) T0; B) T1; C) T2, and D) T3*

8. 3.6 Discussion

Systematic Trends Related To Status At Birth

Evidence from this study suggest a progressive change over time in urine metabolome of babies with perinatal asphyxia treated with hypothermia. Several discriminant metabolites have been found persistently decreasing (i.e. lactic acid, taurine, lysine and mannitol) or increasing (citric acid, lactose, and galactose) over time. The decreasing trend of lactic acid over time may indicate the progressive recovery of aerobic metabolism. Notably, lactic acid was found significantly increased in the three dead babies, at both T0 and T2. In the developing brain, this metabolite act as exchangeable substrate between astrocytes, the more abundant neuroglial cell type, and neurons. It is both a precursor of lipids and an energy source for neurons. During hypoxia-anoxia, astrocytes consistently increase the lactic acid production rate by the activation of anaerobic glycolysis pathway, with a progressive accumulation of this metabolite and, in turn, acidosis. In particular, the latter phenomenon exerts a negative impact on astrocyte metabolism, leading to

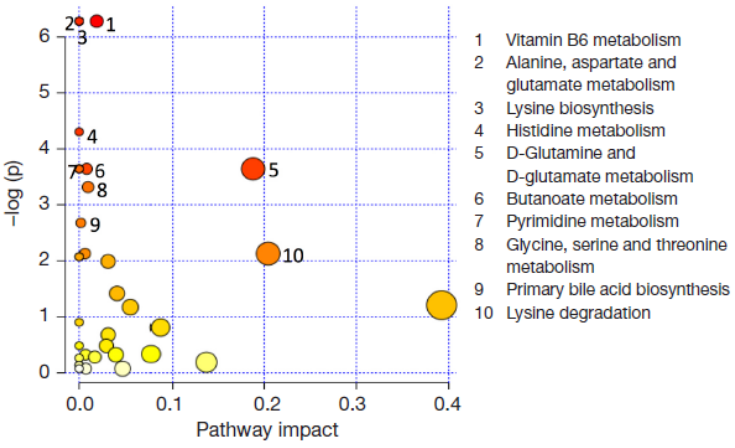

Fig. 8.3.5: *Metabolic pathway analysis at T4*

serious and irreversible astrocytes damage and cytolysis [294]. Furthermore, the progressive loss in astrocytes number triggers a redox imbalance caused by a massive generation of ROS. Therefore, in addition to deprivation of energy source deriving from astrocytes, neurons are further damaged. Interestingly, lactic acid was previously reported as a biomarker for poor outcome in perinatal hypoxia and HIE [295]. Similarly to lactic acid, taurine decreased over time from T1 to T4 and it was found increased at T2 in the group of dead babies. Taurine is synthesised from methionine and cysteine in the presence of vitamin B6. This metabolite is involved in the maintenance of intracellular sodium and calcium homeostasis and in the balance of neurotransmitters. Moreover, taurine and its analogues exert anti-neurotoxic and anti-inflammatory effects [296]. Being an intracellular metabolite, alterations in plasma membrane permeability and cytolysis produces accumulation of extracellular taurine and therefore it may be considered a biomarker of cellular injury and death. As a consequence, the decrease over time in urinary taurine concentration can be explained by the progressive recovery of injured tissues and organs. Conversely, the high taurine urinary level in the group of dead babies may be indicative of cellular necrosis and death due to hypoxia. The importance of this metabolic compound was also supported by Pathway analysis. Lysine trend over time was similar to that of lactic acid and taurine. Lysine is an essential amino acid mainly involved as a precursor in protein biosynthesis; furthermore, lysine is a precursor in the biosynthesis of free carnitine and its esterified form acylcarnitine, two key metabolites for β-oxidation. In hypoxia-ischemia, the decrease of fatty acid oxidation causes an increase in carnitines concentrations [297]. At birth, higher urinary levels of lysine may be associated with the increasing need of energy source by cells during hypoxia. Indeed, lysine can be used as an alternative fuel for cells, partially replacing the unavailability of aerobic metabolism [298]. It may be reasonable that the progressive decrease of mannitol over time together with its accumulation in the urine of dead babies at T2 may be due to the presence of this metabolic inert substrate within pharmaceutical products as excipient [299]. Therefore, its decrease may be related to the reduction in drugs administration due to the amelioration of clinical conditions, while its increase in dead babies at T3, may be caused be the intensification of therapy in critical clinical conditions. Since persistent brain hypoxia and ischemia lead to brain hyperosmolality [300], the simultaneous increase of mannitol exacerbates the process [301]. Nevertheless, the hypothesis of gut dysbiosis in these babies cannot be excluded. In particular, Clostridium sp. HGF2, Streptococcus sp. M143, Streptococcus sp. M334 were found to be significantly associated with mannitol [302]. On the other hand, the dysbiosis-induced hyperpermeability of the gut mucosa should contribute to increased mannitol excretion [303]. Citric acid was found persistently increasing from T1 to T4 when compared with T0. Citric acid is an intermediate in the TCA cycle. This metabolic pathway is the central metabolic hub of the cell,

being the gateway to the aerobic metabolism of any molecule that can be transformed into an acetyl group or dicarboxylic acid. In addition, TCA cycle is a source of precursors for the building blocks of amino acids, nucleotide bases, cholesterol, and porphyrin. The increase of citric acid over time can be correlated with the progressive re-activation of oxygen-dependent ATP production pathways, namely the TCA cycle. Interestingly, survivors were characterised by higher levels of 2-ketoglutaric acid, an intermediate of TCA cycle, both at birth and at T3. This strongly supports the hypothesis that, while in these babies aerobic pathways have been re-activated, it has not been prompted within dead babies' group. Regarding carbohydrates alterations, decrease of fructose together with the simultaneous increase of lactose, galactose, and galactitol can be observed. Fructose is metabolised in the liver, primarily to glycogen; the accumulation of fructose at birth and the subsequent decrease are consistent with the recovery of liver function over time. Lactose, a disaccharide of D-glucose and D-galactose, is present in milk and is the principal dietary source of galactose. Lactose is the primary carbohydrate source for developing mammals and in humans, constituting 40% of the energy consumed during the nursing period. Therefore, an explanation for the progressive increase of lactose, galactose, and galactitol may reside in feeding. Another increased molecule throughout recovery was 4-hydroxyproline. Interestingly, enzymatic hydroxylation of proline during hypoxia is involved in proteolysis of hypoxia-inducible factor alpha subunit (HIF-1α) [304]. Being HIFs transcription factors responding to changes in available oxygen within the cellular environment, hydroxyproline higher levels may be due to the positive response of the organism to the hypoxic condition. Related to it, the high level of proline in dead babies at birth may be considered as an absence of proline hydroxylation. Moreover, degradation of 4-hydroxyproline results in the formation of glyoxylate, which is converted into oxalate through glyoxylate reductase (GR) [305]. Nevertheless, the progressive decrease over time of oxalic acid may be due to the utilisation of this metabolite for the synthesis of uracil and orotic acid [306], involved in the cellular replication occurring during tissues and organs recovery after hypoxia.

Metabolisms Differences at Different Time Points

Among the metabolisms highlighted by Pathway analysis for T0, tyrosine and ubiquinone seemed to play a particularly important role. Indeed, tyrosine is a precursor of neurotransmitters via transformation of dopamine in L-norepinephrine and then in L-epinephrine. Since chronic hypoxia/ischemia may reduce these enzymes' activity, causing neuronal deficiency, an involvement may be expected [307]. Regarding ubiquinone, its implication may be explained through its production of ROS; however, the role of mitochondrial ROS in the regulation of HIF-1 under hypoxia is still unclear [308]. Other relevant metabolisms, i.e. glycerolipid, purine, and fatty acids metabolisms, may

be related to the need for fuel to maintain cellular homeostasis. Considering the metabolic pathways at T1, activation of phenylalanine metabolism was observed together with processes connected to glycolysis, gluconeogenesis, or fatty acid. While the first metabolic pathway may be indicative of neurotransmission alteration, the others are implied in energy supply. Calculations on T2 group underlined pyrimidine biosynthesis as the most relevant pathway, being of importance for cell proliferation and for TCA cycle intermediates. Interestingly, eight other metabolisms provide energy after a period characterised by lactic acid overproduction and depletion of ATP. The similarity between T3 and T4 suggested the achievement of recovery by the activation of energetic pathways such as the TCA cycle.

8.4 Monitoring of Necrotising Enterocolitis

8.4.1 Necrotising Enterocolitis

Necrotising enterocolitis (NEC) is a clinical condition characterised by variable damage of the gastrointestinal tract and involving acute inflammatory response, altered bacterial colonisation, and damage from immaturity and compromised mucosa. For these reasons, NEC is considered one of the most adverse events in preterm neonates. The incidence of this occurrence varies depending on the geographic area: 1-8% in Western countries and up to 20% in South Asia. Although its onset is variable, most cases of NEC are reported around 30 weeks of life [309,310]. The exact aetiology of this pathology is still not understood. Indeed, multiple risk factors such as hypoxia, feeding, sepsis, abnormal colonisation of the bowels are thought to influence NEC occurrence. In particular, it seems that recently colonised gut, enteral nutrition, and the rupture of the mucosal integrity may induce translocation of bacteria. These species may then release endotoxins and other mediators in the bloodstream. It is hypothesised that this may be the reason why is NEC incidence is higher in preterm than term infants. Indeed, the immature intestine of preterm infants may display an abnormal inflammatory response compared to a mature intestine. Subsequently, the immune system is more susceptible to pro-inflammatory and anti-inflammatory stimuli and, together with the different gut bacterial colonization and the abnormal expression of some factors such as the toll-like receptor, the onset of food intolerance in preterm children results more frequent [311–317]. Another supporting evidence is that after the 32 weeks of life, the number of NEC cases dramatically decreases, probably due to the complete maturation of the intestine. The application of feeding guidelines, human milk feeding, the use of probiotics, and novel management approaches significantly reduce the onset of conditions such as feeding intolerance. Nevertheless, NEC still represents the most frequent intestinal emergency in most of Western countries and its prevention is

one of the most challenging targets because of the dangerous consequences of mortality and morbidity [318–324].

8.4.2 Aim of the Project

In this study, both ^{1}H-NMR and GC-MS platforms were applied to reveal and monitor changes in the urinary metabolome of NEC affected infants. The window of time considered for this purpose was of about two months: from birth (i.e. prior to NEC onset), at the time of NEC onset, and after the disease onset.

8.4.3 Population

A total of 18 neonates with gestational age < 32 weeks (NEC n = 6, healthy controls n = 6, infants with feeding intolerance who did not developed NEC n = 6) were recruited from the neonatal intensive care unit of Hospital de la Croix Rousse, Hospices Civils de Lyon, Lyon, France (Table 8.4.1). NEC cases were confirmed by clinical and imaging findings according to algorithms of differential diagnosis [325,326]. Each NEC infant was matched with one healthy newborn and one food intolerant infant based on gestational age (± 1 week) and sex. The study was approved by the local Ethics Committee and informed consent forms were signed by infant parents prior to participation.

Variable	**NEC (n = 6)**	**Controls (n = 12)**	
		Infants with food intolerance (n = 6)	**Healthy (n = 6)**
Gestational age (weeks)	25+3 - 29+0	26+3 - 29+4	25+6 - 30+0
Male/Female (number)	3/3	3/3	3/3
Cesarean section delivery (number)	2	5	3
IUGR[a] (number)	1	5	1
Onset of NEC (days)	7 - 54	--	--

Table 8.4.1: *Characteristics of population*

Urines of infants were collected weekly between September 2014 and July 2015, from birth until 8 weeks of life. The first criterion for inclusion in the study was the achievement of a minimum number of 5 samples. Each urine sample (1-2 mL) was collected using a non-invasive method with a ball of cotton inserted into the disposable diaper, aspired with a syringe, transferred to a sterile 2

mL vial and then frozen at -80°C. Samples were air shipped, packed in dry ice, to the University of Cagliari for the metabolomic analysis.

8.4.4 Results

Application of PCA on NMR and GC-MS data revealed no clusterisation among samples according to the clinical status of the subjects: healthy newborns, infants with food intolerance, or NEC cases. Therefore, HCA based on the first three PCs of the previous model was performed to better visualise possible grouping relationships. Results are shown in Fig. 8.4.1. In HCA dendrogramme, the vertical axis is a measure of cluster similarity: the further the distance between two clusters, the less similar they are respectively. Both dendrogrammes delivered similar results, suggesting clustering depending on infant age rather than clinical status. Notably, two major groups could be distinguished. Group 1 included mainly urine samples from infants younger than 25 days and some from NEC infants older than 40 days. Group 2 comprised mainly urine samples from infants older than 25 days.

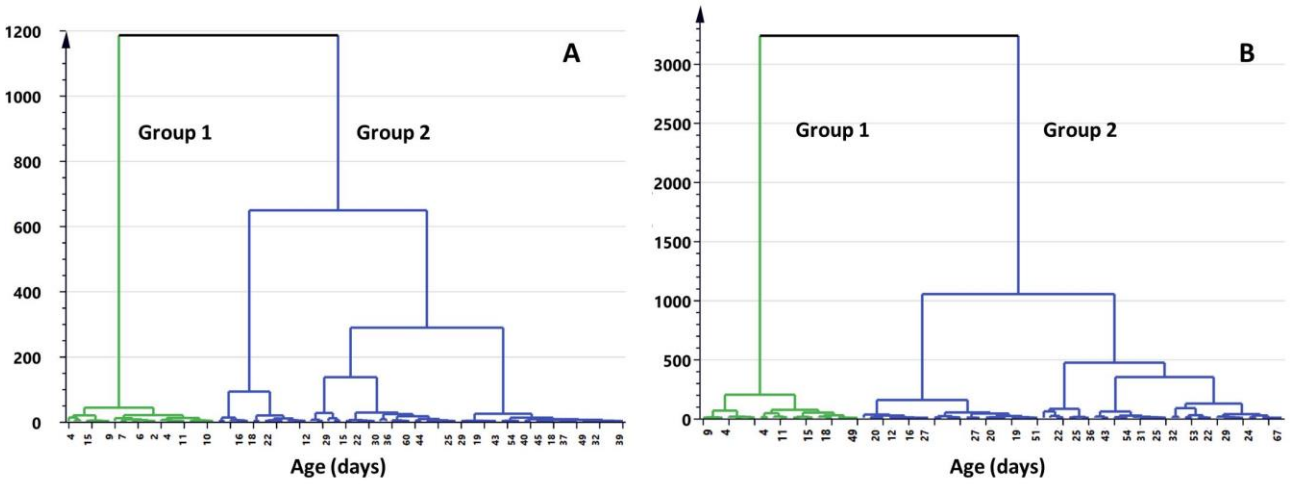

Figure 8.4.1: *HCA dendrogrammes based on 3 PCs obtained from PCA models of A) NMR and B) GC-MS data sets. Dendrogrammes were calculated with Ward clustering method and sorted by size.*

Consequently, the effect of time on urinary profile was explored by means of PCA (NMR model: $R^2 = 0.474$ and $Q^2 = 0.398$; GC-MS model: $R^2 = 0.406$, $Q^2 = 0.353$) (Fig.8.4.2). Interestingly, while healthy newborns (circles) were separated depending on their age, NEC cases (stars) reflected the disease onset.

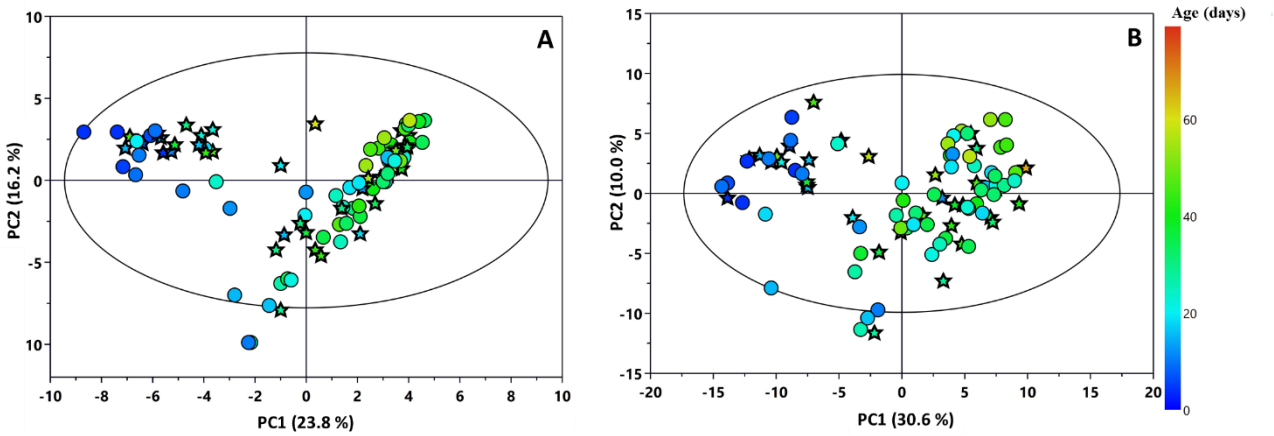

Figure 8.4.2: *PCA scores plot of A) NMR (A) and GC-MS (B) data from all infants collected at different time points from birth over an average period of two months of life. Samples are coloured according to infant age. Stars denotes NEC*

For a better visualisation, Fig. 8.4.3 displays the same plot as in Fig. 2A; however, NEC points of each infant are individually highlighted and arrows show the metabolic change over time. Notably, the time-dependent shift of NEC newborns with early-onset (within 20 days of life) followed the same direction as those of healthy and intolerant subjects (Figures 8.4.3A-C). Conversely, NEC newborns with late-onset (after 40 days of life) showed similar direction only until disease onset. Successively, the metabolome of these patients become similar to that of the first days of life (Figures 8.4.3 D-F).

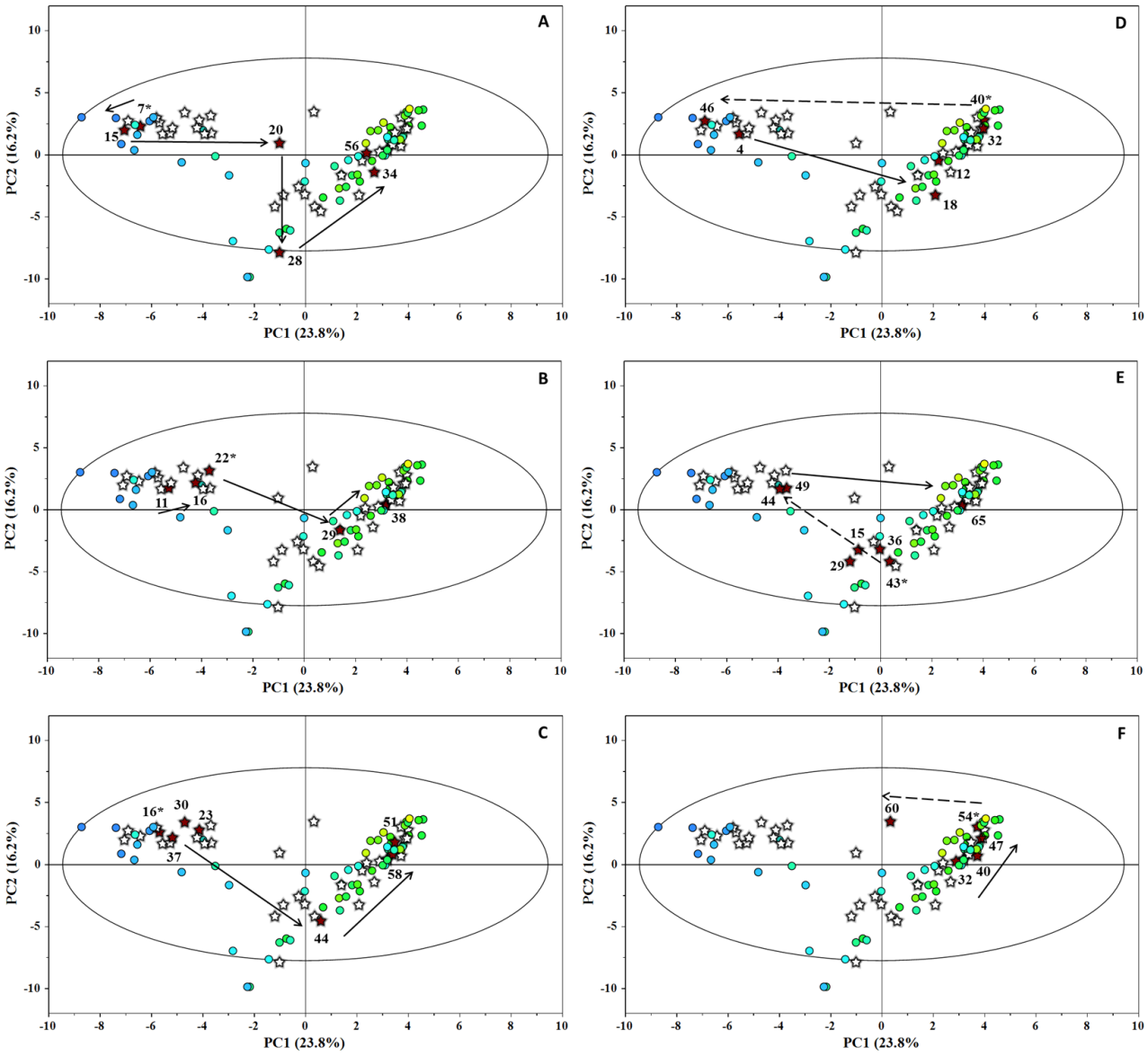

Figure 8.4.3: *Individual metabolic trends of 6 NEC (☆) infants by PCA scores plot of ^{1}H-NMR data set. Numbers indicate NEC infant age in days while * indicate the day of disease onset: A-C) Early onset; D-F) Late onset*

In order to compare the temporal progression of the urine metabolome in relation to the clinical state of infants, PCA models were built for each group of recruited newborns. In particular, due to the different behaviour between NEC infants, these subjects were divided into two sub-groups: early- and late-onset NEC. Fig. 8.4.4 and Fig. 8.4.5 display the score plots of the PCA models built with NMR and GC-MS data together with the metabolites that mostly contributed to the clusterisation. Changes in the urinary metabolome of healthy (Fig. 8.4.4A and Fig. 8.4.5A) and intolerant (Fig. 8.4.4B and Fig. 8.4.5B) infants were very similar. In particular, such alterations included elevations of betaine, choline, glycine, creatinine, *N*,*N*-dimethylglycine, and α-ketoglutaric acid as the infant age increased and decrease in gluconate, fucose, and *N*-acetyl compounds. Higher levels of betaine, glycine, and α-ketoglutaric acid as well as lower levels of the gluconate over time

were also observed in the metabolic changes of early- (Fig. 8.4.4C and Fig. 8.4.5C) and late-onset NEC cases (Fig. 8.4.4D and Fig. 8.4.5D), the latter only until the disease onset. Additionally, both NEC sub-groups exhibited increasing levels of threonine, hydroxyproline, fucose, and *N*-acetyl compounds over time.

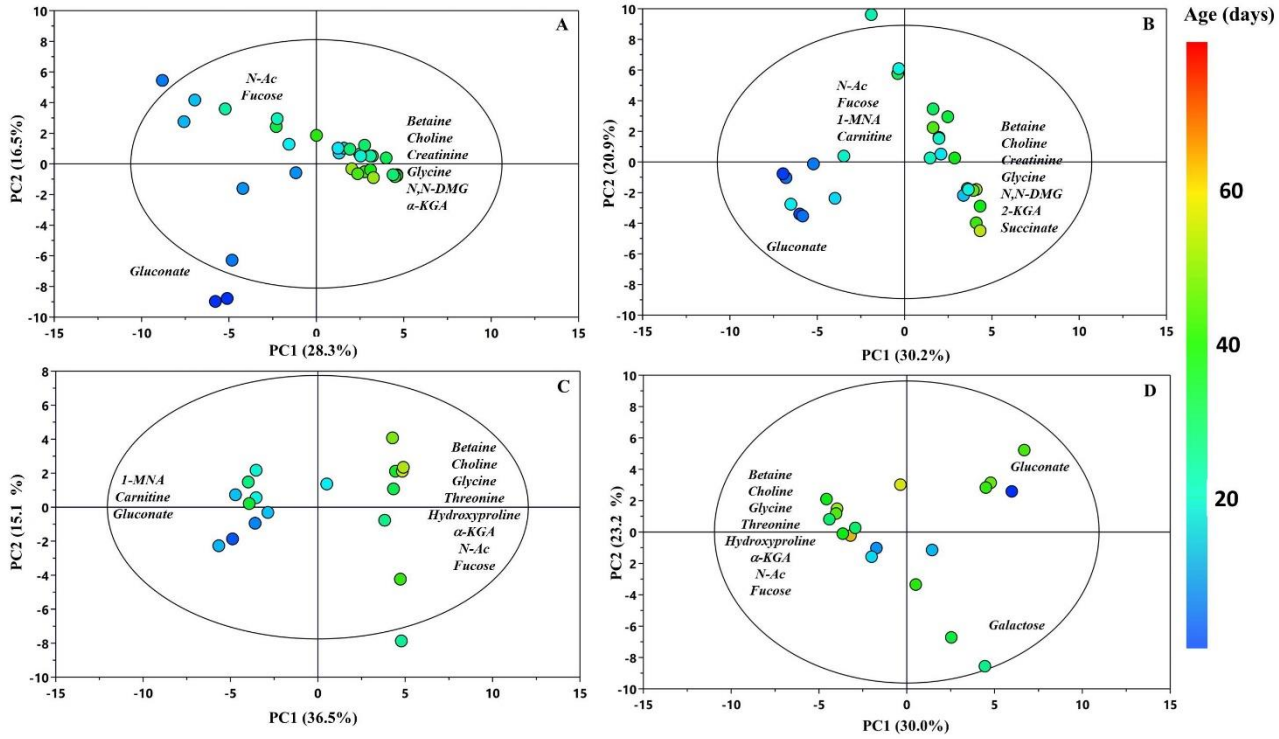

Figure 8.4.4: *PCA scores plots of the ^{1}H-NMR data from A) controls, B) infants with food intolerance, C) early-onset, and D) late-onset NEC. Samples are coloured according to the infant age. N-Ac: N-Acetyl compounds; N,N-DMG: N,N-Dimethylglycine; 1-MNA: 1-Methylnicotinamide; α-KGA: α-Ketoglutaric acid.*

Furthermore, in order to investigate the metabolic differences between early- and late-onset NEC, both groups were separately compared to control patients (healthy and intolerant). Therefore, only data prior to or on the day of disease onset were explored. As reported in Table 8.4.2, only the late-onset NEC vs. controls ^{1}H-NMR model reached statistical significance. The discriminant metabolites for this model are shown in the color-coded coefficient loading plots (Fig. 8.4.6). In details, upward the resonance peaks indicate increased levels of that metabolite in NEC group, while downwards peaks indicate a decrease. Colour is (ii) the hot coloured metabolites (e.g. red) show more significant contribution than the cold coloured (e.g. blue) ones for the intergroup discrimination. Therefore, the separation between late-onset NEC and controls was driven by higher levels of lactate, alanine, and *N*-acetyl compounds and lower levels of gluconate in NEC infants.

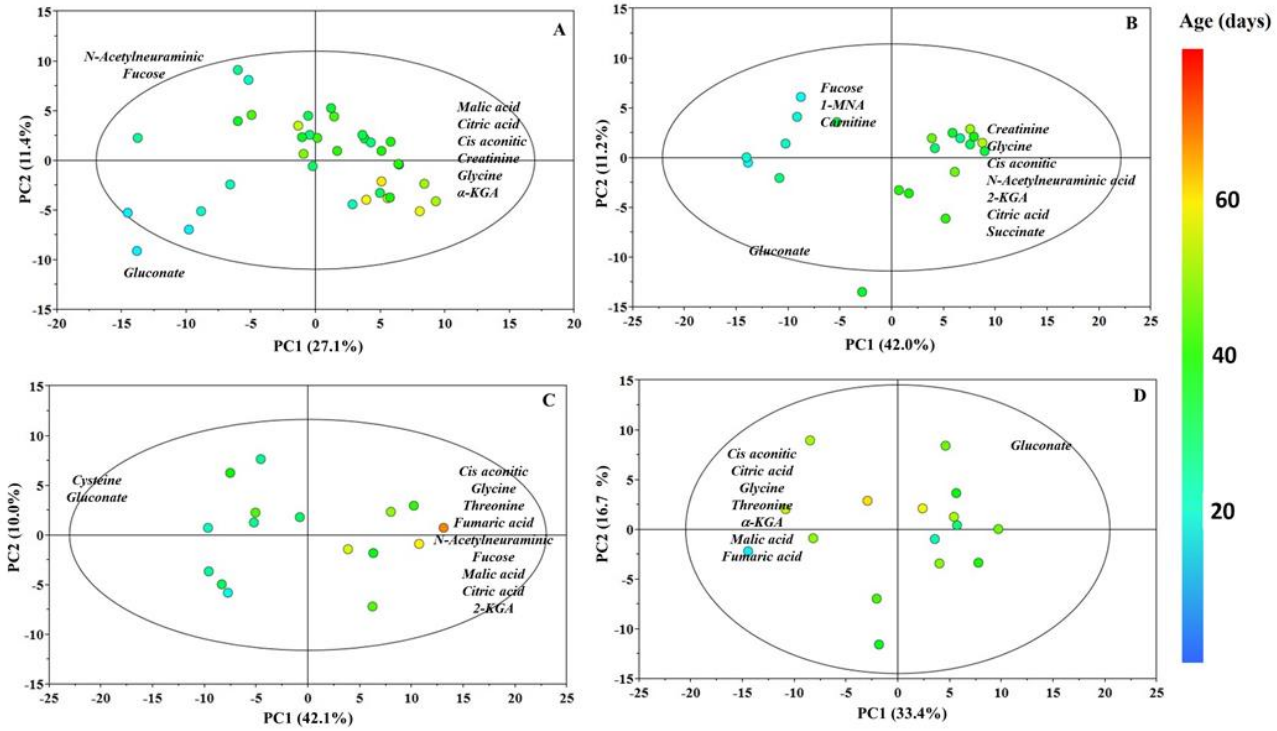

Figure 8.4.5: *PCA scores plots of the GC-MS data from A) controls, B) infants with food intolerance, C) early-onset, and D) late-onset NEC. Samples are coloured according to the infant age*

Analytical Method	Phenotypes	Permutation test					
		R^2X	R^2Y	Q^2Y	R^2Y intercept	Q^2Y intercept	p value
NMR	Early-onset NEC *vs.* controls	0.710	0.996	0.908	0.956	-0.393	0.321
	Late-onset NEC *vs.* controls	0.469	0.813	0.297	0.688	-0.499	0.018
GC-MS	Early-onset NEC *vs.* controls	0.403	0.930	-0.233	/	/	/
	Late-onset NEC *vs.* controls	0.327	0.625	0.044	0.507	-0.333	0.721

Table 8.4.2: *Statistical parameters for the OPLS-DA models built with ^{1}H NMR and GC-MS data*

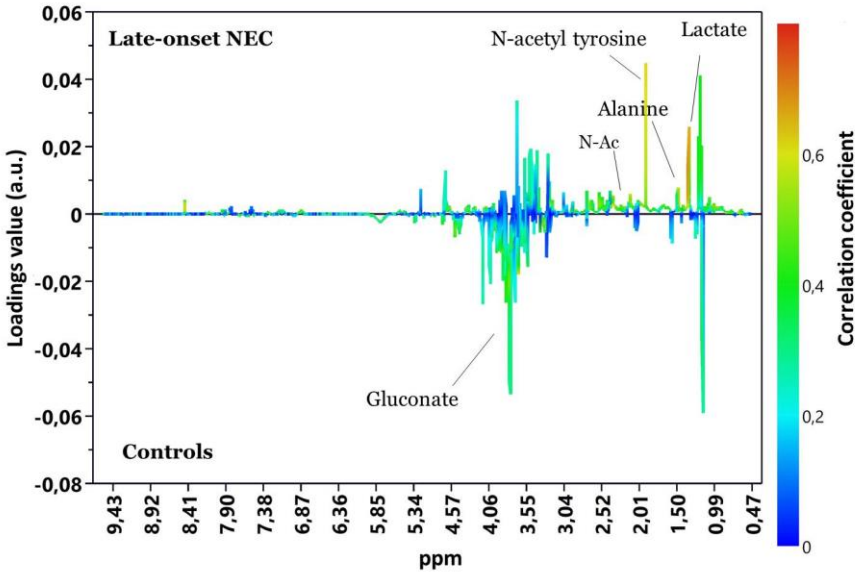

Figure 8.4.6: *OPLS-DA coefficient plots for the models built from the urinary ^{1}H-NMR profiles of late-onset NEC and controls groups, including only urine samples collected prior to or on the day of disease*

8.4.5 Discussion

Age-dependent Trends

Results suggested significant time-dependent metabolic changes for all infants, and in particular for NEC cases, depending on the disease onset. Indeed, while early-onset NEC profiles exhibited the same temporal alteration as controls, late-onset NEC profiles drastically change from the latter group after disease occurrence. The analysis of the temporal metabolic urinary modifications for the three groups of infants identified elevation of choline, betaine, glycine, and α-ketoglutaric acid levels over time. Choline and betaine are two metabolites closely related due to the synthesis of the latter from the former [327]. Choline can either be introduced by diet or autonomously produced by sequential methylation of phosphatidylethanolamine and it is a precursor of membrane, lipoprotein, phospholipids, and the neurotransmitter acetylcholine. For this reasons, choline is an important molecule for cell membranes integrity, lipid metabolism, and cholinergic nerve function. Interestingly, increase of both choline and betaine levels was observed in previous works [328,329]. Regarding glycine, this amino acid is involved in several biological processes such as energy release and synthesis of DNA, phospholipids, and collagen. Moreover, it is a precursor of glutathione, purine nucleotides and porphyrins and it contributes to the biosynthesis of creatine phosphate and folate derivatives [330]. α-Ketoglutaric acid is a key intermediate in the Krebs cycle, playing an important role as nitrogen transporter in metabolic pathways. The impact of time on healthy and intolerant subjects involved a significant increase in *N,N*-dimethylglycine and creatinine levels over time. The concentrations of these two metabolites has been documented to be

age-dependent and positively correlates with body weight/muscle metabolism [331,332]. Showing a different behaviour from controls, hydroxyproline, threonine, fucose, and *N*-acetyl derivatives were found increased in NEC patients. While hydroxyproline is involved in collagen production, hence elevated levels may be an early symptom of tissues degradation, concomitant elevated glycine and threonine levels are supported by previous studies [333]. Interestingly, fucose levels can be associated with early state of intestinal inflammation and liver disease [334,335].

Different Trajectory of Late-onset NEC Group

A significant increase in gluconic acid after disease onset in the late group was detected. Due to the lack of gluconate supplements in the NEC treatment of the patients under investigation, the increase of this metabolite is supposed to be of endogenous nature. This metabolites may be synthesized through the pentose phosphate pathway or microbial activity [336]. Pentose phosphate pathway is an alternative pathway to glucose oxidation and it may provide protection against oxidative stress in several conditions such as hypoxia and excessively fast cells proliferation including malignant cases. Moreover, abnormal concentrations of certain sugars and polyols in body fluids occur in several inborn errors of carbohydrate metabolism. Indeed, normal human gut bacteria are able to degrade and use polysaccharides, including both host-synthesized glycans and diet-derived polysaccharides resistant to host-mediated degradation, by means of enzymes and transporters.

Late-onset NEC vs. Controls

Late-onset NEC specimens were characterized by higher levels of lactate, alanine, and *N*-acetyl compounds and lower content of gluconic acid. Although the mechanisms behind these findings are of difficult interpretation, the increase of the glycolysis end products, lactate and alanine, may be related to energy metabolism impairment. Nevertheless, the statistically significant differences with controls, potentially highlighted a metabolic fingerprint for NEC predisposition. However, further investigation are necessary.

8.5 PROM: Effect of the Onset of Labour

8.5.1 Premature Rapture of Membrane

The early diagnosis of pregnancy-related complications and the prediction of pregnancy outcome are considered strategic clinical goals to ensure the health of mothers and of their babies. Among these, premature rupture of membranes (PROM) consists of the rupture of the foetal membranes before the onset of labour. It can be observed at any gestational age [337] and occurs in approximately 10% of pregnant women and in roughly 40% of preterm deliveries [338]. Foetal membranes are of

pivotal importance because offer a robust barrier against infection ascending from the reproductive tract; after their rupture, both mother and foetus are at risk of infection and other complications. The most commonly diagnosed maternal infections in case of PROM are chorioamnionitis and endometritis, which may be further promoted by frequent vaginal exams and the presence of meconium in AF [339]. Foetal complications of PROM include neonatal sepsis, abnormal foetal presentation, cord prolapse or compression, abruptio placentae, and it may increase the risk of neonatal intraventricular haemorrhage, leading to neurodevelopmental disability as a direct consequence [340]. Therefore, from PROM diagnosis may derive different medical procedures such as hospitalization, antibiotic prophylaxis, and induction of labour through oxytocin [341,342], i.e. increased medicalization and caesarean section rates. These practices may in turn affect several women in the positive experience of birth [343]. Moreover, given the increasing antibiotic resistance, alerts have been issued about the use and abuse of prophylactic antibiotics administration [344]. Indeed, growing evidences on this phenomenon suggest possible short and long term risks on maternal and foetal microbiota, resulting in long term sequelae such as obesity, food allergies and intolerances, autoimmune diseases, and possible neurodevelopmental involvement. Although the exact aetiology of PROM is unclear, known factors are collagen remodelling, apoptosis [345], increased transcription of matrix metalloproteinases (MMP) such as MMP9, AF apoptotic activators [346,347], and polymorphism promoter of tumour necrosis factor α (TNF-α), interleukin-1 (IL-1) and MMP1 [348,349]. Notably, there is no universally accepted method for the diagnosis of PROM. Strategies currently performed consist of sterile speculum examination, nitrazine or Fern tests [350], while ultrasound is useful to identify an AF reduction in case of suspect membrane rupture [351]. Albeit these techniques have been employed for more than 60 years, the nitrazine test has been recently discouraged [351]. Moreover, since the AF concentration of several biomarkers is higher than in normal vaginal secretion, many studies investigated the diagnostic value of vaginal AF for an early and accurate diagnosis of PROM. As a result, a number of potential biomarkers including prolactin, AFP, β-subunit of human chorionic gonadotropin (β-HCG), foetal fibronectin, diamine oxidase, lactate, creatinine, urea, and insulin growth factor binding protein-1 (IGF-BP1) has been proposed and tested [352,353]. In particular, IGF-BP1 is the major protein in AF and its presence confirms AF contamination in vaginal secretions. Interestingly, most of these biomarkers seem to accurately distinguish patients with intact membranes from unequivocal membrane rupture; however, they are not routinely applied due to their complex procedure, cost, and low sensitivities in patients with equivocal rupture. For these reasons, further investigations are necessary for the development of novel, versatile, and timely accurate diagnostic means.

8.5.2 Aim of the Project

This study applied a GC-MS-metabolomic approach to investigate the urinary metabolome in relation to PROM occurrence and labour. To pursue this goal, metabolic differences were observed in women with intact membranes and out of labour, with PROM and prior to labour, and with PROM during labour.

8.5.3 Population

Between October 2013 and July 2014, 38 pregnant women at term, age 29-42 years old (gestational age between 38 weeks + 0 days and 40 weeks + 4 days) were admitted at the Unit of Obstetrics and Gynaecology of the University-Hospital of Cagliari and enrolled in this study. Women were divided into 3 phenotypical groups. The first phenotypical group Ph1 consisted of 11 healthy pregnant women enrolled long time before labour (out of labour, intact membranes). Group Ph2 consisted of 10 pregnant women with PROM diagnosed long time before labour (out of labour and PROM). Group Ph3 consisted of 17 pregnant women with PROM and samples collected during labour (in labour and PROM). Diagnosis of PROM was based on women history, direct visualisation of fluid leakage, and speculum examination. When direct visualisation of AF loss was unreliable, qualitative immunochromatographic dipstick test for AF IGF-BP1 presence, together with ultrasound AF evaluation, were performed. Diagnosis was then retrospectively confirmed after delivery. Patients gave written informed consent at the time of admission. The study was conducted in accordance with the Declaration of Helsinki (1964) and previously approved by the local ethics committee.

8.5.4 Samples Collection and Storage

A spot urine sample was collected from each pregnant woman enrolled in the study. Therefore, hence a total of 38 samples were collected and analysed. For Ph1 group, urine were collected 3-14 days before delivery (median value 7 days, interquartile range - IQR 5-11 days); for group Ph2, 15-50 hours before delivery (median value 28.5 hours; IQR 25.5-40 hours), and for group Ph3, 0.25-19 hours before delivery (median value 10 hours, IQR 5-13 hours). Sampling was performed through a sterile, preservatives-free urine beaker equipped with a transfer device (VACUETTE®, Greiner Bio-One International GmbH, Kremsmünster, Austria) which allowed for the automatic filling of a vacuum urine tube without any external contamination. In details, urine passes from the beaker to the vacuum tube by pushing it into the transfer device. The tube is then automatically filled for about 10 mL. After collection, all tubes were centrifuged and supernatant was immediately frozen and stored at -80 °C until analysis.

8.5.5 Results

Three Phenotypes Model

First, statistical analysis and comparisons were conducted on all three different phenotypes at the same time. Appling ANOVA with Tukey's HSD post-hoc test on the three classes Ph1, Ph2, and Ph3 resulted in 58 significant metabolites belonging to five different chemical categories: carbohydrates, oxidised carbohydrate, aminoacids, sugar related, and miscellaneous. The detail list of metabolites is reported in the appendix (Appendix Table A8.5.1). PLS-DA of the same classes produced an unsatisfactory model scoring accuracy=0.67, R^2=0.88, and Q^2=0.33. Moreover, permutation test delivered a p=0.04 (Fig.8.5.1)

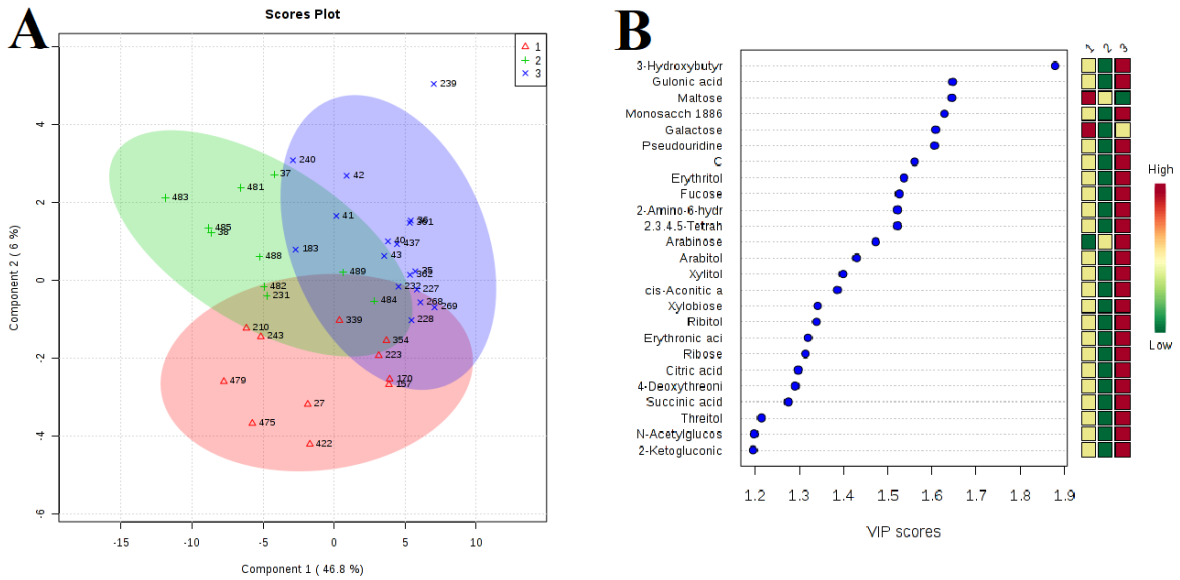

Fig. 8.5.1: *A) 2D scores plot showing PLS-DA discrimination between Ph1 (red, out of labour, intact membranes), Ph2 (green, out of labour, PROM) and Ph3 (blue, in labour, PROM) and B) the corresponding VIP score plot.*

PROM Model: Ph1 (out of labour, intact membranes) vs. Ph2 (out of labour, PROM)

In order to investigate the metabolic differences caused solely by the rupture of membranes, t-test was performed on Ph1 and Ph2 groups. This calculation highlighted 9 significant metabolites: galactose, uric acid, 3,4-dihydroxybutyric acid, galactitol, alanine, lysine, 4-hydroxyphenylacetic acid, serine, hydroxy proline dipeptide. Notably, the entire set of metabolites resulted more abundant in Ph1, except for uric acid. This means that these metabolites are significantly consumed during PROM events. Also in this case, PLS-DA analysis produced an unsuitable model with accuracy = 0.76, R^2 = 0.43, Q^2 = 0.29, and p = 0.09. However, the first 9 metabolites from PLS-DA correspond to those obtained from t-test and as higher levels for all metabolites were observed in

Ph1 group. Power analysis calculated the number of samples for a predictive power of 0.83 as 120 per group (Fig. 8.5.2).

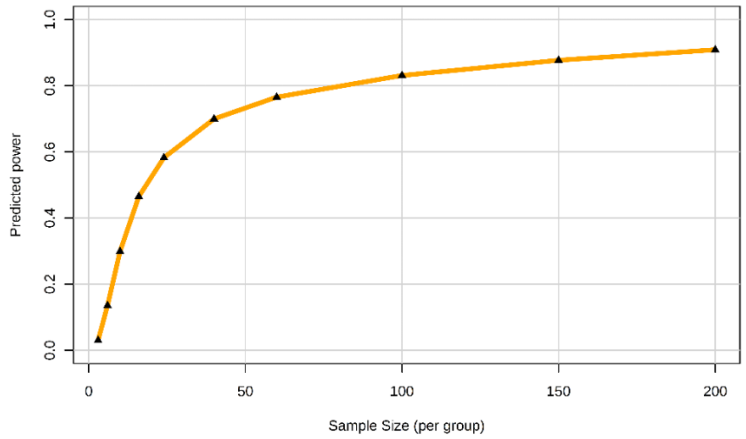

Fig. 8.5.2: *Power analysis calculations indicated a predictive power of 0.83 for 120 samples per group and FDR of 0.1.*

Labour Model: Ph2 (out of labour PROM) vs. Ph3 (in labour PROM)

Labour effects on the metabolome were highlighted by the comparison of Ph2 and Ph3 groups. T-test indicated 60 significant metabolites between the two groups of interest (Appendix Table 8.5.2). Notably, unsatisfactory PLS-DA results delivered a model with accuracy = 0.88, R^2 = 0.96, Q^2 = 0.54, and p = 0.04. Scores and VIP plots are shown in Fig. 8.5.3.

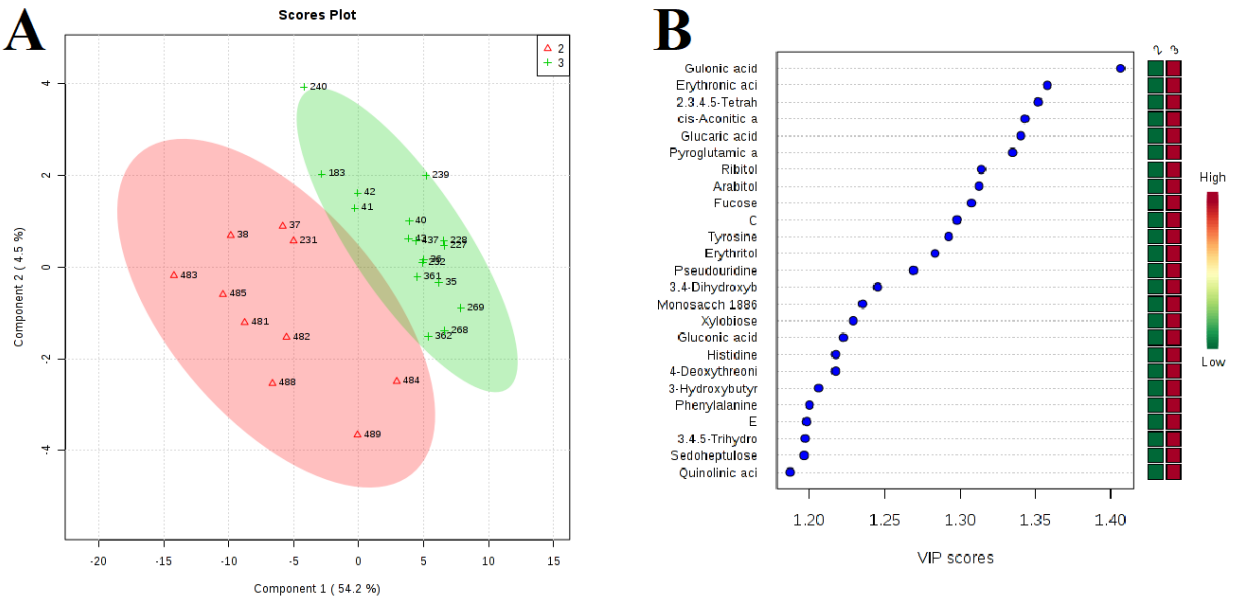

Figure 8.5.3: *A) Score plot showing the separation and clustering between Ph2 (2, triangles) and Ph3 (3, crosses) and B) the corresponding VIP score plot.*

The majority of the metabolites responsible for such phenotype discrimination showed higher levels in Ph3 group (in labour with PROM), while phosphate, lactose, and uric acid were more abundant

in Ph2. Therefore, the metabolites are mainly produced during labour. Power Analysis indicated better results for this model: predictive power of 0.83 for 50 samples per group (Fig. 8.5.4).

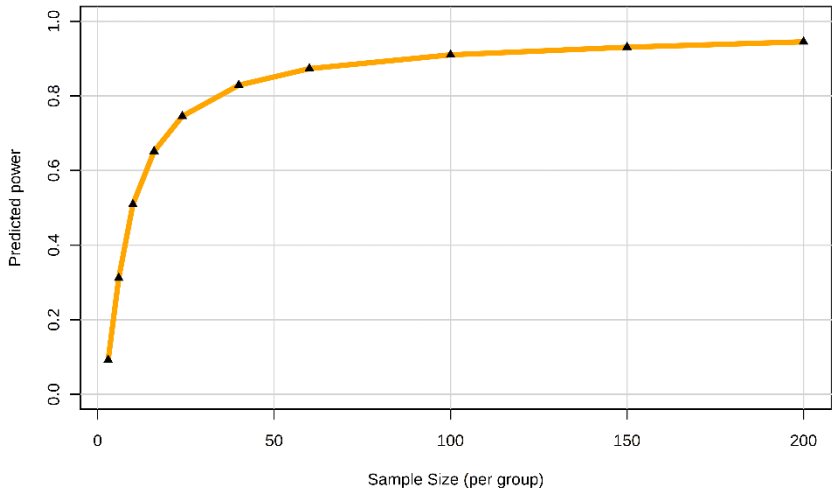

Fig. 8.5.4: *Power analysis calculations indicated a predictive power of 0.83 for 50 samples per group and FDR of 0.1.*

8.5.6 Discussion

Currently, assessment of PROM is mainly based on external genital leakage and/or direct observation of AF loss by direct visualization through speculum examination. Other options are biochemical tests and ultrasound AF evaluation, but none of these strategies may securely confirm diagnosis [354]; subsequently, confirmation of PROM often occurs during labour. Nevertheless, it is of crucial importance to make accurate and timely diagnosis in order to define appropriate clinical interventions, hence to avoid complications for the patients. In this study, although multivariate analysis could not reach statistical significance, univariate calculations identified several discriminant metabolites for the 3 phenotypes; 35 out of 58 could distinguish between at least two comparisons. Therefore, the metabolic profiles are indeed altered due to PROM and/or labour. Nevertheless, more samples are necessary to provide a holistic model that may describe such a heterogeneous and particular conditions. In particular, the separation between Ph2 and Ph3, which are characterised by PROM and differ on the onset of labour, seem to require the lowest number of samples and showed the highest number of discriminant metabolites through t-test. For these reasons, it may be hypothesised that labour event affects the system more than PROM. Furthermore, the fact that PROM model (Ph1 *vs.* Ph2) produced the lowest values for the statistical parameters may also suggest the eventuality that these two phenotypes are actually similar. Indeed, PROM *per se* may not represent a pathological event in the absence of complications. Therefore, further analysis should consider the outcome of delivery in PROM subjects. In details, analysing alteration due to PROM, the almost totality of the discriminant compounds showed higher levels in

the intact membranes group, hence the consumption of the same in the case of broken membranes. Unfortunately, discriminant metabolites are of difficult interpretation. Observing the labour model (Ph2 *vs.* Ph3), in labour subjects excreted the majority of the significant metabolites, consuming phosphate, lactose, and uric acid. Among the several significant metabolites, 3,4-dihydroxybutyric acid is a product of the oxidative metabolism of fatty acids and its increase can be observed in case of inflammations to satisfy the need for a surplus of energy due to stress conditions. Interestingly, it seems that inflammation processes may trigger preterm delivery [355]. Another sign of oxidative stress are the higher levels of glucuronic, gulonic, glucaric, and gluconic acids, and other oxidised carbohydrates which derive from oxidative conversion [355,356]. Moreover, the discriminant uric acid is involved in antioxidant activity in blood toward peroxyl radicals, which are released due to oxidative stress and ROS overproduction in labour [357]. Comparing the results from labour model calculations to those reported [358], only *cis*-aconitic acid showed an analogous trend. Indeed, this metabolite showed an up-regulation characterising the active labour phase. *Cis*-aconitic acid is a well-known intermediate of the tricarboxylic acids (TCA) cycle and its high level may be explained by the increased energy demand during labour.

8.6 pPROM Characterisation: Gestational Age and Bacterial influence

8.6.1 Preterm Premature Rapture of Membrane

Depending on the gestational age at which PROM occurs, before or after 37 weeks of gestation, preterm PROM (pPROM) and PROM are defined, respectively [359,360]. Approximately 10% of pregnancies experience PROM, while pPROM incidence is from 2% to 3.5%, being the leading cause of the 30-40% of preterm deliveries and of the 85% of consequent perinatal morbidity and mortality for both the foetus and the mother worldwide [361–364]. Although several factors are involved in the onset of pPROM including smoking, excessive alcohol consumption, drugs, and anaemia, bacterial infections and related conditions (e.g. cervical insufficiency and uterine shortening and overdistention) appear to be the main causes [365–370]. On the basis of these evidences, pPROM may occur when infection is confirmed, requiring the application of appropriate therapy. Several protocols are available to predict the onset of pPROM, but they often use invasive sampling. For example, amniotic fluid volume is scarce in most pPROM cases, requiring the performance of amniocentesis and, despite the experience, potential risks of foetal and/or maternal complications is not negligible [371]. Percutaneous umbilical cord blood sampling is significantly associated with haemorrhage in the puncture site, foetomaternal haemorrhage with mixing of foetal and maternal blood, foetal bradycardia, and cord hematoma [372]. Placental sampling may cause miscarriage and amniotic fluid leakage, leading to oligohydramnios and pPROM [373–375]. Other tests

using specimens easier to collect such as vaginal secretion and plasma may lack diagnostic accuracy because of false positive and/or false negative due to sample contaminations. Moreover, these strategies are expensive and show technical difficulty [366]. Therefore, it is of the utmost importance to design a reliable, non-invasive, and not expensive method to diagnose infections that may trigger pPROM.

8.6.2 Aim of the Project

The present work aimed at the GC-MS characterisation of the urinary metabolome of women experiencing pPROM. Indeed, the differences with PROM metabolic profile may deliver useful information to better understand its physiopathology (e.g. triggering by bacterial infection) or to evaluate the impact of gestational age.

8.6.3 Population

Forty-three urine samples were collected from 43 women, from 24 to 44 years old, who experienced PROM in singleton pregnancy and without clinical signs of infection. Depending on the pregnancy condition of the women, urine samples were divided into the following groups: 1) at term (≥37 weeks) not in labour (NLPROM) (n = 10); 2) at term in labour (LPROM) (n = 17); 3) preterm (<37 weeks) not in labour (NLpPROM) (n = 16). The subjects' median gestational age was of 38 weeks. Subjects were recruited from the Department of Obstetrics and Gynecology, Azienda Ospedaliera Universitaria (AOU) in Cagliari, Italy, between October 2013 and May 2015. Following collection, samples were centrifuged and supernatants were collected, frozen, and stored at -80 °C until metabolomic analysis. The study conformed to the principles outlined in the Declaration of Helsinki, and was approved by the ethics committee of the AOU, Cagliari, Italy. All patients gave their written informed consent prior to their participation in the study.

8.6.4 Results

Univariate Analysis: Lactic acid, erythritol, and ethanolamine contents in NLpPROM and PROM samples

Student's t-test highlighted significant changes in several metabolites. Among them, lactic acid was of particular interest because of its involvement in bacterial infection and other delivery related complication [358,376]. For this reason, Pearson correlation was applied, highlighting similar trends in erythritol and ethanolamine contents. The boxplot in Fig. 8.6.1 shows lactic acid levels in NLpPROM (samples labelled as 1) and PROM (samples labelled as 2). Its mean was significantly higher in NLpPROM (0.24 ± 0.21 arbitrary units -a.u.-) than in both PROM conditions (0.09 ± 0.1

a.u.) considered as one single group (NLPROM+LPROM) ($p<0.01$, **). Similar results are reported for ethanolamine (Fig. 8.6.2; NLpPROM: 0.6 ± 0,3 a.u.; PROM: 0.14 ± 0.08 a.u.; $p<0.001$, ***).

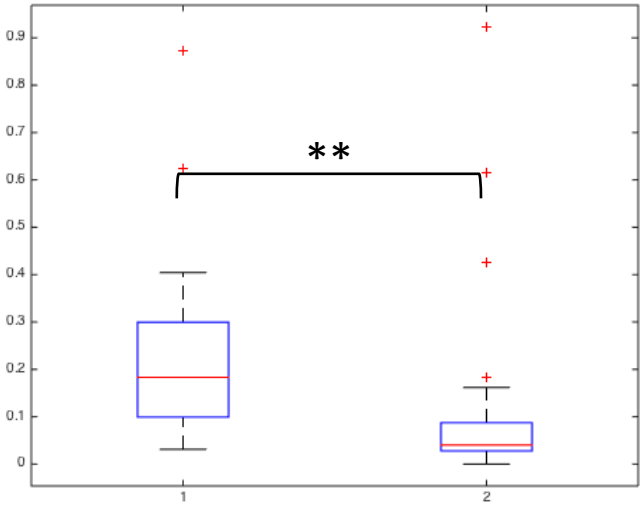

Fig. 8.6.1: *Boxplot showing significant differences in lactic acid level between NLpPROM (1) and PROM (2)*

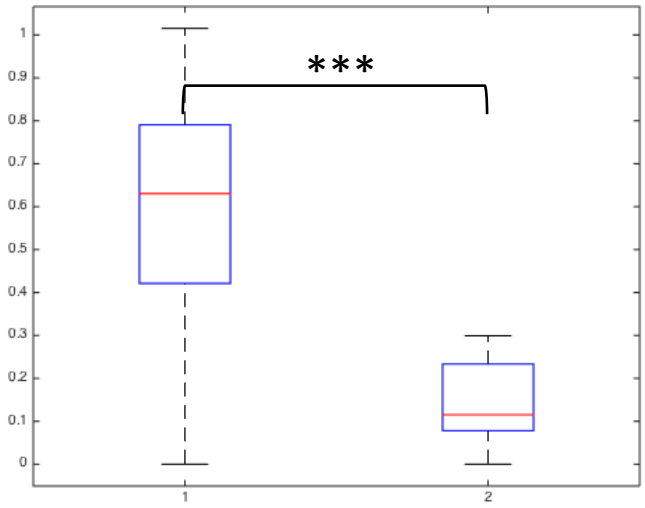

Fig. 8.6.1: *Boxplot showing significant differences in ethanolamine level between NLpPROM (1) and PROM (2)*

Multivariate Analysis: PROM and NLpPROM Metabolites

Interestingly, PLS-DA separation between NLpPROM and (NLPROM+LPROM), considered as one single group, was satisfactory (accuracy = 1.0, R^2 = 0.96803, and Q^2 = 0.92981 by 10-fold CV), while no separation was statistically relevant for NLPROM *vs.* LPROM. Results in Fig. 8.6.3 shows the clusterisation of NLpPROM and PROM conditions in urine samples.

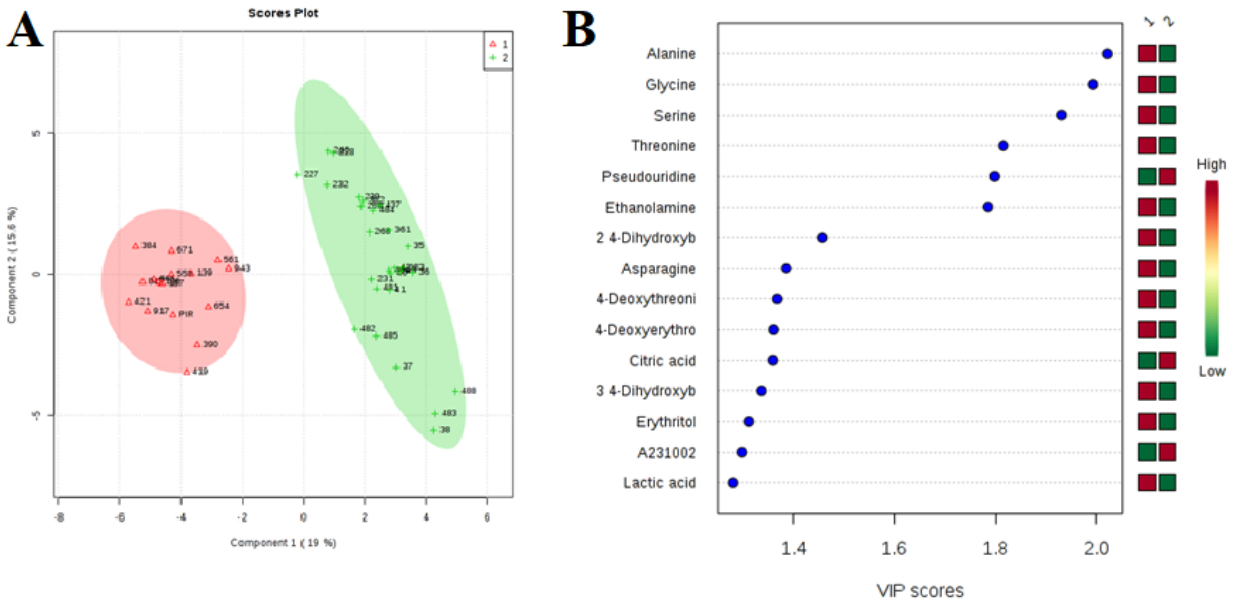

Figure 8.6.3: *A) Score plot showing the clustering between NLpPROM (1) and PROM (2) and B) the corresponding VIP score plot.*

In particular, alanine, glycine, serine, threonine, ethanolamine, 2,4-dihydroxybutyric acid, asparagine, 4-deoxythreonic acid, 4-deoxyerythronic acid, 3,4-dihydroxybutyric acid, erythritol, and lactic acid increased in NLpPROM class, while pseudouridine, citric acid, and the unknown metabolite A231002 decrease.

8.6.5 Discussion

Interestingly, while PCA and PLS-DA separations between NLpPROM subjects was statistically significant with the entire set of PROM, the two PROM conditions showed no significant alterations. Such results may be due to the small number of samples collected for this preliminary study. However, it may also be informative of the fact that the premature birth is the prevalent event in the metabolic profile modification. Notably, among the identified discriminant metabolites with higher concentrations in NLpPROM than in PROM condition, lactic acid and ethanolamine are associated with bacterial infection. Lactic acid is considered one of the most significant markers involved in several adverse events during pregnancy in women with suspected sepsis [377]. Indeed, it is the most relevant metabolic end product of carbohydrate fermentation by lactic acid bacteria, belonging to the order of Lactobacillales. Among them, bacteria of the genus *Lactobacillus* are known for their presence in the gastrointestinal microbiota, although to a lesser extent compared to other genera. In addition, *Lactobacillus* is known for its beneficial effects as probiotics and it is widely used to restore gut microbiota and its function when altered by pathological conditions [377]. However, lactic acid does not always derive from non-pathogenic bacteria. For example,

Streptococcus is another genus of lactic acid bacteria and several of them such as *S. pyogenes, S. agalactiae,* and *S. pneumoniae* are known for their pathogenicity which may cause pharyngitis, sepsis, and pneumonia, respectively [378,379]. Therefore, lactic acid increase may indicate an ongoing infection that could trigger preterm birth. Ethanolamine is present in bacteria and mammals' cells, as well as introduced by human diet. It may derive from the breakage of phosphatidylethanolamine contained in bacteria as constituent of cell membrane phospholipids, particularly in epithelial intestinal cells [380]. Therefore, ethanolamine higher levels, as in the case of NLpPROM condition, may be associated with bacterial growth. For this reason, a dysbiosis, i.e. a change in the microbiotic balance, may be a manifestation of infection and consequent NLpPROM. Another interesting finding was the lower concentration of 4-deoxythreonic acid in PROM specimens. This common urinary metabolite may be consumed by several strains of *E. coli, S. mercescens* or *P.aeruginosa* [381], suggesting a different microbiota within the two groups under study. However, the outcome of such difference in microorganisms is of difficult determination. Pseudouridine is a ubiquitous constituent of RNA material, playing a pivotal role in several biological mechanisms [382]. Therefore, the lower levels observed in NLpPROM excretions may be related to its use in microorganisms' RNA for bacterial growth and function. Probably not related to ongoing infections were the lower levels of several amino acids, namely alanine, glycine, serine, threonine, and asparagine in PROM group. Although subjective variables such as hormonal secretions, diet, and behaviour are involved, this data may be explained by the different degree of protein turnover at different gestational ages [383]. This process is enhanced during the latest part of gestation, using amino acids for protein synthesis in foetus, placenta, and mother tissues. Supporting data reported longer babies at birth in cases of prompted protein turnover [384]. Notably, 4-deoxyerythronic acid derives from threonine, hence its lower concentration in PROM may be a consequence of the amino acid lower content within the same samples [385].

8.7 Systemic Sclerosis: Preliminary Investigation on Early Diagnosis and Classification Potential

8.7.1 Systemic Scleroderma

Systemic sclerosis (SSc), or scleroderma, is a chronic autoimmune disorder affecting the connective tissues and characterised by induration and thickening of the skin, vascular obliteration, Raynaud's phenomenon, excessive extracellular matrix deposition, and fibrosis of the connective tissues [386,387] Moreover, musculoskeletal manifestations, and involvement of gastrointestinal tract, lungs, heart, and kidneys may be observed. Indeed, SSc may present in two forms; limited systemic sclerosis (lcSSc), which is confined to the skin and surrounding tissue, and a diffuse systemic sclerosis

(dcSSc) or diffuse skin involvement, and a localized form [388]. The age of onset is generally comprised between 45 and 65 years old, and the causes of such morbidity are not fully understood [29]. Although the disease is not hereditary, SSc is thought to be a polygenic disease in which several genes are involved in its origin and development [387,389]. Nevertheless, there is an association with certain medications or exposure to some environmental toxicants (vinyl chloride, trichloroethylene, and silicone) [387,390]. The prevalence of such disease in the US is of 27.6 cases per 100,000, with 4.6 higher incidence for women [388]. Due to symptoms overlap with a number of other diseases, the diagnosis is usually performed though auto-antibody pattern such as antinuclear antibodies, anticentromere antibodies, anti-Scl-70, etc. [387].

8.7.2 Aim of the Project

The aim of this study was to identify urinary molecular descriptors of SSc by means of GC-MS platform. Given the potential environmental component in its aetiology, modification in urine's metabolome may be of interest. Furthermore, clusterisation between lcSSc and dcSSc was attempted to highlight different mechanisms.

8.7.3 Population

In this study, 30 subjects affected by SSc (28 female, and 2 males), and 20 healthy controls were enrolled. SSc diagnosis was performed following classification criteria of the American College of Rheumatology for SSc [391]. Among pathological patients, 18 showed lcSSc, while 11 were characterised by dcSSc. Median age of enrolled subjects was 58 years old, while median onset age was 45 years old. Patients gave informed consent for the study, which was approved by the local ethics committee.

8.7.4 Results

Controls vs. SSc

PLS-DA produced a robust 5 components-model that could clearly discriminate SSc subjects from controls (accuracy = 0.98, R^2 = 0.98909, and Q^2 = 0.82359 by LOOCV) (Fig. 8.7.1). Such phenotypical separation was possible due to specific metabolites showed in the VIP score figure (Fig. 8.7.1B): monoglycerides 1-monostearin and 1-monopalmitin, inositol, caffeine, β-alanine, glycolic acid, 5-hydroxyindolacetic acid, and other eight unknown compounds. Among these, two seem to be unidentified carbohydrates and one is, supposedly, a derivative of glycine. However, all the mentioned metabolites decreased within SSc group.

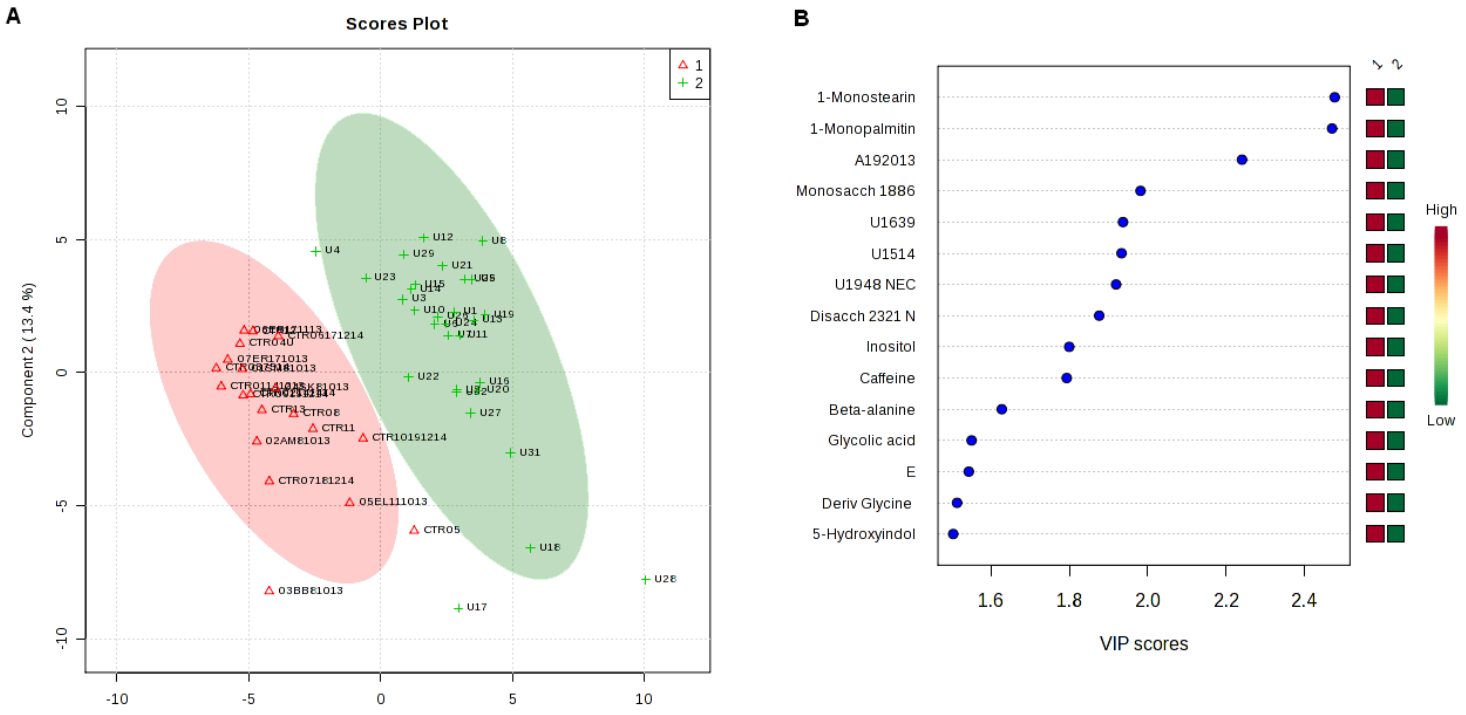

Fig. 8.7.1: *A) Score plot showing clear discrimination between controls (red) and SSc affected subjects (green). B) VIP scores showing increment the importance of the different metabolites for control (1) and SSc (2) subjects.*

Metabolic Pathways analysis was applied to the same data matrix highlighting alterations in several biological processes. In order, pyrimidine (1), β-alanine (2), and propanoate (3) metabolisms, pantothenate and CoA biosynthesis (4), caffeine (5) metabolism, glyoxylate and dicarboxylate metabolism (6), aminoacyl-tRNA biosynthesis (7), inositol phosphate (8), and arginine and proline (9), tryptophan metabolisms (10), and phenylalanine, tyrosine and tryptophan biosynthesis (11) were identified as the most affected pathways (Fig. 8.7.2). The application of power analysis highlighted a sample size of 200 specimens per group for a power of 0.64 and FDR of 0.1.

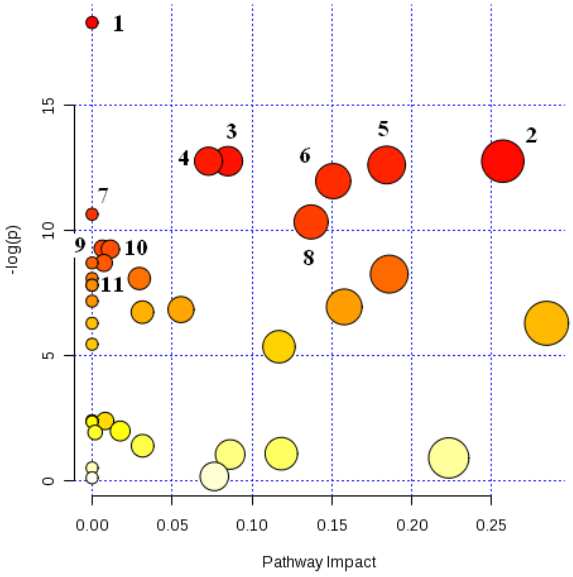

Fig. 8.7.2*: Metabolic Pathways analysis for controls vs. SSc cases.*

LcSSc vs. DcSSc

When comparing lcSSc patients with those characterised by dcSSc, the obtained PLS-DA model did not reach statistical significance. This may be due to the exiguous sample size as well as for the noise present in within the two phenotypical groups.

8.7.5 Discussion

Results showed potentially reliable measure only for the separation between SSc affected and healthy control subjects. The main discriminants for this clusterisation were found to be a series of compounds belonging to a variety of classes. Among the different metabolites, the most interesting is 5-hydroxyindoleacetic acid. Indeed, such compound is the end product of serotonin metabolism. Although there are only hypothesis on the involved mechanisms, serotonin seems to play an important role in promoting vasoconstriction and supporting the developed fibrosis [392]. This particular compound is accumulated in platelet specialised granules and, following endothelium damage and subsequent binding to collagen type I and III, is released in the plasma during platelets aggregation [393]. Notably, serotonin values are lower inside platelets and higher in plasma of patients affected by certain forms of SSc [394,395]. Moreover, after L-tryptophan loading, 5-hydroxyindoleacetic acid and total indoles levels seem to decrease in scleroderma subjects, probably due to impaired activity of monoamine oxidase, which leads to accumulation of tryptophan amine derivatives (serotonin and tryptamine) in the skin [396].

8.8 Conclusions on Urine

Metabolomics strategy was applied on several study cases, highlighting interesting aspects about the physiological state of the phenotypes under examination. Considering the analysis to discriminate preterm neonates exposed to HC from those who were not exposed, altered metabolic pathways associated to chorioamnionitis were highlighted. Notably, signs of bacterial infections were predominant in these results. Most interestingly, to the best of our knowledge, this was the first study exploiting urinary metabolomics to this aim [31,397]. The study on asphyxiated babied delivered several insights on the modification of the metabolic profile following hypothermia treatment. In particular, taurine could be considered as a potential biomarker for the assessment and the monitoring of cellular injuries and death during a hypoxic-anoxic insult. Nevertheless, several events seemed to influence these alterations such as brain and enzymes impairment, TCA cycle re-activation, HIFs modulation, treatment, duration of feeding, and cellular proliferation [32]. Following the alteration of the temporal dynamics in NEC related cases, significant changes were mainly dependent on two factors: newborns age and NEC onset. Indeed, while the metabolome of most samples seemed to reflect the first variable (healthy, intolerant, and early-onset), late-onset displayed a different trend after disease occurrence. Moreover, the metabolic differences in NEC profiles prior to onset, suggested a potential metabolic detectable predisposition to this pathology [30,398]. Regarding the study related to PROM and the effect of labour onset, univariate chemometric analysis was able to discriminate among the different conditions, highlighting variation in the

phenotypes' metabolome. An interesting feature of these data is that labour conditions seem to have greater influence over the system than the actual PROM occurrence, suggesting that further studies are in need for this delicate diagnosis [28,399]. Notably, the exploration of pPROM occurrences suggested that premature birth, rather than the onset of labour, is a major variable affecting the metabolome. Indeed, amino acids alteration, probably due to enhanced late pregnancy protein turnover, contributed to the discrimination of the two classes. Nevertheless, results could indicate the presence of dysbiosis and infections in different body districts in pregnant women. In the case of heathy *vs*. SSc cases, calculations highlighted serotonin platelets accumulation and/or involvement of monoamine oxidase as discriminant features. Regarding classification between the two forms of SSc, further studies are necessary [29]. Therefore, metabolomics analysis on urine samples could deliver useful information on a number of diverse pathological conditions.

9. Limitations

The limitations of this project are mainly constituted by the samples size explored. Indeed, although Julious criteria [274] were respected in most cases, complex biological phenomena may require larger population in order to be accurately described. Furthermore, most of these studies were monocentric studies. In order to provide more strength to the results, cohorts should be expanded in future investigations by collecting specimens from diverse centres. This would not only validate the results observed, but also allow for the construction of a more general model that could be extensively applied. Nevertheless, it has to be reminded that these were all explorative pilot studies to provide a direction for further investigations. Moreover, it would have been interesting to collect different biofluid from the same patient in the context of the same pathological status. These data could be of use to better understand the physiopathological adaptation of the different body compartments. However, these works put the basis for such development. Another limitation may be the lack of microbiological analysis to identify a more reliable association between clinical status and patients' metabolic outcomes. During the PhD programme, other projects on diverse conditions such as autism, drug response, lymphomas, pyelonephritis, physiological gestation, obesity in pregnancy, etc. or by means of other platforms were conducted. However, due to their extremely early stage, were not included in this work.

10. Conclusions

Within this project, several were the biofluids, tissues, and pathological conditions investigated by means of metabolomics. In particular, AF, intact kidney tissue, extracts from placenta, plasma, saliva, and urine were considered for the clusterisation of the different phenotypes. In most studies, metabolomic strategy was able to highlight significant alteration related to diverse mechanisms (e.g. dietary intake and oxidative stress) that affected the relative concentrations of the metabolome. Interestingly, the successful preliminary exploration of extremely diverse events such as pregnancy-related, perinatal, cancerous, autoimmune status, treatment response, etc. confirmed the versatility of this potentially powerful tool. Although the analysis on GDM and apical periodontitis could not deliver statistically important results, further studies may overcome the samples size limitation. In conclusions, while larger, multicentre samples size and parallel microbiological analyses should be used to confirm data, these metabolomics-based findings are an interesting promise for the future discovery of novel biomarkers, phenotypical investigations, and translation into medical setting to improve clinical practice.

11. Acknowledgement

This work contains results that were published on Molecules [5], Journal of Pediatric and Neonatal Individualized Medicine [17,21,26,28–31,37], Annals of Translational Medicine [32], Clinica Chimica Acta [18], Data in Brief [19], Expert Review of Molecular Diagnostics [4], Clinical Chemistry [20], Placenta [156], PlosOne [397], Disease Markers [399], and NMR in Biomedicine [2].

Francesco Palmas gratefully acknowledges Sardinia Regional Government for the financial support of his PhD scholarship (P.O.R. Sardegna F.S.E. Operational Programme of the Autonomous Region of Sardinia, European Social Fund 2007–2013—Axis IV Human Resources, Objective l.3, Line of Activity l.3.1.).

This work was supported by Legge Regionale 7 (07/08/2007): 'Promotion of scientific research and technologic innovation in Sardinia' CRP60413/2012 'Metabolomic study for new predictive and prognostic biomarkers in the diagnosis of labour'.

The Author acknowledge support by NIH grant CA115746 and the A.A. Martinos Center for Biomedical Imaging.

12. Appendix

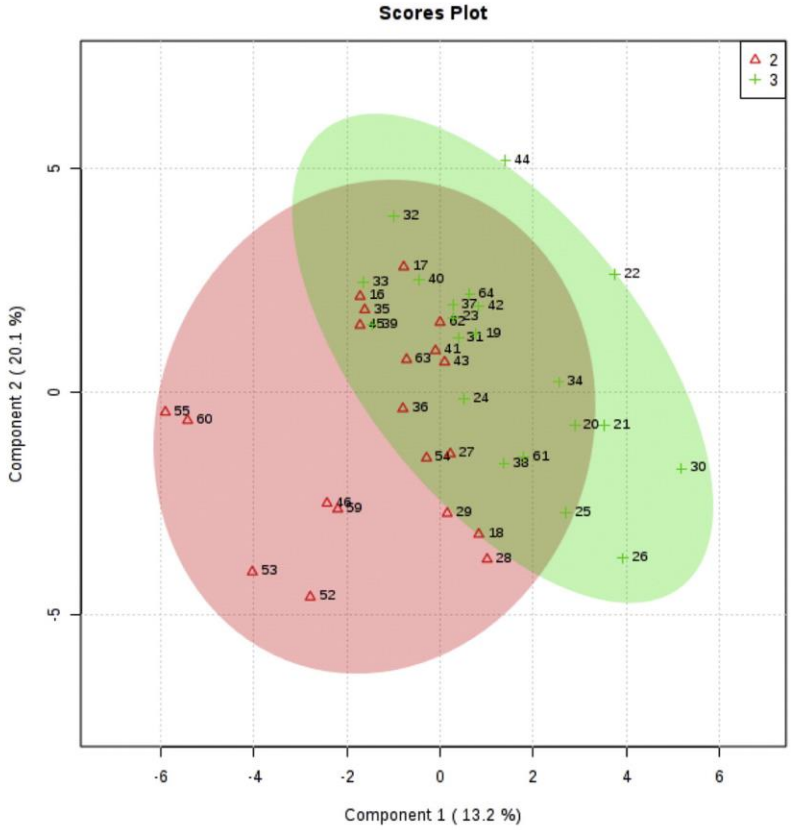

A

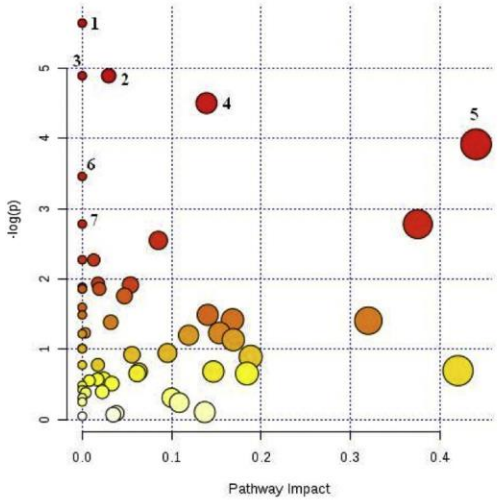

B

No.	Metabolic Pathway/Metabolisms
1.	Fatty acid biosynthesis
2.	Fatty acid metabolism
3.	Fatty acid elongation (in mithocondria)
4.	Glutamine and glutamate
5.	Alanine, aspartate and glutamate
6.	Arginine and ornithine
7.	Pyrimidine

C

Fig. A3.5.1:. *Comparison between transmitters and non-transmitters. A = 2D scores plot showing PLS-DA discrimination for transmitters (2) vs. non-transmitters (3) groups. B = metabolic hubs mainly affected in the comparison between transmitters and non-transmitters. C = corresponding list of metabolic hubs mainly affected by HCMV presence*

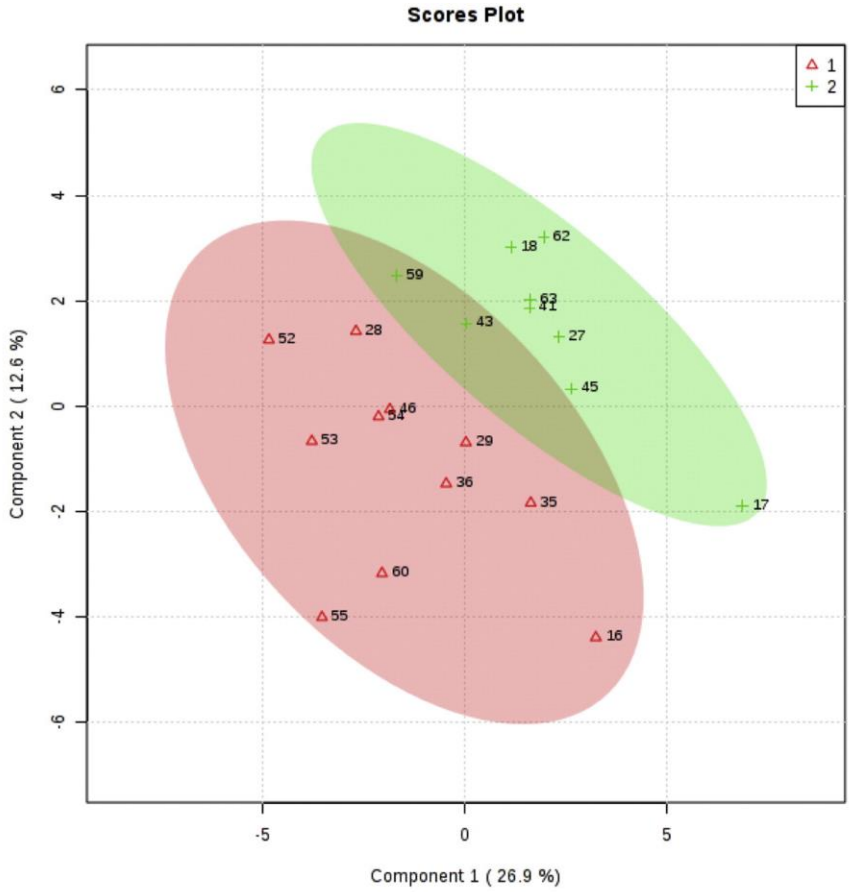

A

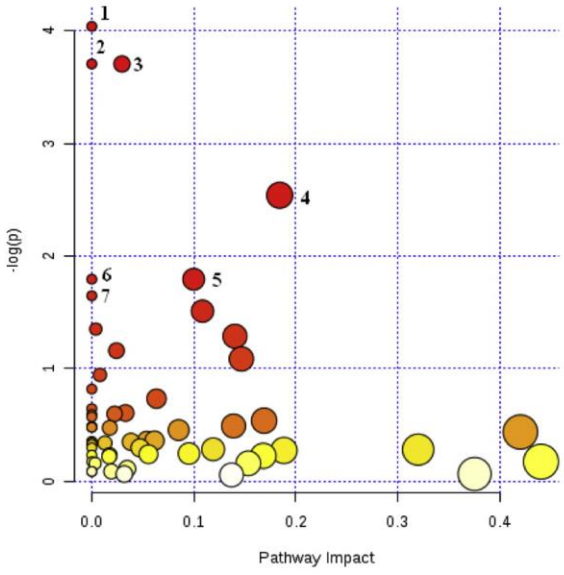

B

No.	**Metabolic Pathway/Metabolisms**
1.	Fatty acid biosynthesis
2.	Fatty acid metabolism
3.	Fatty acid elongation (in mithocondria)
4.	Caffeine
5.	Lysine
6.	Biotin
7.	β-Alanine

C

Fig. A3.5.2: *Comparison between ACI and SCI transmitters. A = 2D scores plot showing PLS-DA discrimination for ACI transmitters (1) vs. SCI transmitters (2) groups. B = metabolic hubs mainly affected in the comparison between ACI transmitters vs. SCI transmitters. C = corresponding list of metabolic hubs mainly affected.*

For discussion purpose, these compounds were divided into 5 groups corresponding to different chemical classes: carbohydrates (Carb), oxidised carbohydrates (Ox), aminoacids (AA), sugar related (SR), and miscellaneous (Misc).

Metabolite	**Chemical Class**	**p value**	**FDR**	**Tukey's HSD**
cis-Aconitic acid	*Misc*	2,01E-03	0.00015894	2-1; 3-1; 3-2
2,3,4,5-Tetrahydroxypentanoic acid 1,4-lactone	*Ox*	8,63E-02	0.00026357	2-1; 3-1; 3-2
Erythronic acid	*Ox*	1,20E-01	0.00026357	2-1; 3-1; 3-2
3-Hydroxybutyric acid	*Misc*	1,75E-01	0.00026357	3-1; 3-2
3,4-Dihydroxybutyric acid	*Misc*	1,95E-01	0.00026357	2-1; 3-2
Glucaric acid	*Ox*	2,00E-01	0.00026357	2-1; 3-2
Unknown C	*Misc*	2,91E-01	0.00029809	3-1; 3-2
Pseudouridine	*Misc*	3,02E-01	0.00029809	3-1; 3-2
Erythritol	*SR*	3,98E-01	0.00030706	3-1; 3-2
Gulonic acid	*Ox*	4,00E-01	0.00030706	3-1; 3-2
Monosaccharide 1886	*SR*	4,28E-01	0.00030706	3-1; 3-2
Pyroglutamic acid	*Misc*	5,02E-01	0.00033075	2-1; 3-2
Arabitol	*SR*	5,44E-01	0.00033075	3-1; 3-2
Fucose	*Carb*	5,94E-01	0.00033536	3-1; 3-2
Ribitol	*SR*	6,53E-01	0.00034397	2-1; 3-2
Tyrosine	*AA*	0.00011408	0.00056327	2-1; 3-2
Xylobiose	*Carb*	0.00016349	0.00075975	3-2
3,4,5-Trihydroxypentanoic acid	*Misc*	0.00023492	0.0010311	2-1; 3-2
Histidine	*AA*	0.00027084	0.0011261	2-1; 3-2
Gluconic acid	*Ox*	0.00040226	0.0015889	3-2
Serine	*AA*	0.00050574	0.0019025	2-1; 3-2
Lysine	*AA*	0.0005569	0.0019615	2-1; 3-2
Monosaccharide E	*SR*	0.00058834	0.0019615	3-2
Xylitol	*SR*	0.00059589	0.0019615	3-1; 3-2
Phenylalanine	*AA*	0.00089953	0.0028425	2-1; 3-2
Threonine	*AA*	0.00098451	0.0029914	2-1; 3-2
Quinolinic acid	*Misc*	0.0012588	0.003683	2-1; 3-2
4-Deoxythreonic acid	*SR*	0.0014511	0.0040942	3-2
Cystine	*AA*	0.0015954	0.004346	3-2
Succinic acid	*Misc*	0.0024091	0.0063441	3-2
Alanine	*AA*	0.0027785	0.0070807	2-1; 3-2
N-Acetylglucosamine	*SR*	0.0035822	0.0088435	3-2
Phosphate	*Misc*	0.0037469	0.0089697	3-2
Ribonic acid	*Ox*	0.0042205	0.0098065	3-2

2-Amino-6-hydroxy-7-methyl-7H-purine	*Misc*	0.0043539	0.0098274	3-1; 3-2
Hydroxy proline dipeptide	*AA*	0.0048016	0.010537	2-1; 3-2
Maltose	*Carb*	0.0050599	0.010804	2-1; 3-1
Glutamine	*AA*	0.0055744	0.011425	2-1; 3-2
Glycine, *N*-4-hydroxybenzoyl	*Misc*	0.0057479	0.011425	2-1; 3-2
Threonic acid	*Ox*	0.005785	0.011425	2-1; 3-2
2-O-Glycerol-galactopyranoside	*SR*	0.006708	0.012925	2-1; 3-2
Lactose	*Carb*	0.0077141	0.01451	2-1; 3-2
Ribose	*Carb*	0.0088787	0.016312	3-2
Citric acid	*Misc*	0.0092274	0.016567	3-2
Galactose	*Carb*	0.010113	0.017412	3-1
4-Hydroxyphenylacetic acid	*Misc*	0.010139	0.017412	2-1; 3-2
Glucose	*Carb*	0.012002	0.020173	2-1
Glycine *N*-4-hydroxybenzoyl derivative	*Misc*	0.018028	0.029671	3-2
Uric acid	*Misc*	0.0197	0.031761	3-2
Threitol	*SR*	0.020579	0.032514	3-2
Galactitol	*SR*	0.021507	0.033314	2-1
Hippuric acid	*Misc*	0.023726	0.035603	3-2
Creatinine	*Misc*	0.023885	0.035603	2-1; 3-2
2,4-Dihydroxybutyric acid	*Misc*	0.026377	0.038588	3-2
2-Ketogluconic acid	*Ox*	0.027386	0.039336	3-2
Arabinose	*Carb*	0.028179	0.039753	3-1
Sedoheptulose	*Carb*	0.028971	0.040153	3-2
4-Deoxyerythronic acid	*Ox*	0.034187	0.046565	3-2

Table A8.5.1: *Statistically significant (FDR < 0.05) metabolites from univariate analysis (ANOVA with Tukey's HSD post-hoc test) of the three classes Ph1, Ph2, and Ph3.*

Metabolite	**Chemical Class**	**p.value**	**FDR**	**Ph2 vs. Ph3**
Gulonic acid	*Ox*	7,31E-04	5,63E-01	Down
Erythronic acid	*Ox*	3,00E-02	7,03E-01	Down
2,3,4,5-Tetrahydroxypentanoic acid 1.4-lactone	*Ox*	3,53E-03	7,03E-01	Down
cis-Aconitic acid	*Misc*	4,44E-02	7,03E-01	Down
Glucaric acid	*Ox*	4,76E-03	7,03E-01	Down
Pyroglutamic acid	*Misc*	5,48E-02	7,03E-01	Down
Ribitol	*SR*	9,12E-02	9,12E-01	Down
Arabitol	*SR*	9,47E-02	9,12E-01	Down
Fucose	*Carb*	1,07E-01	9,14E-02	Down

Unknown C	*Misc*	1,34E-01	0.00010306	Down
Tyrosine	*AA*	1,52E-01	0.0001065	Down
Erythritol	*SR*	1,87E-01	0.00011968	Down
Pseudouridine	*Misc*	2,55E-01	0.00015105	Down
3,4-Dihydroxybutyric acid	*Misc*	4,19E-01	0.00023071	Down
Monosaccharide 1886	*Carb*	5,13E-01	0.00026311	Down
Xylobiose	*Carb*	5,80E-01	0.00027903	Down
Gluconic acid	*Ox*	6,60E-01	0.00029457	Down
Histidine	*AA*	7,26E-01	0.00029457	Down
4-Deoxythreonic acid	*Ox*	7,27E-01	0.00029457	Down
3-Hydroxybutyric acid	*Misc*	9,00E-01	0.00034512	Down
Phenylalanine	*AA*	0.00010095	0.00034512	Down
Monosaccharide E	*Carb*	0.0001043	0.00034512	Down
3,4,5-Trihydroxypentanoic acid	*Ox*	0.00010624	0.00034512	Down
Sedoheptulose	*Carb*	0.00010757	0.00034512	Down
Quinolinic acid	*Misc*	0.00012733	0.00039216	Down
Xylitol	*SR*	0.00017953	0.00053168	Down
Phosphate	*Misc*	0.00020953	0.00059755	Up
Lysine	*AA*	0.000373	0.0010074	Down
Succinic acid	*Misc*	0.00037941	0.0010074	Down
Ribose	*Carb*	0.00049401	0.001268	Down
Threonine	*AA*	0.00055591	0.0013069	Down
Cystine	*AA*	0.00056022	0.0013069	Down
2-Amino-6-hydroxy-7-methyl-7H-purine	*Misc*	0.00056835	0.0013069	Down
Serine	*AA*	0.00057708	0.0013069	Down
N-Acetylglucosamine	*SR*	0.00074989	0.0016498	Down
Citric acid	*Misc*	0.0009237	0.0019757	Down
Ribonic acid	*Ox*	0.0013077	0.0027213	Down
Glutamine	*AA*	0.0014072	0.0028515	Down
Lactose	*Carb*	0.0020445	0.0040365	Up
Glucose	*Carb*	0.0024816	0.004777	Down
Hydroxy proline dipeptide	*AA*	0.0028275	0.0053102	Down
Glycine, *N*-4-hydroxybenzoyl	*Misc*	0.0038577	0.0070724	Down
2-Ketogluconic acid	*Ox*	0.0045002	0.0080016	Down
2,4-Dihydroxybutyric acid	*Misc*	0.0045723	0.0080016	Down
Threonic acid	*Ox*	0.0047704	0.0081627	Down
4-Hydroxyphenylacetic acid	*Misc*	0.0051136	0.0085598	Down
Alanine	*AA*	0.0052474	0.0085968	Down
2-O-Glycerol-galactopyranoside	*SR*	0.0071983	0.011547	Down
Threitol	*SR*	0.0091347	0.014354	Down

Glycine, *N*-4-hydroxybenzoyl derivative	*Misc*	0.010305	0.015869	Down
Creatinine	*Misc*	0.012953	0.019557	Down
Uric acid	*Misc*	0.014046	0.020799	Up
3-Methylhistidine	*AA*	0.014579	0.02117	Down
Glyceromannoheptonic acid	*Ox*	0.014847	0.02117	Down
Hippuric acid	*Misc*	0.015776	0.022086	Down
Inositol	*SR*	0.016169	0.022232	Down
Arabinose	*Carb*	0.017089	0.023086	Down
4-Deoxyerythronic acid	*Ox*	0.017767	0.023587	Down
Ethanolamine	*Misc*	0.024206	0.031591	Down
Mannitol	*SR*	0.026258	0.033697	Down

Table A8.5.2: *Statistically significant (FDR < 0.05) metabolites from t-test of the classes Ph2 vs. Ph3.*

13. References

1. Lindon JC, Nicholson JK, Holmes E. *Handbook of Metabonomics and Metabolomics*. Amsterdam: Elsevier; 2007.
2. Dietz C, Ehret F, Palmas F, et al. Applications of high - resolution magic angle spinning MRS in biomedical studies II — Human diseases. *NMR Biomed*. 2017;30:e3784. doi:10.1002/nbm.3784.
3. Piras D, Locci E, Palmas F, et al. Rare disease: a focus on metabolomics. *Expert Opin Orphan Drugs*. 2016;4(12):1229-1237. doi:10.1080/21678707.2016.1252671.
4. Palmas F, Fattuoni C, Noto A, Barberini L, Dessì A, Fanos V. The choice of amniotic fluid in metabolomics for the monitoring of fetus health. *Expert Rev Mol Diagn*. 2016;7159(April):1-14. doi:10.1586/14737159.2016.1139456.
5. Fattuoni C, Palmas F, Noto A, Fanos V, Barberini L. Perinatal asphyxia: A review from a metabolomics perspective. *Molecules*. 2015;20:7000-7016. doi:10.3390/molecules20047000.
6. Romero R, Mazaki-tovi S, Vaisbuch EDI, et al. Metabolomics in premature labor : a novel approach to identify patients at risk for preterm delivery. *J Matern Neonatal Med*. 2010;23(December):1344-1359. doi:10.3109/14767058.2010.482618.
7. Bodenhausen G, Freeman R, Morris G. A Simple Pulse Sequence for Selective Excitation in Fourier Transform NMR. *J Magn Reson*. 1976;75:171-175.
8. Morris G, Freeman R. Selective excitation in Fourier transform nuclear magnetic resonance. *J Magn Reson*. 1978;29:433-462.
9. Taylor JL, Wu C, Cory D, Gonzalez RG, Bielecki A, Cheng LL. High-Resolution Magic Angle Spinning Proton NMR Analysis of Human Prostate Tissue With Slow Spinning Rates. *Magn Reson Med*. 2003;50:627-632. doi:10.1002/mrm.10562.
10. Burns MA, Taylor JL, Wu C, et al. Reduction of Spinning Sidebands in Proton NMR of Human Prostate Tissue With Slow High-Resolution Magic Angle Spinning. *Magn Reson Med*. 2005;54:34-42. doi:10.1002/mrm.20523.
11. Martınez-Bisbal MC, Esteve V, Martınez-Granados B, Celda B. Magnetic Resonance Microscopy Contribution to Interpret High-Resolution Magic Angle Spinning Metabolomic Data of Human Tumor Tissue. *J Biomed Biotechnol*. 2011;2011:1-8. doi:10.1155/2011/763684.
12. Haukaas TH, Moestue SA, Vettukattil R, et al. Impact of Freezing Delay Time on Tissue Samples for Metabolomic Studies. *Front Oncol*. 2016;6(January):1-9. doi:10.3389/fonc.2016.00017.
13. Jordan KW, He W, Halpern EF, Wu C, Cheng LL. Evaluation of Tissue Metabolites with High Resolution Magic Angle Spinning MR Spectroscopy Human Prostate Samples After Three-Year Storage at – 80 ºC. *Biomark Insights*. 2007;2:147-154.
14. Swanson MG, Zektzer AS, Tabatabai ZL, et al. Quantitative Analysis of Prostate Metabolites Using 1 H HR-MAS Spectroscopy. *Magn Reson Med*. 2006;55:1257-1264. doi:10.1002/mrm.20909.
15. Dunn WB, Broadhurts D, Begley P, et al. Procedures for large-scale metabolic profiling of serum and plasma using gas chromatography and liquid chromatography coupled to mass spectrometry. *Nat Protoc*. 2011;6:1060-1083.
16. Shen Q, Li X, Qiu Y, Su M, Liu Y, Li H. Metabonomic and metallomic profiling in the amniotic fluid of malnourished pregnant rats. *J Proteome Res*. 2008;7:2151-2157.
17. Zavattoni M, Palmas F, Fattuoni C, et al. PRIMARY HCMV INFECTION IN PREGNANCY: PRELIMINARY METABOLOMIC DATA ON AMNIOTIC FLUID. *J Pediatr Neonatal Individ Med*. 2015;4(2):36-37.
18. Fattuoni C, Palmas F, Noto A, et al. Primary HCMV infection in pregnancy from classic data towards metabolomics: An exploratory analysis. *Clin Chim Acta*. 2016;460:23-32. doi:10.1016/j.cca.2016.06.005.
19. Barberini L, Noto A, Saba L, et al. Multivariate data validation for investigating primary HCMV infection in pregnancy. *Data Br*. 2016;9:220-230. doi:10.1016/j.dib.2016.08.050.
20. Mussap M, Noto A, Fattuoni C, et al. Primary Human Cytomegalovirus (HCMV) Infection in Pregnancy: Unrevealing the Metabolic Network. *Clin Chem*. 2016:S219.
21. Palmas F, Barberini L, Noto A, et al. METABOLOMIC STUDY OF AMNIOTIC FLUID IN GESTATIONAL DIABETES. *J Pediatr Neonatal Individ Med*. 2015;4(2):131-132.
22. Chi Y, Pei L, Chen G, et al. Metabonomic profiling of human placentas reveals different metabolic patterns among subtypes of neural tube defects. *J Proteome Res*. 2014;13(2):934-945. doi:10.1021/pr4009805.
23. Dunn WB, Brown M, Worton SA, et al. The metabolome of human placental tissue: Investigation of first trimester tissue and changes related to preeclampsia in late pregnancy. *Metabolomics*. 2012;8(4):579-597. doi:10.1007/s11306-011-0348-6.
24. Beckonert O, Keun HC, Ebbels TMD, et al. Metabolic profiling, metabolomic and metabonomic procedures for NMR spectroscopy of urine, plasma, serum and tissue extracts. *Nat Protoc*. 2007;2(11):2692-2703. doi:10.1038/nprot.2007.376.
25. McCombie G, Medina-Gomez G, Lelliott CJ, Vidal-Puig A, Griffin JL. Metabolomic and Lipidomic Analysis of the Heart of Peroxisome Proliferator-Activated Receptor-γ Coactivator 1-β Knock Out Mice on a High Fat Diet. *Metabolites*. 2012;2(2):366-381. doi:10.3390/metabo2020366.

26. Fattuoni C, Mandò C, Palmas F, et al. METABOLOMIC ANALYSIS OF PLACENTA TISSUE IN OBESE PREGNANCIES. *J Pediatr Neonatal Individ Med*. 2017;6:81.
27. Zheng J, Dixon RA, Li L. Development of Isotope Labeling LC−MS for Human Salivary Metabolomics and Application to Profiling Metabolome Changes Associated with Mild Cognitive Impairment. *Anal Chem*. 2012;84:10802-10811.
28. Meloni A, Barberini L, Mereu R, et al. PRE-LABOR RUPTURE OF MEMBRANES (PROM) AND MODERN METABOLOMICS. *J Pediatr Neonatal Individ Med*. 2015;4(2):71-73.
29. Noto A, Amador C, Palmas F, et al. NEW PERSPECTIVES FOR THE STUDY OF SYSTEMIC SCLERODERMA. *J Pediatr Neonatal Individ Med*. 2015;4(2):125-126.
30. Palmas F, Magistris A De, Noto A, et al. METABOLOMICS STUDY ON NEC OCCURRENCE BY GC-MS. *J Pediatr Neonatal Individ Med*. 2016;5(2):65-66.
31. Palmas F, Biggio D, Pugni L, et al. GC-MS METABOLOMICS IDENTIFICATION OF NEW BIOMARKERS OF CHORIOAMNIONITIS: A PILOT STUDY. *J Pediatr Neonatal Individ Med*. 2016;5(2):59-60.
32. Noto A, Pomero G, Mussap M, et al. Urinary gas chromatography mass spectrometry metabolomics in asphyxiated newborns undergoing hypothermia: from the birth to the first month of life. *Ann Transl Med*. 2016;4(21):417-430. doi:10.21037/atm.2016.11.27.
33. Jordan KW, Adkins CB, Su L, et al. Lung Cancer Comparison of squamous cell carcinoma and adenocarcinoma of the lung by metabolomic analysis of tissue – serum pairs. *Lung Cancer*. 2010;68(1):44-50. doi:10.1016/j.lungcan.2009.05.012.
34. Burns MA, Taylor JL, Wu C, et al. Reduction of Spinning Sidebands in Proton NMR of Human Prostate Tissue With Slow High-Resolution Magic Angle Spinning. *Magn Reson Med*. 2005;42:34-42. doi:10.1002/mrm.20523.
35. Xia J, Mandal R, Sinelnikov I V, Broadhurst D, Wishart DS. MetaboAnalyst 2.0—a comprehensive server for metabolomic data analysis. *Nucleic Acids Res*. 2012;40(May):127-133. doi:10.1093/nar/gks374.
36. Xia J, Wishart DS. Comprehensive Metabolomics Data Analysis. *Curr Protoc Bioinforma*. 2016;55(September):1-91. doi:10.1002/cpbi.11.
37. Barberini L, Grapov D, Noto A, et al. ORTHOGONALIZATION METHODS IN METABOLOMICS. HYPOTHESIS AND TESTS FOR VALIDATION. *J Pediatr Neonatal Individ Med*. 2015;4(2):46-49.
38. Brace R, Cheung C. Regulation of amniotic fluid volume: evolving concepts. *Adv Exp Med Biol*. 2014;814:49-68.
39. Pelizzo G, Ballico M, Mimmi MC, et al. Metabolomic profile of amniotic fluid to evaluate lung maturity : the diaphragmatic hernia lamb model. *Multidiscip Respir Med*. 2014;9:1-8. doi:10.1186/2049-6958-9-54.
40. Feng J, Yan Y, Liang G, et al. Maternal and fetal metabonomic alterations in prenatal nicotine exposure-induced rat intrauterine growth retardation. *Mol Cell Endocrinol*. 2014;394(1-2):59-69. doi:10.1016/j.mce.2014.06.016.
41. Graca G, Duarte IF, Barros S, et al. Impact of Prenatal Disorders on the Metabolic Profile of Second Trimester Amniotic Fluid : A Nuclear Magnetic Resonance Metabonomic Study. *J Proteome Res*. 2010;9:6016-6024.
42. Pasquinelli F. *Diagnostica E Tecniche Di Laboratorio Parte Seconda*.; 1985.
43. Duarte IF, Barros S, Goodfellow BJ, Carreira IM, Couceiro AB, Gil AM. H NMR Based Metabonomics of Human Amniotic Fluid for the Metabolic Characterization of Fetus Malformations. *J Proteome Res*. 2009;8:4144-4150.
44. Hill M, Parizek A, RadmilaKanchevaa, MichaelaDuˇskováa M, Lubomír Kˇríˇza, MichaelaKlímkováb, AndreaPaˇskováb, Zdenˇek ˇZiˇzkab P, Milan Melounc L. Steroid metabolome in plasma from the umbilical artery, umbilical vein, maternal cubital vein and in amniotic fluid in normal and preterm labor_. *J Steroid Biochem Mol Biol*. 2010;121:594-610. doi:10.1016/j.jsbmb.2009.10.012.
45. Persson M, Winkvist A, Mogren I. Lifestyle and health status in a sample of Swedish women four years after pregnancy: a comparison of women with a history of normal pregnancy and women with a history of gestational diabetes mellitus. *B*. 2015.
46. Arfi A, Cohen J, Canlorbe G, Bendifallah S, Thomassin-naggara I, Darai E. European Journal of Obstetrics & Gynecology and Reproductive Biology First-trimester determination of fetal gender by ultrasound : measurement of the ano-genital distance. *Eur J Obstet Gynecol*. 2016;203:177-181. doi:10.1016/j.ejogrb.2016.06.001.
47. Mckeown BT, Record RG. THE INFLUENCE OF PLACENTAL SIZE ON FOETAL From the Department of Social Medicine , University of Birmingham { Received Birth weight. *J Endocrinol*. 1953;10:73-81.
48. Cvitic S, Longtine MS, Hackl H, et al. The Human Placental Sexome Differs between Trophoblast Epithelium and Villous Vessel Endothelium. *PLoS One*. 2013;8(10):e79233. doi:10.1371/journal.pone.0079233.
49. Efrat Z, Akinfenwa O, Nicolaides K. First-trimester determination of fetal gender by ultrasound. *Ultrasound Obs Gynecol*. 1999;13:305-307.
50. Emerson D, Felker R, Brown D. The sagittal sign. An early second trimester sonographic indicator of fetal gender. *J Ultrasound Med*. 1989;8:293-297.
51. Efrat Z, Perri T, Ramati E, Tugendreich D, Meizner I. Fetal gender assignment by first-trimester ultrasound.

Ultrasound Obs Gynecol. 2006;27:619-621.
52. Pedreira D. In search for the third point. *Ultrasound Obs Gynecol*. 2000;15:262-263.
53. Salazar-Martinez E, Romano-Riquer P, Yanez-Marquez, E Longnecker M, Hernandez-Avila M. Anogenital distance in human male and female newborns: a descriptive, cross-sectional study. *Environ Heal Glob Access Sci Source*. 2004;3:8.
54. Papadopoulou E, Vafeiadi M, Agramunt S. Anogenital distances in newborns and children from Spain and Greece: predictors, tracking and reliability. *Pediatr Perinat Epidemiol*. 2013;27:89-99.
55. Costa J-M, Benachi A, Gautier E. New strategy for prenatal diagnosis of X-linked disorders. *N Engl J Med*. 2002;346:1502.
56. Larson G. Globoseries Glycosphingolipids of Human Meconium. *Arch Biochem Biophys*. 1986;246(2):531-545.
57. Hanisch F-G, Peter-Katalinic J. Structural studies on fetal mucins from human amniotic fluid. *Eur J Biochem*. 1992;535:527-535.
58. Chen WYJ, Abatangelo G. Perspective article Functions of hyaluronan in wound repair. *Wound Repair Regen*. 1999;7:79-89.
59. Singh KK, ed. *Oxidative Stress, Disease And Cancer*. London: Imperial College Press; 2006.
60. Araújo LU, Grabe-guimarães A, Furtado Mosqueira CV, Martins Carneiro C, Silva-Barcellos NM. Profile of wound healing process induced by allantoin. *Wound Heal*. 2010;25(5):460-466.
61. Zitanova I, Koryta P, Garaiova I, Pueschel S. Uric acid and allantoin levels in Down syndrome : antioxidant and oxidative stress mechanisms ? ˇ ustrova ˇ itn ˇ kova. *Chim Clin Acta*. 2004;341:139-146. doi:10.1016/j.cccn.2003.11.020.
62. Fahrmann J, Grapov1 D, Yang J, et al. Systemic Alterations in the Metabolome of Diabetic NOD Mice Delineate Increased Oxidative Stress Accompanied by Reduced Inflammation and Hypertriglyceremia. *Am J Physiol Metab*. 2015;308(11):e978-989. doi:10.1152/ajpendo.00019.2015.
63. Yuan W, Zhang J, Li S, Edwards JL. Amine Metabolomics of Hyperglycemic Endothelial Cells using Capillary LC À MS with Isobaric Tagging. *J Proteome Res*. 2011;10:5242-5250.
64. Pero RW, Lund H, Leanderson T. Antioxidant Metabolism Induced by Quinic Acid . Increased Urinary Excretion of Tryptophan and Nicotinamide. *Phyther Res*. 2009;346(October 2008):335-346. doi:10.1002/ptr.
65. Jimenez E, Marin ML, Martin R, et al. Is meconium from healthy newborns actually sterile ? *Res Microbiol*. 2008;159:187-193. doi:10.1016/j.resmic.2007.12.007.
66. Zavattoni M, Lombardi G, Rognoni V, Furione M, Klersy C, Stronati M. Review and meta-analysis of the epidemiology of congenital cytomegalovirus (CMV) infection. *J Med Virol*. 2014;86:2163-2170.
67. Zavattoni M, Lombardi G, Rognoni V, Furione M, Klersy C, Stronati M. Pre- and periconceptional primary cytomegalovirus infection: risk of vertical transmission and congenital disease. *J Med Virol*. 2014;86:2163-2170.
68. Zavattoni M, Lombardi G, Rognoni V, Furione M, Klersy C, Stronati M. Congenital cytomegalovirus infection following primary maternal infection in the third trimester. *J Med Virol*. 2014;86:2163-2170.
69. Zavattoni M, Lombardi G, Rognoni V, Furione M, Klersy C, Stronati M. Human cytomegalovirus in utero transmission: follow-up of 524 maternal seroconversions. *J Med Virol*. 2014;86:2163-2170.
70. Zavattoni M, Lombardi G, Rognoni V, Furione M, Klersy C, Stronati M. Intrauterine transmission and clinical outcome of 248 pregnancies with primary cytomegalovirus infection in relation to gestational age. *J Med Virol*. 2014;86:2163-2170.
71. Zavattoni M, Lombardi G, Rognoni V, Furione M, Klersy C, Stronati M. Role of prenatal diagnosis and counseling in the management of 735 pregnancies complicated by primary human cytomegalovirus infection: a 20-year experience. *J Med Virol*. 2014;86:2163-2170.
72. Zavattoni M, Lombardi G, Rognoni V, Furione M, Klersy C, Stronati M. Maternal, fetal, and neonatal parameters for prognosis and counseling of HCMV congenital infection. *J Med Virol*. 2014;86:2163-2170.
73. Revello MG, Zavattoni M, Furione M, Lilleri D, Gorini G, Gerna G. Diagnosis and outcome of preconceptional and periconceptional primary human cytomegalovirus infections. *J Infect Dis*. 2002;186:553-557.
74. Pass RF, Stagno S, Myers GJ, Alford CA. Outcome of symptomatic congenital cytomegalovirus infection: results of long-term longitudinal follow-up. *Pediatrics*. 1980;66:758-762.
75. Dollard SC, Grosse SD, Ross DS. New estimates of the prevalence of neurological and sensory sequelae and mortality associated with congenital cytomegalovirus infection. *Rev Med Virol*. 2007;17:355-363.
76. Saigal S, Lunyk O, Larke RP, Chernesky MA. The outcome in children with congenital cytomegalovirus infection. A longitudinal follow-up study. *Am J Dis Child*. 1982;136:896-901.
77. Boppana SB, Fowler KB, Pass RF, Rivera LB, Bradford RD, Lakeman FD. Congenital cytomegalovirus infection: association between virus burden in infancy and hearing loss. *J Pediatr*. 2005;146:817-823.
78. Lanari M, Lazzarotto T, Venturi V, Papa I, Gabrielli L, Guerra B. Neonatal cytomegalovirus blood load and risk of sequelae in symptomatic and asymptomatic congenitally infected newborns. *Pediatrics*. 2006;117:76-83.
79. Guerra B, Lazzarotto T, Quarta S, Lanari M, Bovicelli L, Nicolosi A. Prenatal diagnosis of symptomatic congenital cytomegalovirus infection. *Am J Obstet Gynecol*. 2000;183:476-482.
80. Revello MG, Zavattoni M, Furione M, Baldanti F, Gerna G. Quantification of human cytomegalovirus DNA in

amniotic fluid of mothers of congenitally infected fetuses. *J Clin Microbiol*. 1999;37:3350-3352.
81. Gouarin S, Gault E, Vabret A, Cointe D, Rozenberg F, Grangeot-Keros L. Real-time PCR quantification of human cytomegalovirus DNA in amniotic fluid samples from mothers with primary infection. *J Clin Microbiol*. 2002;40:1767-1772.
82. Picone O, Costa JM, Leruez-Ville M, Ernault P, Olivi M, Ville Y. Cytomegalovirus (CMV) glycoprotein B genotype and CMV DNA load in the amniotic fluid of infected fetuses. *Pediatr Diagnostic*. 2004;24:1001-1006.
83. Goegebuer T, Meensel B Van, Beuselinck K, Cossey V, Ranst M Van, Hanssen M. Clinical predictive value of real-time PCR quantification of human cytomegalovirus DNA in amniotic fluid samples. *J Clin Microbiol*. 2009;47:660-665.
84. Fabbri E, Revello MG, Furione M, Zavattoni M, Lilleri D, Tassis B. Prognostic markers of symptomatic congenital human cytomegalovirus infection in fetal blood. *BJOG*. 2011;118:448-456.
85. Bodéus M, Hubinont C, Bernard P, Bouckaert A, Thomas K, Goubau P. Prenatal diagnosis of human cytomegalovirus by culture and polymerase chain reaction: 98 pregnancies leading to congenital infection. *Prenat Diagn*. 1999:314-317.
86. Liesnard C, Donner C, Brancart F, Gosselin F, Delforge ML, Rodesch F. Prenatal diagnosis of congenital cytomegalovirus infection: prospective study of 237 pregnancies at risk. *Obstet Gyncology*. 2000;95:881-888.
87. Enders G, Bäder U, Lindemann L, Schalasta G, Daiminger A. Prenatal diagnosis of congenital cytomegalovirus infection in 189 pregnancies with known outcome. *Prenat Diagn*. 2001;21:362-377.
88. Goegebuer T, Meensel B Van, Beuselinck K, Cossey V, Ranst M Van, Hanssens M. Clinical predictive value of real-time PCR quantification of human cytomegalovirus DNA in amniotic fluid samples. *J Clin Microbiol*. 2009;47:660-665.
89. Revello MG, Zavattoni M, Sarasini A, Percivalle E, Simoncini L, Gerna G. Human cytomegalovirus in blood of immunocompetent persons during primary infection: prognostic implications for pregnancy. *J Infect Dis*. 1998;177:1170-1175.
90. Fanos V, Locci E, Noto A, Lazzarotto T, Manzoni P, Atzori L. Urinarymetabolomics in newborn infected by human cytomegalovirus: a preliminary investigation. *Early Hum Dev*. 2013;89:S58-S61.
91. Noto A, Dessi A, Puddu M, Mussap M, Fanos V. Metabolomics technology and their application to the study of the viral infection. *J Matern Neonatal Med*. 2014;7058:53-57. doi:10.3109/14767058.2014.955963.
92. Locci E, Noto A, Lanari M, Lazzarotto T, Fanos V, Atzori L. Metabolomics: a new tool for the investigation of metabolic changes induced by cytomegalovirus. *J Matern Neonatal Med*. 2013;26(S2):17-19. doi:10.3109/14767058.2013.829684.
93. Munger J, Bajad SU, Coller HA, Shenk T, Rabinowitz JD. Dynamics of the Cellular Metabolome during Human Cytomegalovirus Infection. *PLoS Pathog*. 2006;2(12):e132. doi:10.1371/journal.ppat.0020132.
94. Munger J, Bennett BD, Parikh A, et al. Systems-level metabolic flux profiling identifies fatty acid synthesis as a target for antiviral therapy. *Nat Biotechnol*. 2008;26(10):1179-1186. doi:10.1038/nbt.1500.
95. Chambers JW, Maguire TG, Alwine JC. Glutamine Metabolism Is Essential for Human Cytomegalovirus Infection □. *J Virol*. 2010;84(4):1867-1873. doi:10.1128/JVI.02123-09.
96. Yu Y, Clippinger AJ, Alwine JC. Viral affects on metabolism: changes in glucose and glutamine utilization during human cytomegalovirus infection. *Trends Microbiol*. 2012;19(7):360-367. doi:10.1016/j.tim.2011.04.002.Viral.
97. Liu STH, Sharon-friling R, Ivanova P, Milne SB, Myers DS, Rabinowitz JD. Synaptic vesicle-like lipidome of human cytomegalovirus virions reveals a role for SNARE machinery in virion egress. *PNAS*. 2011;108(31):12869–12874. doi:10.1073/pnas.1109796108.
98. Paradowska E, Przepiórkiewicz M, Nowakowska D, Studzińska M, Wilczyński J, Emery VC. Detection of cytomegalovirus in human placental cells by polymerase chain reaction. *APMIS*. 2006;114:764-771.
99. Ridge CA, Pua BB, Madoff DC. Epidemiology and Staging of Renal Cell Carcinoma. *Semin Intervent Radiol*. 2014;31:3-8.
100. Ljungberg B, Campbell SC, Yong H, et al. The Epidemiology of Renal Cell Carcinoma. *Eur Urol*. 2011;60:615-621. doi:10.1016/j.eururo.2011.06.049.
101. Hancock SB, Georgiades CS. Kidney Cancer. *Cancer J*. 2016;22(6):387-392. doi:10.4135/9781412963855.n671.
102. Siegel RL, Miller KD, Jemal A. Cancer Statistics , 2015. *CA Cancer J Clin*. 2015;65(1):5-29. doi:10.3322/caac.21254.
103. Decastro GJ, Mckiernan JM. Epidemiology , Clinical Staging , and Presentation of Renal Cell Carcinoma. *Urol Clin North Am*. 2008;35(4):581-592. doi:10.1016/j.ucl.2008.07.005.
104. Scoll BJ, Wong Y, Egleston BL, Kunkle DA, Saad IR, Uzzo RG. Age, Tumor Size and Relative Survival of Patients With Localized Renal Cell Carcinoma: A Surveillance, Epidemiology and End Results Analysis. *J Urol*. 2009;181(2):506-511. doi:10.1016/j.juro.2008.10.026.Age.
105. Podo F. Tumour phospholipid metabolism. *NMR Biomed*. 1999;12:413-439.
106. Foster DA, Xu L. Phospholipase D in Cell Proliferation and Cancer. *Mol Cancer Res*. 2003;1(September):789-

800.
107. Ackerstaff E, Glunde K, Bhujwalla ZM. Choline Phospholipid Metabolism : A Target in Cancer Cells ? *J Cell Biochem*. 2003;90:525–533. doi:10.1002/jcb.10659.
108. Sitter B, Bathen T, Hagen B, Arentz C, Skjeldestad FE, Gribbestad IS. Cervical cancer tissue characterized by high-resolution magic angle spinning MR spectroscopy. *Magn Reson Mater Physics, Biol Med*. 2004;16:174-181. doi:10.1007/s10334-003-0025-5.
109. Meister A, Anderson ME. GLUTATHIONE. *Annu Rev Biochem*. 1983;52:711-760.
110. Balendiran GK, Dabur R, Fraser D. The role of glutathione in cancer. *Cell Biochem Funct*. 2004;22(October 2003):343-352.
111. Moreadiths RW, Lehningert AL. The Pathways of Glutamate and Glutamine Oxidation by Tumor Cell Mitochondria. Role of mitochondrial NAD(P)+-dependent malic enzyme. *J Biol Chem*. 1984;259:6215-6221.
112. Michaelis T, Helms G, Merboldt K, Hanicke W, Bruhn H, Frahm J. Identification of Scyllo-Inositol in Proton. *NMR Biomed*. 1993;6(June 1992):105-109.
113. Koppenol WH, Bounds PL, Dang C V. Otto Warburg's contributions to current concepts of cancer metabolism. *Nat Rev Cancer*. 2011;11(May):325-337. doi:10.1038/nrc3038.
114. Unwin RD, Craven RA, Harnden P, et al. Proteomic changes in renal cancer and co-ordinate demonstration of both the glycolytic and mitochondrial aspects of the Warburg effect. *Proteomics*. 2003;3:1620-1632. doi:10.1002/pmic.200300464.
115. Xu XD, Shao SX, Jiang HP, et al. Warburg Effect or Reverse Warburg Effect ? A Review of. *Oncol Res Treat*. 2015;38(59):117-122. doi:10.1159/000375435.
116. Gonzalez CD, Alvarez S, Ropolo A, Rosenzvit C, Bagnes MFG, Vaccaro MI. Autophagy , Warburg , and Warburg Reverse Effects in Human Cancer. *Biomed Res Int*. 2014;2014:1-10.
117. Lee M, Yoon J. Metabolic interplay between glycolysis and mitochondrial oxidation: The reverse Warburg effect and its therapeutic implication. *World J Biol Chem*. 2015;6(3):148-162. doi:10.4331/wjbc.v6.i3.148.
118. Fenger F. Chemical Composition of Placenta. *J Biol Chem*. 1916;29:19-23.
119. Pratt JP, Kaucher M, Richards AJ, Williams HH, Macy IC. Composition of the human placenta. *Am J Obstet Gynecol*. 1946;52:402-408. doi:10.1016/S0002-9378(15)30252-0.
120. Yetter JF. Examination of the Placenta. *Am Fam Physician*. 1998;57(5):1045-1054.
121. Dunn WB, Brown M, Worton SA, et al. Changes in the Metabolic Footprint of Placental Explant-Conditioned Culture Medium Identifies Metabolic Disturbances Related to Hypoxia and Pre-Eclampsia. *Placenta*. 2009;30(11):974-980. doi:10.1016/j.placenta.2009.08.008.
122. Heazell AEP, Brown M, Dunn WB, et al. Analysis of the Metabolic Footprint and Tissue Metabolome of Placental Villous Explants Cultured at Different Oxygen Tensions Reveals Novel Redox Biomarkers. *Placenta*. 2008;29:691-698. doi:10.1016/j.placenta.2008.05.002.
123. Horgan RP, Broadhurst DI, Dunn WB, et al. Changes in the Metabolic Footprint of Placental Explant-Conditioned Medium Cultured in Different Oxygen Tensions from Placentas of Small for Gestational Age and Normal Pregnancies. *Placenta*. 2010;31(10):893-901. doi:10.1016/j.placenta.2010.07.002.
124. Tissot van Patot MC, Murray AJ, Beckey V, et al. Human placental metabolic adaptation to chronic hypoxia , high altitude : hypoxic preconditioning. *Am J Physiol Regul Integr Comp Physiol*. 2010;(15):166-173. doi:10.1152/ajpregu.00383.2009.
125. Cindrova-Daves T, Tissot van Patot M, Gardner L, Jauniaux E, Burton GJ, Charnock-Jones DS. Energy status and HIF signalling in chorionic villi show no evidence of hypoxic stress during human early placental development. *Mol Hum Reprod*. 2015;21(3):296-308. doi:10.1093/molehr/gau105.
126. Korkes HA, Sass N, Moron AF, et al. Lipidomic Assessment of Plasma and Placenta of Women with Early-Onset Preeclampsia. *PLoS One*. 2014;9(10):e110747. doi:10.1371/journal.pone.0110747.
127. Austdal M, Cecilie L, Thomsen V, Haugstad L, Iversen A. Metabolic pro fi les of placenta in preeclampsia using HR-MAS MRS metabolomics. *Placenta*. 2015;36(12):1455-1462. doi:10.1016/j.placenta.2015.10.019.
128. Mumme K, Gray C, Reynolds CM, et al. Maternal-fetal hepatic and placental metabolome profiles are associated with reduced fetal growth in a rat model of maternal obesity. *Metabolomics*. 2016;12:83-92. doi:10.1007/s11306-016-1014-9.
129. Catalano PM, Shankar K. Obesity and pregnancy : mechanisms of short term and long term adverse consequences for mother and child. *Br Med J*. 2017;360:1-16. doi:10.1136/bmj.j1.
130. Zilberlicht A, Feferkorn I, Younes G, Damti A, Auslender R, Riskin-mashiah S. The mutual effect of pregestational body mass index , maternal hyperglycemia and gestational weight gain on adverse pregnancy outcomes The mutual effect of pregestational body mass index , maternal hyperglycemia and gestational weight gain on adverse preg. *Gynecol Endocrinol*. 2016;3590(April):416-420. doi:10.3109/09513590.2015.1127911.
131. Wallace JM, Horgan GW, Bhattacharya S. Placental weight and ef fi ciency in relation to maternal body mass index and the risk of pregnancy complications in women delivering singleton babies. *Placenta*. 2012;33(8):611-618. doi:10.1016/j.placenta.2012.05.006.
132. Taricco E, Radaelli T, Santis MSN De, Cetin I. Foetal and Placental Weights in Relation to Maternal Characteristics in Gestational Diabetes. *Placenta*. 2003;24:343-347.

133. Mandò C, Calabrese S, Mazzocco MI, et al. Sex speci fi c adaptations in placental biometry of overweight and obese women. *Placenta*. 2016;38:1-7. doi:10.1016/j.placenta.2015.12.008.
134. Leon-garcia SM, Roeder HA, Nelson KK, et al. Maternal obesity and sex-speci fi c differences in placental pathology. *Placenta*. 2016;38:33-40. doi:10.1016/j.placenta.2015.12.006.
135. Rasmussen KM, Yaktine AL, Guidelines I of M (US) and NRC (US) C to RIPW, eds. *Weight Gain During Pregnancy: Reexamining the Guidelines*. Washington (DC): National Academies Press (US); 2009.
136. Hod M, Kapur A, Sacks DA. The International Federation of Gynecology and Obstetrics (FIGO) Initiative on gestational diabetes mellitus: A pragmatic guide for diagnosis, management, and care. *Int J Gynecol Obstet*. 2015;131:S173-211.
137. Cetin I. Amino Acid Interconversions in the Fetal-Placental Unit : The Animal Model and Human Studies In Vivo. *Pediatr Res*. 2001;49(2):148-154.
138. Jansson T. Reviews of Placental Amino Acid Transport and Metabolism Amino Acid Transporters in the Human Placenta. *Pedriatric Res*. 2001;49(2):141-147.
139. Jansson N, Rosario FJ, Gaccioli F, et al. Activation of Placental mTOR Signaling and Amino Acid Transporters in Obese Women Giving Birth to Large Babies. *Endocr Care*. 2013;98(January):1-9. doi:10.1210/jc.2012.
140. Murakami S. Role of taurine in the pathogenesis of obesity. *Mol Nutr Food Res*. 2015:1353-1363. doi:10.1002/mnfr.201500067.
141. Ditchfield AM, Desforges M, Mills TA, et al. Maternal obesity is associated with a reduction in placental taurine transporter activity. *Int J Obes*. 2015;(January):557-564. doi:10.1038/ijo.2014.212.
142. Yang M, Vousden KH. Serine and one-carbon metabolism in cancer. *Nat Rev Cancer*. 2016;16:650-662. doi:10.1038/nrc.2016.81.
143. Houtkooper RH, Canto C, Wanders RJ, Auwerx J. The Secret Life of NAD ⁺ : An Old Metabolite Controlling New Metabolic Signaling Pathways. *Endocr Rev*. 2015;31(April 2010):194-223. doi:10.1210/er.2009-0026.
144. Cetin I, Parisi F, Berti C, Mandò C, Desoye G. Placental fatty acid transport in maternal obesity ` 1. *J Dev Orig Health Dis*. 2012;3:409-414. doi:10.1017/S2040174412000414.
145. Larner J, Ph D. D-Chiro-Inositol – Its Functional Role in Insulin. *Int J Experimantal Diabetes Res*. 2002;3:47-60.
146. Mandò C, Novielli C, Anelli G. Alterations of Mitochondrial Content in Obese Placentas. *Reprod Sci*. 2015;22:374A-374A.
147. Taricco E, Radaelli T, Rossi G, et al. Effects of gestational diabetes on fetal oxygen and glucose levels in vivo. 2009:1729-1735. doi:10.1111/j.1471-0528.2009.02341.x.
148. Hospital BC, Cetin PI, Sacco OL. PLACENTAL MITOCHONDRIAL CONTENT AND FUNCTION IN INTRAUTERINE GROWTH RESTRICTION AND PREECLAMPSIA. *Am J Physiol Metab*. 2013;306:E404-413. doi:10.1152/ajpendo.00426.2013.
149. Lassance L, Haghiac M, Leahy P, Basu S. HHS Public Access. 2016;212(5):1-18. doi:10.1016/j.ajog.2015.02.026.Identification.
150. Anelli GM, Cardellicchio M, Novielli C. Mitochondrial content and hepcidin are increased in obese pregnant mothers. *J Matern Neonatal Med*. 2017;4:1-8.
151. Scifres CM, Chen B, Nelson DM, Sadovsky Y. Fatty Acid Binding Protein 4 Regulates Intracellular Lipid Accumulation in Human Trophoblasts. *J Clin Endocrinol Metab*. 2015;96(July 2011):1083-1091. doi:10.1210/jc.2010-2084.
152. Mennitti L V, Oliveira JL, Morais CA, et al. ScienceDirect Type of fatty acids in maternal diets during pregnancy and / or lactation and metabolic consequences of the offspring. *J Nutr Biochem*. 2014;26:99-111. doi:10.1016/j.jnutbio.2014.10.001.
153. Berti C, Cetin I, Agostoni C, et al. Critical Reviews in Food Science and Nutrition Pregnancy and infants â€™ outcome : nutritional and metabolic implications . *Crit Rev Food Sci Nutr*. 2016;56:82-91. doi:10.1080/10408398.2012.745477.
154. Scholtens DM, Muehlbauer J, Daya NR, et al. Metabolomics Reveals Broad-Scale Metabolic Perturbations in Hyperglycemic Mothers During Pregnancy. *Diabetes Care*. 2014;37(January):158-166. doi:10.2337/dc13-0989.
155. Cetin I, Santis MSN De, Taricco E, et al. Maternal and fetal amino acid concentrations in normal pregnancies and in pregnancies with gestational diabetes mellitus. *Am J Obstet Gynecol*. 2005;192:610-617. doi:10.1016/j.ajog.2004.08.011.
156. Fattuoni C, Palmas F, Anelli GM, et al. Preliminary metabolomics analysis of placenta in maternal obesity. *Placenta*. 2018;61:89-95. doi:https://doi.org/10.1016/j.placenta.2017.11.014.
157. The University of Sydney. PLASMA. http://sydney.edu.au/science/biology/learning/blood_composition/Plasma.shtml.
158. O'Neil D. Blood Components. https://web.archive.org/web/20130605052544/http://anthro.palomar.edu/blood/blood_components.htm.
159. Tenesa A, Dunlop MG. association studies. *Nat Rev Genet*. 2009;10:353-358.
160. Zhou ZY, Wan XY, Cao JW. Dietary methionine intake and risk of incident colorectal cancer: A meta-analysis of 8 prospective studies involving 431,029 participants. *PLoS One*. 2013;8(12):6-12.

doi:10.1371/journal.pone.0083588.
161. Lin Y, Ma C, Liu C, Wang Z, Yang J. NMR-based fecal metabolomics fingerprinting as predictors of earlier diagnosis in patients with colorectal cancer. 2016;7(20).
162. AHLQUIST DA, ZOU H, DOMANICO M, et al. Next-Generation Stool DNA Test Accurately Detects Colorectal Cancer and Large Adenomas. *Gastroenterology*. 2014;142(2). doi:10.1053/j.gastro.2011.10.031.AHLQUIST.
163. Gastroenterologi PEN, Quintero E. Gastroenterología y Hepatología. 2009;32(8):565-576. doi:10.1016/j.gastrohep.2009.01.179.
164. Oncology R, Surgical S, Ahmed FE, et al. Diagnostic MicroRNA Markers to Screen for Sporadic Human Colon Cancer in Stool : I . Proof of Principle. 2013;114:93-113.
165. Chan ECY, Koh PK, Mal M, et al. Metabolic Profiling of Human Colorectal Cancer Using High-Resolution Magic Angle Spinning Nuclear Magnetic Resonance (HR-MAS NMR) Spectroscopy and Gas Chromatography Mass Spectrometry (GC / MS) research articles. *J Proteome Res*. 2009;8:352-361.
166. Denkert C, Budczies J, Weichert W, et al. Metabolite profiling of human colon carcinoma – deregulation of TCA cycle and amino acid turnover. *Mol Cancer*. 2008;7(72):1-15. doi:10.1186/1476-4598-7-72.
167. Qiu Y, Cai G, Zhou B, et al. A Distinct Metabolic Signature of Human Colorectal Cancer with Prognostic Potential. *Clin Cancer Res*. 2014;20(8):2136-2147. doi:10.1158/1078-0432.CCR-13-1939.
168. Moriwaki K, Noda K, Furukawa Y, et al. Deficiency of GMDS Leads to Escape from NK Cell-Mediated Tumor Surveillance Through Modulation of TRAIL Signaling. *Gastroenterology*. 2009;137(1):188-198.e2. doi:10.1053/j.gastro.2009.04.002.
169. Kannagi R, Yin J, Miyazaki K, Izawa M. Current relevance of incomplete synthesis and neo-synthesis for cancer-associated alteration of carbohydrate determinants-Hakomori's concepts revisited. *Biochim Biophys Acta - Gen Subj*. 2008;1780(3):525-531. doi:10.1016/j.bbagen.2007.10.007.
170. Nakayama K, Moriwaki K, Imai T, et al. Mutation of GDP-Mannose-4,6-Dehydratase in Colorectal Cancer Metastasis. *PLoS One*. 2013;8(7):4-8. doi:10.1371/journal.pone.0070298.
171. Moriwaki K, Shinzaki S, Miyoshi E. GDP-mannose-4,6-dehydratase (GMDS) deficiency renders colon cancer cells resistant to tumor necrosis factorrelated apoptosis-inducing ligand (TRAIL) receptor- and CD95-mediated apoptosis by inhibiting complex II formation. *J Biol Chem*. 2011;286(50):43123-43133. doi:10.1074/jbc.M111.262741.
172. Wang Z, Uchida K, Ohnaka K, et al. Sugars, sucrose and colorectal cancer risk: the Fukuoka colorectal cancer study. *Scand J Gastroenterol*. 2014;49(5):581-588. doi:10.3109/00365521.2013.822091.
173. Charrez B, Qiao L, Hebbard L. The role of fructose in metabolism and cancer. *Horm Mol Biol Clin Investig*. 2015;22(2):79-89. doi:10.1515/hmbci-2015-0009.
174. Michaud DS, Fuchs CS, Liu S, Willett WC, Colditz GA, Giovannucci E. Dietary glycemic load, carbohydrate, sugar, and colorectal cancer risk in men and women. *Cancer Epidemiol Biomarkers Prev*. 2005;14(1):138-147. http://www.ncbi.nlm.nih.gov/pubmed/15668487%5Cnhttp://cebp.aacrjournals.org/content/14/1/138.full.pdf.
175. Stamp D, Zhang XM, Medline A, Bruce WR, Archer MC. Sucrose enhancement of the early steps of colon carcinogenesis in mice. *Carcinogenesis*. 1993;14(4):777-779. doi:10.1093/carcin/14.4.777.
176. Port AM, Ruth MR, Istfan NW. Fructose consumption and cancer: is there a connection? *Curr Opin Endocrinol Diabetes Obes*. 2012;19(5):367-374. doi:10.1097/MED.0b013e328357f0cb.
177. Hui H, Huang D, McArthur D, Nissen N, Boros LG, Heaney AP. Direct spectrophotometric determination of serum fructose in pancreatic cancer patients. *Pancreas*. 2009;38(6):706-712. doi:10.1097/MPA.0b013e3181a7c6e5.
178. Liu H, Huang D, McArthur DL, Boros LG, Nissen N, Heaney AP. Fructose induces transketolase flux to promote pancreatic cancer growth. *Cancer Res*. 2010;70(15):6368-6376. doi:10.1158/0008-5472.CAN-09-4615.
179. Tan B, Qiu Y, Zou X. Metabonomics identifies serum metabolite markers of colorectal cancer. *J Proteome Res*. 2013;12(6):3000-3009.
180. Xu W, Tamim H, Shapiro S, Stang MR, Collet J-P. Use of antidepressants and risk of colorectal cancer: a nested case-control study. *Lancet Oncol*. 2006;7(4):301-308. doi:10.1016/S1470-2045(06)70622-2.
181. Coogan PF, Strom BL, Rosenberg L. Antidepressant use and colorectal cancer risk. *Pharmacoepidemiol Drug Saf*. 2009;18:1111-1114. doi:10.1002/pds.
182. Dowling P, Hughes DJ, Larkin AM, et al. Elevated levels of 14-3-3 proteins, serotonin, gamma enolase and pyruvate kinase identified in clinical samples from patients diagnosed with colorectal cancer. *Clin Chim Acta*. 2015;441:133-141. doi:10.1016/j.cca.2014.12.005.
183. Burroughs KD, Dunn SE, Barrett JC, Taylor JA. Insulin-Like Growth Factor-I: a Key Regulator of Human Cancer Risk? *J Natl Cancer Inst*. 1999;91(7):579-581. doi:10.1093/jnci/91.7.579.
184. Nocito A, Dahm F, Jochum W, et al. Serotonin regulates macrophage-mediated angiogenesis in a mouse model of colon cancer allografts. *Cancer Res*. 2008;68(13):5152-5158. doi:10.1158/0008-5472.CAN-08-0202.
185. Dong Z, Kumar R, Yang X, Fidler IJ. Macrophage-derived metalloelastase is responsible for the generation of angiostatin in Lewis lung carcinoma. *Cell*. 1997;88(6):801-810. doi:10.1016/S0092-8674(00)81926-1.

186. Houghton AM, Grisolano JL, Baumann ML, et al. Macrophage elastase (matrix metalloproteinase-12) suppresses growth of lung metastases. *Cancer Res*. 2006;66(12):6149-6155. doi:10.1158/0008-5472.CAN-04-0297.
187. Cornelius L a, Nehring LC, Harding E, et al. Matrix metalloproteinases generate angiostatin: effects on neovascularization. *J Immunol*. 1998;161(12):6845-6852. http://www.ncbi.nlm.nih.gov/pubmed/9862716.
188. Ataee R, Ajdary S, Rezayat M, Shokrgozar MA, Shahriari S, Zarrindast MR. Study of 5HT 3 and 5HT 4 Receptors Expression in HT29 Cell Line and Human Colon Adenocarcinoma Tissues. *Archives*. 2010;13(2):120-125.
189. Wang H, Tso VK, Slupsky CM, Fedorak RN. a Systematic Review. 2010:1395-1406.
190. Miyagi Y, Higashiyama M, Gochi A, et al. Plasma free amino acid profiling of five types of cancer patients and its application for early detection. *PLoS One*. 2011;6(9). doi:10.1371/journal.pone.0024143.
191. Giovannucci E, Rimm EB, Ascherio A, Stampfer MJ, Colditz GA, Willett WC. Alcohol, low-methionine-low-folate diets, and risk of colon cancer in men. *J Natl Cancer Inst*. 1995;87(4):265-273. doi:10.1093/jnci/87.4.265.
192. Giovannucci E. Trans-HHS Workshop : Diet , DNA Methylation Processes and Health Epidemiologic Studies of Folate and Colorectal Neoplasia : a Review 1. *New York*. 2002:2350-2355.
193. Harnck L, Jacobs DR, Nicodemus K, Lazovich D, Anderson K, Folsom AR. Relationship of Folate, Vitamin B-6, Vitamin B-12, and Methionine Intake to Incidence of Colorectal Cancers. *Nutr Cancer*. 2002;43(2):152-158. doi:10.1207/S15327914NC432.
194. Bailey LB, Gregory JF. Folate Metabolism and Requirements. *J Nutr*. 1999;129:779-782.
195. Kune G, Watson L. Colorectal Cancer Protective Effects and the Dietary Micronutrients Folate, Methionine, Vitamins B6, B12, C, E, Selenium, and Lycopene. *Nutr Cancer*. 2009;56(1):11-21. doi:10.1207/s15327914nc5601.
196. Ulrich CM. Nutrigenetics in Cancer Research—Folate Metabolism and Colorectai Cancer. *J Nutr*. 2005;135(7):2698-2702.
197. de Vogel S, Dindore V, van Engeland M, Goldbohm RA, van den Brandt PA, Weijenberg MP. Dietary folate, methionine, riboflavin, and vitamin B-6 and risk of sporadic colorectal cancer. *J Nutr*. 2008;138(12):2372-2378. doi:10.3945/jn.108.091157.
198. Sandhu MS, White IR, McPherson K. Systematic review of the prospective cohort studies on meat consumption and colorectal cancer risk a meta-analytical approach. *Cancer Epidemiol Biomarkers …*. 2001;10(May):439-446. http://cebp.aacrjournals.org/content/10/5/439.short.
199. Uchida H, Yamazaki K, Fukuma M, et al. Overexpression of leucine-rich repeat-containing G protein-coupled receptor 5 in colorectal cancer. *Cancer Sci*. 2010;101(7):1731-1737. doi:10.1111/j.1349-7006.2010.01571.x.
200. Yamanoi K, Fukuma M, Uchida H, et al. Overexpression of leucine-rich repeat-containing G protein-coupled receptor 5 in gastric cancer. *Pathol Int*. 2013;63(1):13-19. doi:10.1111/pin.12013.
201. REZA ALIZADEH-NAVAEI1, ALIREZA RAFIEI1, SAEID ABEDIAN-KENARI2, HOSSEIN ASGARIAN-OMRAN1, REZA VALADAN1, and AKBAR HEDAYATIZADEH-OMRAN1. Comparison of leucine-rich repeat-containing G protein-coupled receptor 5 expression in different cancer and normal cell lines. *Biomed reports*. 2016;5:130-132. doi:10.3892/br.2016.684.
202. Bult CJ, Eppig JT, Kadin JA, et al. The Mouse Genome Database (MGD): Mouse biology and model systems. *Nucleic Acids Res*. 2008;36(SUPPL. 1):724-728. doi:10.1093/nar/gkm961.
203. Meunier D, Patra K, Smits R, et al. Expression analysis of proline rich 15 (Prr15) in mouse and human gastrointestinal tumors. *Mol Carcinog*. 2011;50(1):8-15. doi:10.1002/mc.20692.
204. Liu W, Glunde K, Bhujwalla ZM, Raman V, Sharma A, Phang JM. Proline oxidase promotes tumor cell survival in hypoxic tumor microenvironments. *Cancer Res*. 2012;72(14):3677-3686. doi:10.1158/0008-5472.CAN-12-0080.
205. Ma Y, Liu W, Peng J, et al. A pilot study of gas chromatograph/mass spectrometry-based serum metabolic profiling of colorectal cancer after operation. *Mol Biol Rep*. 2010;37(3):1403-1411. doi:10.1007/s11033-009-9524-4.
206. Ni Y, Xie G, Jia W. Metabonomics of Human Colorectal Cancer: New Approaches for Early Diagnosis and Biomarker Discovery. *J Proteome Res*. 2014;13(9):3857-3870. doi:10.1021/pr500443c.
207. Hough LB. Genomics meets histamine receptors: new subtypes, new receptors. *Mol Pharmacol*. 2001;59(3):415-419. doi:10.1124/mol.59.3.415.
208. Takeuchi Y, Nishibori M, Uomoto M, et al. Increase in histidine decarboxylase activity in tissues of mice bearing Colon-26 tumor cells. *Naunyn Schmiedebergs Arch Pharmacol*. 1999;360(1):92-98. http://www.ncbi.nlm.nih.gov/pubmed/10463338.
209. Masini E, Fabbroni V, Giannini L, et al. Histamine and histidine decarboxylase up-regulation in colorectal cancer: Correlation with tumor stage. *Inflamm Res*. 2005;54(SUPPL. 1):5-6. doi:10.1007/s00011-004-0437-3.
210. Ghosh AK, Hirasawa N, Ohuchi K. Enhancement by histamine of vascular endothelial growth factor production in granulation tissue via H(2) receptors. *Br J Pharmacol*. 2001;134(7):1419-1428. doi:10.1038/sj.bjp.0704372.
211. Pathi SS, Lei P, Sreevalsan S, Chadalapaka G, Jutooru I, Safe S. Pharmacologic Doses of Ascorbic Acid

Repress Specificity Protein (Sp) Transcription Factors and Sp-Regulated Genes in Colon Cancer Cells. *Nutr Cancer*. 2011;63(7):1133-1142. doi:10.1080/01635581.2011.605984.
212. Pires AS, Marques CR, Encarnação JC, et al. 756: Ascorbic acid-induced cytotoxicity in colon cancer cell lines. *Eur J Cancer*. 2014;50:S182. doi:10.1016/S0959-8049(14)50664-8.
213. Yu L, Aa J, Xu J, et al. Metabolomic phenotype of gastric cancer and precancerous stages based on gas chromatography time-of-flight mass spectrometry. *J Gastroenterol Hepatol*. 2011;26(8):1290-1297. doi:10.1111/j.1440-1746.2011.06724.x.
214. Pires AS, Marques CR, Encarnação JC, et al. Ascorbic acid and colon cancer: an oxidative stimulus to cell death depending on cell profile. *Eur J Cell Biol*. 2016;95(6-7):208-218. doi:10.1016/j.ejcb.2016.04.001.
215. Qiu Y, Cai G, Su M. Serum metabolite profiling of human colorectal cancer using GC-TOFMS and UPLC-QTOFMS. *J Proteome Res*. 2009;8(10):4844-4850.
216. Nomura DK, Long JZ, Niessen S. Monoacylglycerol lipase regulates a fatty acid network that promotes cancer pathogenesis. *Cell*. 2010;140(1):49-61.
217. Yang YJ, Lee SH, Hong SJ, Chung BC. Comparison of fatty acid profiles in the serum of patients with prostate cancer and benign prostatic hyperplasia. *Clin Biochem*. 1999;32(6):405-409.
218. Connolly JM, Coleman M, Rose DP. Effects of dietary fatty acids on DU145 human prostate cancer cell growth in athymic nude mice. *Nutr Cancer*. 1997;29(2):114-119.
219. Zheng X, Xie G, Jia W. Metabolomic profiling in colorectal cancer: opportunities for personalized medicine. *Per Med*. 2013;10(7):741-755. doi:10.2217/pme.13.73.
220. Williams MD, Reeves R, Resar LS, Hill HH. Metabolomics of colorectal cancer: Past and current analytical platforms. *Anal Bioanal Chem*. 2013;405(15):5013-5030. doi:10.1007/s00216-013-6777-5.
221. Humphrey SP, Williamson RT. A review of saliva : Normal composition , flow , and function. *J Prosthet Dent*. 2001;85(2):162-169.
222. de Almeida P, Gregio AM, Machado MA, de Lima AA, Azevedo L. Saliva Composition and Functions : *J Contemp Dent Pract*. 2008;9(3):72-80.
223. Figueira J, Gouveia-figueira S, Öhman C, Lif P, Nording ML, Öhman A. Journal of Pharmaceutical and Biomedical Analysis Metabolite quantification by NMR and LC-MS / MS reveals differences between unstimulated , stimulated , and pure parotid saliva. *J Pharm Biomed Anal*. 2017;140:295-300. doi:10.1016/j.jpba.2017.03.037.
224. Cavalla F, Biguetti C, Jain S, et al. Proteomic Profiling and Differential Messenger RNA Expression Correlate HSP27 and Serpin Family B Member 1 to Apical Periodontitis. *J Endod*. 2017;43(9):1486-1493. doi:10.1016/j.joen.2017.03.014.
225. Ingle JI. *Ingle's Endodontics 6*. Vol 13.; 2008.
226. Loesche WJ. The identification of bacteria associated with periodontai disease and dentai caries by enzymatic methods. *Oral Microbiol Immunol*. 1986;1(14):65-70.
227. De Jong MH, Van Der Hoeven JS. The Growth of Oral Bacteria on Saliva. *J Dent Res*. 1987;66(2):498-505.
228. Slots J. *Herpesviruses in Periodontal Disease*.; 2005.
229. Contreras A, Umeda M, Chen C, Bakker I, Morrison JL, Slots J. Relationship Between Herpesviruses and Adult Periodontitis and Periodontopathic Bacteria. *J Periodontol*. 199AD;70(5):478-484.
230. Venturi, Endodonzia AI di. *La Diagnosi-Element Di Anatomia, Fisiologia E Patologia Del Complesso Pulpo-Dentinale*.; 2014.
231. J.Màrton I, Kiss C. Overlapping Protective and Destructive Regulatory Pathways in Apical Periodontitis. *J Endod*. 2014;40(2):155-163. doi:10.1016/j.joen.2013.10.036.
232. Akamine A, Hashinguchi I, Toriya Y, Maed K. Immnohistochemical examination on the localization of macrophages and plasma cells in induced rat periapical lesions. *Dent Traumatol*. 1994;10:121-128.
233. Rodini CDO, Lara VS, Paulo S. Study of the expression of CD68 + macrophages and CD8 + T cells in human granulomas and periapical cysts. *J Endod*. 2001;92(2):221-227. doi:10.1067/moe.2001.116813.
234. Goettel M, Niessner R, Mueller D, Scherer M, Scherer G, Pluym N. Metabolomic Fingerprinting in Various Body Fluids of a Diet- Controlled Clinical Smoking Cessation Study Using a Validated GC- TOF-MS Metabolomics Platform. *J Proteome Res*. 2017;16:3491-3503. doi:10.1021/acs.jproteome.7b00128.
235. Santone C, Dinallo V, Paci M, Ottavio SD, Barbato G, Bernardini S. Journal of Pharmaceutical and Biomedical Analysis Saliva metabolomics by NMR for the evaluation of sport performance. *J Pharm Biomed Anal*. 2014;88:441-446. doi:10.1016/j.jpba.2013.09.021.
236. Kageyama G, Saegusa J, Irino Y, et al. Metabolomics analysis of saliva from patients with primary Sj o syndrome. *Clin Exp Immunol*. 2015;182:149-153. doi:10.1111/cei.12683.
237. Liang Q, Liu H, Li X, Zhang A. High-throughput metabolomics analysis discovers salivary biomarkers for predicting mild cognitive impairment and Alzheimer's disease. *RSC Adv*. 2016;6:75499-75504. doi:10.1039/C6RA16802G.
238. Roberta L, Oliveira P De, Martins C, et al. Salivary Metabolite Fingerprint of Type 1 Diabetes in Young Children. *J Proteome Res*. 2016;15:2491-2499. doi:10.1021/acs.jproteome.6b00007.
239. Sugimoto M, Wong ÆDT. Capillary electrophoresis mass spectrometry-based saliva metabolomics identified

oral , breast and pancreatic cancer-specific profiles. *Metabolomics*. 2010;6:78-95. doi:10.1007/s11306-009-0178-y.
240. Wang Q, Gao P, Wang X, Duan Y. Clinica Chimica Acta Investigation and identi fi cation of potential biomarkers in human saliva for the early diagnosis of oral squamous cell carcinoma. *Clin Chim Acta*. 2014;427:79-85. doi:10.1016/j.cca.2013.10.004.
241. Takayama T, Tsutsui H, Shimizu I, Toyama T, Yoshimoto N. Clinica Chimica Acta Diagnostic approach to breast cancer patients based on target metabolomics in saliva by liquid chromatography with tandem mass spectrometry. *Clin Chim Acta*. 2016;452:18-26. doi:10.1016/j.cca.2015.10.032.
242. Zhang A, Sun H, Wang X. Saliva Metabolomics Opens Door to Biomarker Discovery , Disease Diagnosis , and Treatment. *Appl Biochem Biotechnol*. 2012;168:1718-1727. doi:10.1007/s12010-012-9891-5.
243. Sugimoto M, Saruta J, Matsuki C. Physiological and environmental parameters associated with mass spectrometry-based salivary metabolomic profiles. 2013:454-463. doi:10.1007/s11306-012-0464-y.
244. Cuevas-Cordoba B, Santiago-Garcia J. Saliva: A Fluid of Study for OMICS. *PMICS A J Integr Biol*. 2014;18(2):87-97. doi:10.1089/omi.2013.0064.
245. Tasoulas J, Patsouris E, Giaginis C. Salivaomics for oral diseases biomarkers detection. *Expert Rev Mol Diagn*. 2016;7159(December 2015):285-295. doi:10.1586/14737159.2016.1133296.
246. Wallner-liebmann S, Tenori L, Mazzoleni A, et al. Individual Human Metabolic Phenotype Analyzed by 1 H NMR of Saliva Samples. *J Proteome Res*. 2016;15:1787-1793. doi:10.1021/acs.jproteome.5b01060.
247. Aimetti M, Cacciatore S. Metabonomic analysis of saliva reveals generalized chronic periodontitis signature. *Metabolomics*. 2012;8:465-474. doi:10.1007/s11306-011-0331-2.
248. Pasquinelli F. *Diagnosi E Tecniche Di Laboratorio - Parte Seconda*. 1st ed. Firenze: Rossini Editrice; 1985.
249. Pasquinelli F. *Diagnosi E Tecniche Di Laboratorio - Parte Seconda*. 1st ed. Firenze: Rossini Editrice; 1985.
250. Pasquinelli F. *Diagnosi E Tecniche Di Laboratorio - Parte Seconda*. 1st ed. Firenze: Rossini Editrice; 1985.
251. Khamis MM, Adamko DJ, El-aneed A. MASS SPECTROMETRIC BASED APPROACHES IN URINE METABOLOMICS AND BIOMARKER DISCOVERY. *Mass Spectrom Rev*. 2014;9999:1-20. doi:10.1002/mas.
252. Vaidyanathan K. Urinary proteomics and metabolomics in the diagnosis of pediatric disorders. *Proteomics Clin Appl*. 2015;9:482-489. doi:10.1002/prca.201400093.
253. Emwas A, Roy R, Mckay RT, et al. Recommendations and Standardization of Biomarker Quanti fi cation Using NMR-Based Metabolomics with Particular Focus on Urinary Analysis. *J Proteome Res*. 2016;15:360-373. doi:10.1021/acs.jproteome.5b00885.
254. Sarosiek I, Schicho R, Blandon P, Bashashati M, Ave A, Paso E. Urinary metabolites as noninvasive biomarkers of gastrointestinal diseases : A clinical review. *World J Gastrointest Oncol*. 2016;8(5):459-465. doi:10.4251/wjgo.v8.i5.459.
255. Kim CJ, Romero R, Chaemsaithong P. Acute chorioamnionitis and funisitis: definition, pathologic features, and clinical significance. *Am J Obstet Gynecol*. 2015;213(4):S29-S52. doi:10.1016/j.ajog.2015.08.040.
256. Goldenberg RL, Culhane JF, Iams JD, Romero R. Preterm Birth 1 Epidemiology and causes of preterm birth. *Lancet*. 2008;371:75-84.
257. Lahra MM, Beeby PJ, Jeffery HE. Intrauterine Inflammation, Neonatal Sepsis, and Chronic Lung Disease: A 13 Year Hospital Cohort Study. *Pediatrics*. 2009;123:1314-1319. doi:10.1542/peds.2008-0656.
258. Pugni L, Pietrasanta C, Acaia B, et al. Chorioamnionitis and neonatal outcome in preterm infants : a clinical overview. *J Matern Neonatal Med*. 2016;29(0):1525-1529. doi:10.3109/14767058.2015.1053862.
259. Soraisham AS, Trevenen C, Wood S, Singhal N, Sauve R. Histological chorioamnionitis and neurodevelopmental outcome in preterm infants. *J Perinatol*. 2013;33(1):70-75. doi:10.1038/jp.2012.49.
260. Andrews WW, Goldenberg RL, Faye-petersen O, Cliver S, Goepfert AR, Hauth JC. The Alabama Preterm Birth study : polymorphonuclear and mononuclear cell placental infiltrations , other markers of inflammation , and outcomes in 23- to 32-week preterm newborn infants. *Am J Obstet Gynecol*. 2006;195:803-808. doi:10.1016/j.ajog.2006.06.083.
261. Been J V, Zimmermann LJI. Histological chorioamnionitis and respiratory outcome in preterm infants. *Arch Dis Fetal Neonatal Ed*. 2009;94:F218-F225. doi:10.1136/adc.2008.150458.
262. Edline RAWR, Etersen ONAFAYE, Eller DEH, et al. Amniotic Infection Syndrome : Nosology and Reproducibility of Placental Reaction Patterns. *Pediatr Dev Pathol*. 2003;6:435-448. doi:10.1007/s10024-003-7070-y.
263. Sung J, Choi S, Oh S, Roh C, Kim J. Revisiting the diagnostic criteria of clinical chorioamnionitis in preterm birth. *BJOG an Int J Obstet Gynaecol*. 2016:1-9. doi:10.1111/1471-0528.14176.
264. Tita ATN, Andrews WW. Diagnosis and Management of Clinical Chorioamnionitis. *Clin Perinatol*. 2010;37(2):339-354. doi:10.1016/j.clp.2010.02.003.
265. Been J V, Vanterpool SF, Rooij JDE De, et al. A Clinical Prediction Rule for Histological Chorioamnionitis in Preterm Newborns. *PLoS One*. 2012;7(10):e46217. doi:10.1371/journal.pone.0046217.
266. Buhimschi IA, Nayeri UA, Laky CA, Razeq A, Dulay AT, Buhimschi CS. Advances in medical diagnosis of intra-amniotic infection Advances in medical diagnosis of intra-amniotic infection. *Expert Opin Med Diagn*.

2013;7:5-16. doi:10.1517/17530059.2012.709232.
267. Chaemsaithong P, Romero R, Korzeniewski SJ, Martinez-varea A, Dong Z. A point of care test for interleukin-6 in amniotic fluid in preterm prelabor rupture of membranes : a step toward the early treatment of acute intra-amniotic inflammation / infection. *J Matern Neonatal Med*. 2016;29(0):360-367. doi:10.3109/14767058.2015.1006621.
268. Verani J, McGee L, Schrag S. Prevention of perinatal group B streptococcal disease--revised guidelines from CDC, 2010. *MMWR Recomm Rep*. 2010;59:1-36.
269. Brady MT, Polin RA. Prevention and Management of Infants With Suspected or Proven Neonatal Sepsis. *Pediatrics*. 2014;132:166-168. doi:10.1542/peds.2013-1310.
270. Cotten CM, Taylor S, Stoll B, et al. Prolonged Duration of Initial Empirical Antibiotic Treatment Is Associated With Increased Rates of Necrotizing Enterocolitis and Death for Extremely. *Pediatrics*. 2009;123:58-66. doi:10.1542/peds.2007-3423.
271. Kuppala VS, Meinzen-derr J, Morrow AL, Schibler KR. Prolonged Initial Empirical Antibiotic Treatment is Associated with Adverse Outcomes in Premature Infants. *J Pediatr*. 2011;159(5):720-725. doi:10.1016/j.jpeds.2011.05.033.
272. Alm B, Erdes L, Möllborg P, Pettersson R, Norvenius SG. Neonatal Antibiotic Treatment Is a Risk Factor for. *Pediatrics*. 2008;121:697-702. doi:10.1542/peds.2007-1232.
273. Penders J, Thijs C, Brandt PA Van Den, et al. Gut microbiota composition and development of atopic manifestations in infancy : the KOALA Birth Cohort Study. *Gut*. 2007;56:661-667. doi:10.1136/gut.2006.100164.
274. Julious SA. Sample size of 12 per group rule of thumb for a pilot study. *Pharm Stat*. 2005;4:287-291. doi:10.1002/pst.185.
275. Taylor P, Singer M. The role of mitochondrial dysfunction in sepsis-induced multi-organ failure. *Virulence*. 2014;5(1):66-72. doi:10.4161/viru.26907.
276. Peptidoglycan CW, Park JT, Uehara T, Park JT, Uehara T. How Bacteria Consume Their Own Exoskeletons (Turnover and Recycling of How Bacteria Consume Their Own Exoskeletons (Turnover and Recycling of Cell Wall Peptidoglycan)†. *Microbiol Mol Biol Rev*. 2008;72(2):211-227. doi:10.1128/MMBR.00027-07.
277. Taylor P, Angelis M De, Francavilla R, Piccolo M, Giacomo A De. Autism spectrum disorders and intestinal microbiota. *Gut Microbes*. 2015;6(3):207-213. doi:10.1080/19490976.2015.1035855.
278. Dudzik D, Revello R, Barbas C, Bartha JL. LC − MS-Based Metabolomics Identi fi cation of Novel Biomarkers of Chorioamnionitis and Its Associated Perinatal Neurological Damage. *J Proteome Res*. 2015;14:1432-1444. doi:10.1021/pr501087x.
279. Abehsera D, Rodrigues Y, Mingorance J, Suárez A, Magdaleno F, Bartha JL. Prediction and clinical relevance of pathologic patterns of injury associated with chorioamnionitis. *Placenta*. 2014;35(1):70-71. doi:10.1016/j.placenta.2013.10.009.
280. Prince AL, Ma J, Kannan PS, et al. The placental microbiome is altered among subjects with spontaneous preterm birth with and without chorioamnionitis. *Am J Obstet Gynecol*. 2014;5:e1-627.e16. doi:10.1016/j.ajog.2016.01.193.
281. Peekhaus N, Conway T. What ' s for Dinner ?: Entner-Doudoroff Metabolism in Escherichia coli. *J Bacteriol*. 1998;180(14):3495-3502.
282. P. S. Perinatal asphyxia: an overview. In: Stevenson D, Benitz W, Sunshine P, eds. *Fetal and Neonatal Brain Injury: Mechanisms, Management and the Risks of Practice*. Third. Cambridge (UK): Cambridge University Press; 3003:3-28.
283. Committee on Obstetric Practice AC of O and G. ACOG Committee Opinion. Number 326, December 2005. Inappropriate use of the terms fetal distress and birth asphyxia. *Obstet Gynecol*. 2005;106:1469-1470.
284. Ahearne CE, Boylan GB, Murray DM, et al. Short and long term prognosis in perinatal asphyxia: An update. *World J Clin Pediatr*. 2016;5(1):67-75. doi:10.5409/wjcp.v5.i1.67.
285. Antonucci R, Porcella A, Pilloni MD. Perinatal asphyxia in the term newborn. *J Pediatr Neonatal Individ Med*. 2014;3(2):1-14. doi:10.7363/030269.
286. Shah P, Riphagen S, Beyene J, Perlman M. Multiorgan dysfunction in infants with post-asphyxial hypoxic-ischaemic encephalopathy. *Arch Dis Child Fetal Neonatal Ed*. 2004;89(3):152-156. doi:10.1136/adc.2002.023093.
287. Herrera-Marschitz M, Neira-Pena T, Rojas-Mancilla E, et al. Perinatal asphyxia : CNS development and deficits with delayed onset. *Front Neurosci*. 2014;8(March):1-11. doi:10.3389/fnins.2014.00047.
288. Wassink G, Gunn ER, Paul P, Bennet L, Gunn AJ. The mechanisms and treatment of asphyxial encephalopathy. *Front Neurosci*. 2014;8(February):1-11. doi:10.3389/fnins.2014.00040.
289. Laptook AR. Birth Asphyxia and Hypoxic-Ischemic Brain Injury in the Preterm Infant. *Clin Perinatol*. 2016;43:529-545. doi:10.1016/j.clp.2016.04.010.
290. Azzopardi D V., Strohm B, Edwards AD, et al. Moderate Hypothermia to Treat Perinatal Asphyxial Encephalopathy. *N Engl J Med*. 2009;361:1349-1358.
291. Azzopardi D, Strohm B, Marlow N, et al. Effects of Hypothermia for Perinatal Asphyxia on Childhood

Outcomes. *N Engl J Med*. 2014;371:140-149. doi:10.1056/NEJMoa1315788.
292. Laptook AR, Corbett RJT, Sterett R, Garcia D. Quantitative Relationship between Brain Temperature and Energy Utilization Rate Measured in Vivo Using 3 1 AND â€™ H Magnetic Resonance Spectroscopy. *Pediatr Res*. 1995;38(6):919-925.
293. Bayley N. *Bayley Scales of Infant and Toddler Development*. Third. San Antonio, TX, USA: Harcourt Assessment; 2006.
294. Romero J, Muniz J, Tornatore TL, et al. Dual role of astrocytes in perinatal asphyxia injury and neuroprotection. *Neurosci Lett*. 2014;565:42-46. doi:10.1016/j.neulet.2013.10.046.
295. Ide Bergamaschi N, Clarke P. Is delayed normalization of plasma lactate in cooled babies with hypoxic-ischaemic encephalopathy associated with a poor outcome? *J Pediatr Neonatal Individ Med*. 2015;4:36-37.
296. Marcinkiewicz J, Kontny E. Taurine and inflammatory diseases. *Amino Acids*. 2014;46:7-20. doi:10.1007/s00726-012-1361-4.
297. Ezgü F, Atalay Y, Hasanoğlu A. Serum carnitine levels in newborns with perinatal asphyxia and relation to neurologic prognosis. *Nutr Neurosci*. 2004;7:351-356.
298. Jones LL, Mcdonald DA, Borum PR. Acylcarnitines : Role in brain. *Prog Lipid Res*. 2010;49(1):61-75. doi:10.1016/j.plipres.2009.08.004.
299. Amstrong N. Mannitol. In: Rowe R, Sheskey P, Quinn M, eds. *Handbook of Pharmaceutical Excipients*. Sixth. London (UK): Pharmaceutical Press and American Pharmacists Association; 2009:424-428.
300. Hatashita S, Hoff JT, Salamat SM, Neurosurgery S, Arbor A. Ischemic Brain Edema and the Osmotic Gradient Between Blood and Brain. *J Cereb Blood Flow Metab*. 1988;8:552-559.
301. Polderman KH, van de Kraats G, Dixon JM, Vandertop WP, Girbes ARJ. Increases in spinal fluid osmolarity induced by mannitol. *Neurol Crit Care*. 2003;31(2):584-590. doi:10.1097/01.CCM.0000050287.68977.84.
302. Feng Q, Liu Z, Zhong S, Li R, Xia H, Jie Z. Integrated metabolomics and metagenomics analysis of plasma and urine identified microbial metabolites associated with coronary heart disease. *Sci Rep*. 2016;6:22525. doi:10.1038/srep22525.
303. Nathavitharana K, Lloyd D, Raafat F. Urinary mannitol: lactulose excretion ratios and jejunal mucosal structure. *Arch Dis Child*. 1988;63:1054-1059.
304. Jaakkola P, Jaakkola P, Mole DR, et al. Targeting of HIF- ⎵ to the von Hippel – Lindau Ubiquitylation Complex by O 2 -Regulated Prolyl Hydroxylation. *Science (80-)*. 2001;292:468-472. doi:10.1126/science.1059796.
305. Jiang J, Johnson LC, Knight J, et al. Metabolism of [13 C 5] hydroxyproline in vitro and in vivo : implications for primary hyperoxaluria. *Am J Physionoly-Gastrointestinal Liver Physiol*. 2012;302:637-644. doi:10.1152/ajpgi.00331.2011.
306. Robertson DS. The function of oxalic acid in the human metabolism. *Clin Chem Lab Med*. 2011;49(9):1405-1412. doi:10.1515/CCLM.2011.238.
307. White L, Lawson E. Effects of chronic prenatal hypoxia on tyrosine hydroxylase and phenylethanolamine N-methyltransferase messenger RNA and protein levels in medulla oblongata of postnatal rat. *Pediatr Res*. 1997;42:455-462.
308. Solaini G, Baracca A, Lenaz G, Sgarbi G. Biochimica et Biophysica Acta Hypoxia and mitochondrial oxidative metabolism. *Biochim Biophys Acta*. 2010;1797(6-7):1171-1177. doi:10.1016/j.bbabio.2010.02.011.
309. Cozzi C, Aldrink J, Nicol K, Nicholson L, Cua C. Intestinal location of necrotizing enterocolitis among infants with congenital heart disease. *J Perinatol*. 2013;33(10):783-785. doi:10.1038/jp.2013.49.
310. Mcelroy SJ, Underwood A, Sherman MP. Paneth Cells and Necrotizing Enterocolitis : A Novel Hypothesis for Disease Pathogenesis. *Neonatology*. 2013;103:10-20. doi:10.1159/000342340.
311. Defense B, Gamma EF La, Blau J. Transfusion-Related Acute Gut Injury : Feeding, Flora, Flow, and Barrier Defense. *Semin Perinatol*. 2012;36(4):294-305. doi:10.1053/j.semperi.2012.04.011.
312. Singh R, Shah BL, Frantz ID. Necrotizing Enterocolitis and the Role of Anemia of Prematurity. *Semin Perinatol Perinatol*. 2012;36(4):277-282. doi:10.1053/j.semperi.2012.04.008.
313. Hawkes CP, Adzick NS, Palladino A. Late Presentation of Fulminant Necrotizing Enterocolitis in a Child with Hyperinsulinism on Octreotide Therapy. *Horm Res Paediatr*. 2016;86:131-136. doi:10.1159/000443959.
314. Ohlsson A, Walia R, Ss S. Ibuprofen for the treatment of patent ductus arteriosus in preterm or low birth weight (or both) infants (Review). *Cochrane Database Syst Rev Antibiot*. 2015;(2):1-200. doi:10.1002/14651858.CD003481.pub6.www.cochranelibrary.com.
315. Terrini G, Passariello A, Curtis M De, et al. Ranitidine is Associated With Infections , Necrotizing Enterocolitis , and Fatal Outcome in Newborns. *Pediatrics*. 2012;129:e40-e45. doi:10.1542/peds.2011-0796.
316. Lopez SL, Taeusch HW, Findlay RD, Walther FJ. Time of onset of necrotizing enterocolitis in newborn infants with known prenatal cocaine exposure. *Clin Pediatr (Phila)*. 1995;34:424-429.
317. Hallstrom M, Koivisto A, Janas M, Tammela O. Frequency of and risk factors for necrotizing enterocolitis in infants born before 33 weeks of gestation. *Acta Paediatr*. 2003;92:111-113.
318. Shulman RJ. Effect of different total parenteral-nutrition fuel mixes on small intestinal growth and differentiation in the infant miniature pig. *Gastroenterology*. 1988;95:85–92.

319. Tai I, Huang Y, Lien R, Huang C. Clinical manifestations of a cluster of rotavirus infection in young infants hospitalized in neonatal care units. *J Microbiol Immunol Infect*. 2012;45(1):15-21. doi:10.1016/j.jmii.2011.09.023.
320. Bagci S, Eis-Hübinger AM, Yassin AF. Clinical characteristics of viral intestinal infection in preterm and term neonates. *Eur J Clin Microbiol Infect Dis*. 2010;29:1079–1084.
321. Gonzalez-Rivera R, Culverhouse RC, Hamvas A, Tarr PI, Warner BB. The age of necrotizing enterocolitis onset : an application of Sartwell ' s incubation period model. *J Perinatol*. 2011;31:519-523. doi:10.1038/jp.2010.193.
322. Ta BD, Roze E, Braeckel KN van, Bos AF, Rassouli-Kirchmeier R, Hulscher JB. Long-term neurodevelopmental impairment in neonates surgically treated for necrotizing enterocolitis: enterostomy associated with a worse outcome. *Eur J Pediatr Surg*. 2011;21:58-64.
323. Martin CR, Dammann O, Allred EN. Neurodevelopment of extremely preterm infants who had necrotizing enterocolitis with or without late bacteremia. *J Pediatr*. 2010;157:751-756.
324. SHAH DK, DOYLE LW, ANDERSON PJ, et al. Adverse Neurodevelopment in Preterm Infants with Postnatal Sepsis orNecrotizing Enterocolitis is Mediated by White Matter Abnormalities on Magnetic Resonance Imaging at Term. *J Pediatr*. 2008;153:170-175.
325. Puddu M, Marcialis MA, De Magistris A, et al. From the " old NEC " to the " new NECs ." *J Pediatr Neonatal Individ Med*. 2014;3(2)::e030245. doi:10.7363/030245.
326. De Magistris A, Marcialis MA, Puddu M, Irmesi R, Coni E, Fanos V. Embryological development of the intestine and necrotizing enterocolitis. *J Pediatr Neonatal Individ Med*. 2016;5(2):e050213. doi:10.7363/050213.
327. Ueland PM. Choline and betaine in health and disease. *J Inherit Metab Dis*. 2011;34:3−15.
328. Cesare Marincola F, Corbu S, Lussu M, et al. Impact of early postnatal nutrition on the NMR urinary metabolic profile of infant. *J Proteome Res*. 2016;15:3712-3723. doi:10.1021/acs.jproteome.6b00537.
329. Cesare Marincola F, Dessì A, Pattumelli MG. 1H NMR-based urine metabolic profile of IUGR, LGA, and AGA newborns in the first week of life. *Clin Chim Acta*. 2015;451:28-34.
330. Lopez-Corcuera B, Geerlings A, Aragon C. Glycine neurotransmitter transporters : an update. *Mol Membr Biol*. 2001;18:13-20. doi:10.1080/09687680010028.
331. Chiu CY, Yeh KW, Lin G. Metabolomics Reveals Dynamic Metabolic Changes Associated with Age in Early Childhood. *PLoS One*. 2016;11:e0149823.
332. Gu H, Pan Z, Xi B. 1H NMR metabolomics study of age profiling in children. *NMR Biomed*. 2009;22:826−833.
333. Moltu SJ, Sachse D, Blakstad EW, et al. Urinary Metabolite Profiles in Premature Infants Show Early Postnatal Metabolic Adaptation and Maturation. *Nutrients*. 2014;6:1913-1930. doi:10.3390/nu6051913.
334. Lin H, Edmunds SJ, Helsby NA, Ferguson LR, Rowan DD. Nontargeted Urinary Metabolite Profiling of a Mouse Model of Crohn ' s Disease research articles. *J Proteome Res*. 2009;8:2045-2057.
335. Lin H, Helsby NA, Rowan DD, Ferguson LR. Using Metabolomic Analysis to Understand Inflammatory Bowel Diseases. *Inflamm Bowel Dis*. 2011;17(4):1021-1029. doi:10.1002/ibd.21426.
336. Behrends V, Bell TJ, Liebeke M. Metabolite profiling to characterize disease-related bacteria: gluconate excretion by Pseudomonas aeruginosa mutants and clinical isolates from cystic fibrosis patients. *J Biol Chem*. 2013;21:15098-15109.
337. PARRY S, STRAUSS JF. PREMATURE RUPTURE OF THE FETAL MEMBRANES. *Mech Dis*. 1998;338:663-670.
338. Kumar D, Moore RM, Mercer BM, Mansour JM, Redline RW, Moore JJ. The physiology of fetal membrane weakening and rupture : Insights gained from the determination of physical properties revisited. *Placenta*. 2016;42:59-73. doi:10.1016/j.placenta.2016.03.015.
339. Caughey AB, Robinson JN, Norwitz ER. Contemporary Diagnosis and Management of Preterm Premature Rupture of Membranes. *Diagnosis Manag Updat*. 2008;1(1):11-22.
340. Medina TM, Hill DA. Preterm Premature Rupture of Membranes : Diagnosis and Management. *Am Fam Physician*. 2006;73(4):659-664.
341. Selin L, Almström E, Wallin G, Berg M. Use and abuse of oxytocin for augmentation of labor. *Acta Obstet Gynecol*. 2009;2007(September):1352-1357. doi:10.3109/00016340903358812.
342. Oláh KSJ, Steer PJ. The use and abuse of oxytocin. *Obstet Gynaecol*. 2015;17:265-271. doi:10.1111/tog.12222.
343. Gottvall K, Waldenstro U. Does a traumatic birth experience have an impact on future reproduction ? *BJOG an Int J Obstet Gynaecol*. 2002;109(March):254-260.
344. Mueller N, Whyatt R, Hoepner L, et al. Prenatal exposure to antibiotics, cesarean section and risk of childhood obesity. *Int J Obes*. 2015;39(4):665-670. doi:10.1038/ijo.2014.180.Prenatal.
345. Kumar D, Fung W, Moore RM, et al. Proinflammatory Cytokines Found in Amniotic Fluid Induce Collagen Remodeling , Apoptosis , and Biophysical Weakening of Cultured Human Fetal Membranes 1. *Biol Reprod*. 2017;34(October):29-34. doi:10.1095/biolreprod.105.045328.
346. Mclaren J, Taylor DJ, Bell SC. Increased concentration of pro – matrix metalloproteinase 9 in term fetal membranes overlying the cervix before labor : Implications for membrane remodeling and rupture. *Am J Obstet*

Gynecol. 2000;182:409-416.
347. Fortunato SJ, Menon R, Bryant C. Programmed cell death (apoptosis) as a possible pathway to metalloproteinase activation and fetal membrane degradation in premature rupture of membranes. *Am J Obstet Gynecol*. 182AD;2:1468-1476. doi:10.1067/mob.2000.107330.
348. Herbabdez-Guerrero C, Monzon-Bordonaba F, Jimenez-Zamudio L, et al. In-vitro secretion of proin ¯ ammatory cytokines by human amniochorion carrying hyper-responsive gene polymorphisms of tumour necrosis factor- a and interleukin-1 b. *Mol Hum Reprod*. 2003;9(10):625-629. doi:10.1093/molehr/gag076.
349. Fujimoto T, Parry S, Urbanek M, et al. A Single Nucleotide Polymorphism in the Matrix Metalloproteinase- 1 (MMP-1) Promoter Influences Amnion Cell MMP-1 Expression and Risk for Preterm Premature Rupture of the Fetal Membranes *. *J Biol Chem*. 2002;277(8):6296-6302. doi:10.1074/jbc.M107865200.
350. Simhan HN, Canavan TP. Preterm premature rupture of membranes : diagnosis , evaluation and management strategies. *BJOG an Int J Obstet Gynaecol*. 2005;112(March):32-37.
351. Bulletins-Obstetrics AC on P. ACOG Practice Bulletin No. 80: premature rupture of membranes. Clinical management guidelines for obstetrician-gynecologists. *Obs Gynecol*. 2007;109:1007-1019.
352. Heng YJ, Liong S, Permezel M, Rice GE, Quinzio MKW Di, Georgiou HM. Human cervicovaginal fluid biomarkers to predict term and preterm labor. *Front Physiol*. 2015;6(May):1-18. doi:10.3389/fphys.2015.00151.
353. El-messidi A, Cameron A, Glas F. Diagnosis of Premature Rupture of Membranes : Inspiration From the Past and Insights for the Future. *J Obstet Gynaecol Canada*. 2010;32(6):561-569. doi:10.1016/S1701-2163(16)34525-X.
354. Moore TR. Amniotic Fluid Dynamics Reflect Fetal and Maternal Health and Disease. *Obstet Gynecol*. 2010;116(3):759-765.
355. Díaz-castro J, Florido J, Kajarabille N, et al. A New Approach to Oxidative Stress and Inflammatory Signaling during Labour in Healthy Mothers and Neonates. *Oxid Med Cell Longev*. 2015;2015:1-8. doi:10.1155/2015/178536.
356. Dutton GJ. *Glucuronic Acid Free and Combined: Chemistry, Biochemistry, Pharmacology, and Medicine*. New York, New York, USA: Academic Press Inc.; 1966.
357. Wayner DDM, Burton GW, Ingold KU, Barclay LRC, Locke SJ. The relative contributions of vitamin E, urate, ascorbate and proteins to the total peroxyl radical-trapping antioxidant activity of human blood plasma. *Biochim Biophys Acta*. 1987;924:408-419.
358. Caboni P, Meloni A, Lussu M, et al. Urinary metabolomics of pregnant women at term: a combined GC/MS and NMR approach. *J Matern neonatal Med*. 2014;27(S2):2-12.
359. Sacks M, Baker TH. Spontaneous premature rupture of the membranes. A prospective study. *Am J Obs Gynecol*. 1967;97:888-893.
360. Shubert PJ, Diss E, Iams JD. Etiology of preterm premature rupture of membranes. *Obs Gynecol Clin North Am*. 1992;19:251-263.
361. Practice Bulletin No. 160: Premature Rupture of Membranes. *Obs Gynecol*. 2016;127:e39-e51.
362. Bulletins-Obstetrics. ACoP. ACOG Practice Bulletin No. 80: premature rupture of membranes. Clinical management guidelines for obstetrician-gynecologists. *Obs Gynecol*. 2007;109:1007-1009.
363. Mercer B, C M, M C. Periviable birth at 20 to 26 weeks of gestation: proximate causes, previous obstetric history and recurrence risk. *Am J Obs Gynecol*. 2005;193:1175-1180.
364. Mercer BM. Preterm premature rupture of the membranes. *Obs Gynecol*. 2003;101:178-193.
365. Blencowe H, Cousens S, Chou D, et al. Born too soon: the global epidemiology of 15 million preterm births. *Reprod Heal*. 2013;10:S2.
366. Caughey AB, Robinson JN, Norwitz ER. Contemporary diagnosis and management of preterm premature rupture of membranes. *Rev Obs Gynecol*. 2008;1:11-22.
367. Doyle RM, Alber DG, Jones HE, et al. Term and preterm labour are associated with distinct microbial community structures in placental membranes which are independent of mode of delivery. *Placenta*. 2014;35(12):1099-1101. doi:10.1016/j.placenta.2014.10.007.
368. Gomez R, Romero R, Nien JK, et al. A short cervix in women with preterm labor and intact membranes : A risk factor for microbial invasion of the amniotic cavity. *Am J Obstet Gynecol*. 2005:678-689. doi:10.1016/j.ajog.2004.10.624.
369. Gravett MG, Rubens CE, Nunes TM, Group R. Global report on preterm birth and stillbirth (2 of 7): discovery science. *BMC Pregnancy Childbirth*. 2010;10(Suppl 1):1-16.
370. Lee SE, Romero R, Park C, Jun JK, Yoon BH. The frequency and significance of intraamniotic inflammation in patients with cervical insufficiency. *Obsterics*. 2008;(June):1-8. doi:10.1016/j.ajog.2007.11.047.
371. Jazayeri A. Premature Rupture of Membranes. http://emedicine.medscape.com/article/261137-overview. Published 2016.
372. Berry SM, Johnson D, Berghella V. Fetal blood sampling. *Am J Obstet Gynecol*. 2013;209(3):170-180. doi:10.1016/j.ajog.2013.07.014.
373. Chorionic villus sampling - Risks. https://www.nhs.uk/conditions/chorionic-villus-sampling-cvs/risks/. Published 2015.

374. Spong CY. Preterm premature rupture of the fetal membranes complicated by oligohydramnios. *Clin Perinatol*. 2001;28:753-759.
375. Wu C, Chen C, Chou H. Pulmonary Hypoplasia Induced by Oligohydramnios : Findings from Animal Models and a Population-Based Study. *Pediatr Neonatol*. 2017;58(1):3-7. doi:10.1016/j.pedneo.2016.04.001.
376. Murphy M, Butler M, Coughlan B, Brennan D, Herlihy CO, Robson M. disorders and cesarean delivery in nulliparous women at term. *Am J Obstet Gynecol*. 2015;213(5):673.e1-673.e8. doi:10.1016/j.ajog.2015.06.035.
377. Albright CM, Anderson BL, Ali TN, Rouse DJ. Lactic Acid Measurement to Identify Risk of Morbidity from Sepsis in Pregnancy. *Am J Perinatol*. 2015;32:481-486.
378. Quinto EJ, Jiménez P, Caro I, Tejero J, Mateo J. Probiotic Lactic Acid Bacteria : A Review. *Food Nutr Sci*. 2014;5(September):1765-1775.
379. Krzysciak W, Pluskwa KK, Jurczak A, Koscielniak D. The pathogenicity of the Streptococcus genus. *Eur J Clin Microbiol Infect Dis*. 2013;32:1361-1376. doi:10.1007/s10096-013-1914-9.
380. Garsin DA. Ethanolamine Utilization in Bacterial Pathogens: Roles and Regulation. *Nat Rev Microbiol*. 2010;8(4):290-295. doi:10.1038/nrmicro2334.Ethanolamine.
381. Maeda K. IDENTIFICATION OF ESCHERICHIA COLI BY DETECTION OF HYDROQUINONE AND URACIL IN THE URINE SYSTEM. *J Chromatogr*. 1985;345:11-18.
382. Charette M, Gray MW. Pseudouridine in RNA : What , Where , How , and Why. *IUBMB Life*. 2000;49:341-351.
383. Duggleby SL, Jackson AA. Protein , amino acid and nitrogen metabolism during pregnancy : how might the mother meet the needs of her fetus ? *Curr Opin Clin Nutr Metab Care*. 2002;5:503-509.
384. Duggleby SL, Jackson AA. Relationship of maternal protein turnover and lean body mass during pregnancy and birth length. *Clin Sci*. 2001;72:65-72.
385. Kassel DB, Martin M, Schall W, Sweeley CC. Urinary metabolites of L-threonine in type 1 diabetes determined by combined gas chromatography/chemical ionization mass spectrometry. *Biomed Env Mass Spectrom*. 1986;13(10):535-540.
386. Masi AT, Rodnan GP, Medsger TA, et al. PRELIMINARY CRITERIA FOR THE CLASSIFICATION OF SYSTEMIC SCLEROSIS (SCLERODERMA). *Arthritis Rheum*. 1980;23:581-590.
387. Donzelli G, Carnesecchi G, Amador C, et al. Fetal programming and systemic sclerosis. *Am J Obstet Gynecol*. 2015;213:e1-e8.
388. Helmick CG, Felson DT, Lawrence RC, et al. Estimates of the Prevalence of Arthritis and Other Rheumatic Conditions in the United States Part I. *Arthritis Rheum*. 2008;58(1):15-25. doi:10.1002/art.23177.
389. Agarwal SK. The Genetics of Systemic Sclerosis. *Discov Med*. 2010;10:134-143.
390. Varga J, Abraham D. Review series Systemic sclerosis : a prototypic multisystem fibrotic disorder. *J Clin Invest*. 2007;117(3):557-567. doi:10.1172/JCI31139.ed.
391. van de Hoogen F, Khanna D, Fransen J, et al. 2013 classi fi cation criteria for systemic sclerosis : an American college of rheumatology / European league against rheumatism collaborative initiative. *Ann Rheum Dis*. 2013;72:1747-1755. doi:10.1136/annrheumdis-2013-204424.
392. Dees C, Akhmetshina A, Zerr P, et al. Platelet-derived serotonin links vascular disease and tissue fibrosis. *J Exp Med*. 2011;208(5):961-972. doi:10.1084/jem.20101629.
393. Coleiro B, Marshall S, Denton C, et al. Treatment of Raynaud's phenomenon with the selective serotonin reuptake inhibitor fluoxetine. *Rheumatol*. 2001;40:1038-1043.
394. Beretta L, Cossu M, Marchini M, et al. Research article A polymorphism in the human serotonin 5-HT 2A receptor gene may protect against systemic sclerosis by reducing platelet aggregation. *Arthritis Res Ther*. 2008;10(5):R103. doi:10.1186/ar2495.
395. KLIMIUK PS, GRENNAN A, WEINKOVE C, JAYSON MI V. Platelet serotonin in systemic sclerosis. *Ann Rheum Dis*. 1989;48:586-589.
396. Stachow A, Jablonska S, Skiendzielewska A. 5-Hydroxytryptamine and tryptamine pathways in scleroderma. *Br J Dermatol*. 1977;97:147-154.
397. Fattuoni C, Pietrasanta C, Pugni L, et al. Urinary metabolomic analysis to identify preterm neonates exposed to histological chorioamnionitis : A pilot study. *PLoS One*. 2017;12:e0189120. doi:https://doi.org/10.1371/journal.pone.0189120.
398. De Magistris A, Corbu S, Cesare Marincola F, et al. NMR-BASED METABOLOMICS ANALYSIS OF URINARY CHANGES IN NEONATAL NECROTIZING ENTEROCOLITIS. *J Pediatr Neonatal Individ Med*. 2015;4:37.
399. Meloni A, Palmas F, Barberini L, et al. PROM and Labour Effects On Urinary Metabolome : A Pilot Study. *Dis Markers*. 2017:1-19.

Thanks to…

This PhD project could not be done without some important people who I have to thank. First of all, my supervisors, Dr Claudia Fattuoni and Prof Mariano Casu who believed in me and in my abilities. I am truly grateful for what they taught me over these years and the possibilities they opened up for me. I would like to thank Prof L.L. Cheng, who welcomed me twice in his group. He guided me, trusted me, and fuelled my passion, curiosity, and instinct. He has been a great mentor to me. I thank all the physicians I had the pleasure to collaborate with, such as Adam Feldman, Alessandra Meloni, Maurizio Zavattoni, etc. who shared their knowledge and professionalism, stimulating my curiosity in this interesting field. The experts who aided me throughout this path, such as Luigi Barberini, broadening my expertise. The colleagues who joined me in this journey (Estefania Parejo Laucidina, Lindsey Vandergrift, Christopher Dietz, Felix Ehret, Meghan Fenlock, Yanni Jiang, and Taylor Fuss) and the minions I was glad to have (Laura Buccoli, Deborah Biggio, Emanuele Porcedda, and Federico Luiu) had a big role too… Obviously, special thanks go to my family that supported me, no matter what, over these challenging years. Last but not least, my friends Sara Mariani, Roberta Sclocco, Stefania Bartoletti, Pavle Kisin-Rajlic, Kevin Ronan, Tiziana Ibba, Giulia Spada, Giovanna Zappu, Marina Lai, Giulia Sileno, Eleni Skandalaki, and the plethora of other people who provide me with an awesome safety net.